Technische Universiteit
Eindhoven
University of Technology

Numerical simulation of external flames in ventilation-controlled fires

CFD-study with Fire Dynamics Simulator

Master thesis Reem Shakerchi

Beoordeling: Ruud van Herpen MSc. FIFireE
R.A.P.v.Herpen@tue.nl
6 april 2017
Notitie: 20170406.rhe (2 pagina's)

De afstudeerscriptie is een onderzoek naar modellering van uitslaande vlammen met behulp van een veldmodel (FDS) en de validatie daarvan aan de hand van kleinschalige experimenten.

Uitslaande vlammen vormen een bedreiging voor omgeving en eigen gebouw (vluchtroutes, andere compartimenten, draagconstructies buiten de brandruimte), omdat met name vanwege de stralingsflux risico van een hoge thermische belasting aanwezig is.

Om dergelijke risico's te kunnen inschatten bestaan diverse al dan niet genormeerde bepalingsmethoden, elk met een eigen doel. Echter, geen van die bepalingsmethoden kan worden toegepast in projectspecifieke maatwerkoplossingen met FSE-technieken.

Het is in FSE daarom wenselijk om het risico van uitslaande vlammen met een veldmodel (CFD-model) te kunnen vaststellen. Daarin kunnen automatisch projectspecifieke kenmerken worden gewaardeerd. Voorwaarde daarvoor is wel dat het CFD-model goed daarmee kan omgaan en behalve gasstromingen ook verbranding en de daarbij behorende turbulenties in de uitslaande vlam goed kan modelleren.

Een belangrijke conclusie in het afstudeerrapport van Reem is dat de uitslaande vlam in CFD betrouwbaar kan worden gemodelleerd, in verglijking met de experimenten. Echter, daarvoor is wel een relatief fijn grid noodzakelijk. Uiteraard geldt dat een fijner grid de nauwkeurigheid van LES gebaseerde CFD simulaties (zoals FDS: Fire Dynamics Simulator) vergroot. In het algemeen wordt een

grid voldoende fijn verondersteld wanneer voldaan wordt aan:

$$D^* = \left[\frac{\dot{Q}}{\rho_\infty C_\infty T_\infty \sqrt{g}} \right]^{2/5}$$

Hierin is D de gridsize en Q het brandvermogen.

Deze formule volstaat niet voor de gridsize bij modellering van een uitslaande vlam. Voor de modellering van de uitslaande vlam is een fijner grid noodzakelijk. Waarschijnlijk wordt dat veroorzaakt doordat het vermogen in de uitslaande vlam kleiner is dan het vermogen in de brandruimte.

Daarnaast heeft Reem een methode ontwikkeld om turbulenties zodanig uit te middelen dat de hoogte van de uitslaande vlam kan worden bepaald.

Tenslotte heeft ze vanuit het kleine model aanbevelingen gedaan hoe dat geëxtrapoleerd kan worden om de uitslaande vlam in een real-scale model te modelleren.

Het onderzoek is degelijk afgebakend en uitgevoerd, waardoor de conclusies en aanbevelingen betrouwbaar zijn. Het afstudeeronderzoek van Reem is dan ook met een 8,5 gewaardeerd.

Eindhoven, 6 april 2017

Ruud van Herpen MSc. FIFireE
Fellow Fire Safety Engineering

Technische Universiteit Eindhoven University of Technology

Numerical simulation of external flames in ventilation-controlled fires

Master Thesis

Department of the Built Environment
Building Physics and Services

Den Dolech 2, 5612 AZ Eindhoven
P.O. Box 513, 5600 MB Eindhoven
The Netherlands
www.tue.nl

Supervisors:
prof. ir. W. (Wim) Zeiler
ir. R.A.P. (Ruud) van Herpen FIFireE
ir. I.M.M.M.C. (Ingrid) Naus

Author
ing. R (Reem) Shakerchi-Ritmeijer
0863348

Date
April 2017

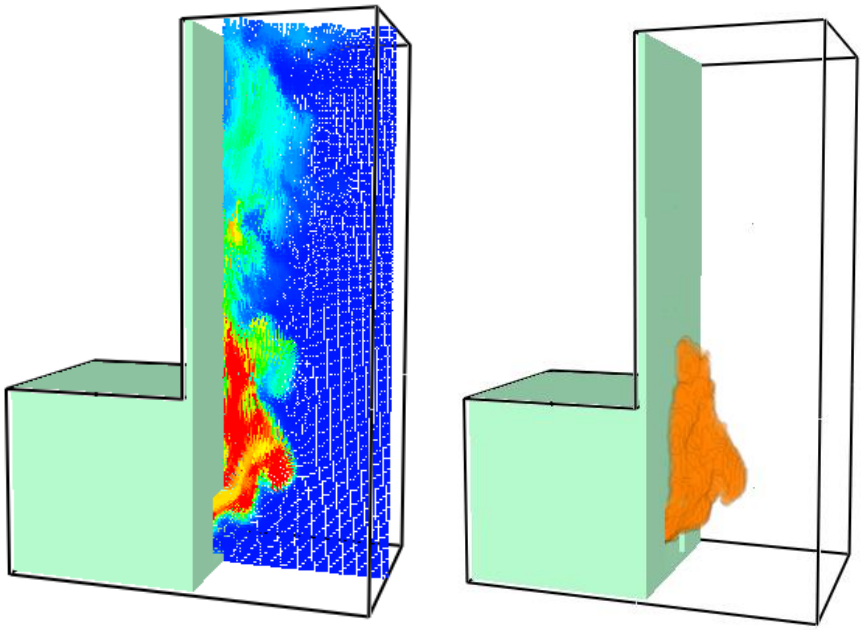

FELLOW/fse Stichting Fellowship FSE WO² Eindhoven

DPA Cauberg-Huygen

Technische Universiteit Eindhoven University of Technology

Where innovation starts

Graduation project

Title:	Numerical simulation of external flames of ventilation-controlled fires
Autor:	ing. R (Reem) Shakerchi-Ritmeijer
Supervisors:	prof. ir. W. (Wim) Zeiler
	ir. R.A.P. (Ruud) van Herpen FIFireE
	ir. I.M.M.M.C. (Ingrid) Naus
Date:	3 April 2017

Preface

This master thesis is created for my graduation project on the department Building Physics and Services at the Eindhoven University of Technology. This master thesis is performed to investigate if ventilation-controlled fires inside enclosures can be predicted by using CFD simulation models. This study has been realized in cooperation with the foundation Fellowship FSE WO² and the specialized consultancy agency DPA Cauberg-Huygen. Without the support of these participants this graduation thesis would not have been possible. Therefore I would like to take this opportunity to thank my supervisors Mr. Wim Zeiler (TU/e), Mr. Ruud van Herpen (TU/e and Fellowship FSE WO²) and Miss Ingrid Naus (Heijmans) for their support, guidance, insights and shared knowledge during the graduation process. Furthermore I would like to thank DPA Cauberg-Huygen for the possibilities and support that was offered to conduct this research. This made it possible to use multiple computers to perform the needed CFD simulations for a long period. Additionally I would like to thank Mr. Bart Merci and Mr. Guoxiang Zhao from the University of Gent who shared an example CFD model with external flames which is used for the validation study. Finally I want to thank my family and my husband for their support throughout this graduation project.

Reem Shakerchi-Ritmeijer

Eindhoven, 28 February 2017

Table of content

Glossary 5
Nomenclature 6
Summary 7
1. Introduction 9
1.1 Aim & objectives 10
1.2 Research relevance 10
1.3 Research limitations 10
1.4 Research approach 11
2. Literature study 12
2.1 Compartment fires in buildings 12
2.2 Experimental study 14
2.3 Numerical study 17
3. Methodology 18
3.1 Numerical simulation of compartment fires 18
3.2 FDS combustion model 20
3.3 Validation study 21
3.4 Sensitivity of building and fire parameters 29
3.5 Full-scale fire compartment 32
4. Research results 35
4.1 Validation study 35
4.2 Sensitivity of building and fire parameters 47
4.3 Full-scale fire compartment 49
5. Discussion 51
5.1 Experimental study 51
5.2 Validation study 52
5.3 Sensitivity of building and fire parameters 53
5.4 Full-scale fire compartment 54
6. Conclusions 55
Bibliografie 57

Appendix I	experimental study - procedure
Appendix II	article review – University Ghent
Appendix III-a	external flame height – calculation method 1
Appendix III-b	external flame height – calculation method 2
Appendix IV-a	fds2acii script
Appendix IV-b	Matlab script
Appendix V	FDS script (full-scale model)
Appendix VI-a	simulation results – HRR Per Unit Volume
Appendix VI-b	simulation results – gas temperature
Appendix VI-c	simulation results – horizontal air velocity
Appendix VI-d	simulation results – external flame
Appendix VII-a	simulation results – sensitivity of building and fire parameters
Appendix VII-b	simulation results – linear correlation
Appendix VIII-a	simulation results – full-size model propane fire (10 cm grid cell size)
Appendix VIII-b	simulation results – full-size model cellulose fire (10 cm grid cell size)
Appendix VIII-c	simulation results – full-size model cellulose fire (5 cm grid cell size)

Glossary

Actual HRR:
Is the fire release rate inside the enclosure as result of the fire release rate of the fire source inside the enclosure (kW).

Adiabatic construction:
Is a construction which remains at a fixed ambient temperature. There is no heat transfer (radiative or convective) from the gas to an adiabatic solid. All heat release rate inside the enclosure will be at maximum because the walls do not allow heat transfer.

Cellulose:
Is a polymer made up by repetition of glucose residues. Glucose is a sugar and consists of C-H-O chains.

Combustion:
Is a rapid chemical reaction between substances like fuel, heat and oxidant (the medium). A fire naturally occurs when the elements are presented and combined in the right mixture.

Compartment:
A typical compartment is described as a closed enclosure in a building communicating with the unconfined atmosphere through one or more vertical openings to be referred to 'windows'.

CO yield and soot yield:
The fraction of fuel mass converted into carbon monoxide (kg/kg) or smoke particles (kg/kg).

Extinction model:
Shows at which flame temperature and oxygen concentration fire will extinguish.

Façade heat flux:
On the façade is the emitted radiation at a distance. As result of external flaming the heat flux on the façade will increase by decreasing the distance to the fire source (W/m^2).

Fire spread:
Is transferring the heat energy through combustible materials.

Fuel controlled fire:
After ignition and at the start of a fire development the fire is described as fuel controlled as there is sufficient air for combustion and the fire development is controlled entirely by the fuel properties and arrangement. A fire can be fuel controlled at a later stage of development.

Heat release rate (HRR):
Is a critical parameter to characterize fire. When a material (fuel) combusts heat will be released to surrounding. The heat release is measured in (kW).

Ignition temperature:
Is the lowest temperature of a material or fuel when it spontaneously ignites in normal atmosphere boundary conditions without an external source of ignition such as a flame.

Mass flow rate:
The mass inflow or outflow rate through an opening is the substance of air which passes per unit of time (kg/s).

Neutral plane:
Is the position where there is no in- and outflow through the opening. The horizontal air velocity at this height is then nearly zero. The neutral plane height shows the boundary line between the inflow and outflow through the external opening.

Temperature lower flammability limit (LFL):
Is the temperature where combustion can not occur. Although there is enough oxygen concentration, below this temperature the fire will not occur.

Theoretical HRR:
Is the heat release rate of the fire source inside the enclosure (kW).

Thermal conductivity:
Of a material is the amount of heat flow through the construction by 1 Kelvin temperature difference.

Thermal diffusivity:
Is the thermal conductivity divided by density and specific heat capacity at constant pressure.

Two-zone model:
The idea of two zone models is that a fire compartment consists of two zones: one hot upper layer and one cold lower layer. The gas temperature inside the enclosure is homogeneous in the upper and lower layer.

Under-ventilated fire:
Fire inside the enclosure becomes under-ventilated when the amount of oxygen through the opening is not enough for combustion. The result of under-ventilated fires are external flames.

Ventilation-controlled fire:
As the fire grows it becomes ventilation-controlled when there is no longer sufficient oxygen to combust. The fire's heat release rate is then controlled completely by the amount of air which is available through external openings.

Nomenclature

A	Area of the opening (m^2)
c	Heat capacity (kJ/kgK)
E	Emitted energy per square meter (W/m^2)
h	height (m)
H	Height of the opening (m)
H_f	Flame height (m)
HRRPUV	Heat release rate per unit volume (Mw/m^3)
$\dot{m}$	Mass flow rate (kg/s)
O_x	Oxygen concentration inside (mol/mol)
Q	Energy release rate of fuel (kW)
Q_{in}	Energy release rate inside (kW)
qx	Heat flux per unit area (W/m^2)
T	Temperature (℃ or K)
u	Air velocity (m/s)
V	Volume (m^3)
N_p	Mean flame height from location of neutral plane height (m)
λ	Thermal conductivity (W/m.K)
ρ	Density (kg/m^3)
ε	Emissivity (-)
σ	Stefan-Boltzmann constant (5.670 $10^{-8}\ w.m^{-2}.k^{-4}$)

Summary

One of the fastest ways of fire spread to other floors is via external openings along the façade (Mammoser & Battaglia, 2002). This way of fire spread is the most dangerous because it is difficult to recognize by the building users. Fire CFD simulations are increasingly used for improvements in the fire protection and the fire safety engineering for reducing and preventing fire victims in the building environment.
External flames occur as results of a limited oxygen concentration inside the enclosure. Unburned gases will then burn outside the enclosure along the façade with enough oxygen concentration. When external flames occur the heat release rate (HRR) outside will result in higher temperatures and heat fluxes. The emitted radiation from the enclosure fire will increase the façade heat fluxes by decreasing the distance. Therefore reducing external flaming is necessary to reduce the risk of fire spread to upper fire compartments. In this research Computational Fluid Dynamics (CFD) simulations with external flames are performed for understanding the sensitivity of external flaming. By using CFD simulations it is possible to estimate the influence of different building and/or fire parameters on the external flaming behaviour.

Due to several complex variables in CFD calculations which depend on the fire scenario, the simulation should be validated with measurements of similar fire scenario. Therefore a CFD simulation model with external flames of ventilation controlled fire is validated based on a literature study (experimental and numerical). An own validated simulation model is used as a reference model to investigate the influence of different building and fire parameters on the external flaming.

Validation study
To investigate which grid cell size is minimal needed to reproduce accurate simulation results a grid sensitivity analyses is performed. Two grid cell sizes (2 cm and 1 cm) are simulated and compared to the measurements. All mentioned measured variables show a lower deviation with the measurements by using 1 cm grid cell size rather than 2 cm. Using 1 cm grid cell size shows a new empirical correlation of $1350\ A\sqrt{H}$ for the actual HRR. This means the simulated actual HRR inside the model deviates approximately 10% from the measurements. The simulated mass inflow rate shows an empirical correlation of $0.47\ A\sqrt{H}$ (deviation of approximately 6% with the measurements). The simulated neutral plane height shows agreement with the empirical correlation of 0.4H. For determining the external flame height from the flame temperature distribution two calculation methods are introduced in this research. Both calculation methods are compared to the external flame height from the experiments. From the results it can be concluded that using calculation method 1 gives a good agreement with the measurements. Because measured data always deals with certain measurement uncertainties the deviation of maximum 10% between the measurements and the simulations is accepted in this research for the validation of the CFD model.

Sensitivity of building and fire parameters
Four different parameters with boundary conditions are simulated (a window-like opening, narrowed opening, adiabatic construction and an increased theoretical HRR) with 2 cm and 1 cm grid cell size. From the simulation results it can be concluded that using the simulation results of a 2 cm grid cell size does not predict similar relative changes with the reference model as simulated with 1 cm grid cell size. All the results show a higher actual HRR inside the model simulated by 2 cm grid cell size compared to the actual HRR inside the model simulated by 1 cm grid cell size. A higher actual HRR inside the model means that the actual HRR outside the model will be lower. A lower actual HRR outside results in a higher external flame (according calculation method 1.

From the results it can be concluded that increasing the theoretical HRR inside the model shows similar results as the reference model. Narrowing the opening and using adiabatic constructions shows similar results for the actual HRR and neutral plane height. But not for the mass inflow rate and the external flame height. However all simulation models show a higher external flame tip relative compared to the reference model, the model with the highest external flame tip is the model with the shifted opening. To investigate if the new empirical correlation fits all opening surfaces more simulation models with different opening geometries need to be investigated.

Full-scale real fire compartment
The cubic scale model with adiabatic constructions (from the sensitivity analyses) is expanded to a full-scale fire compartment (factor 10) with a door-like opening and cellulose fire. The full-scale model is simulated by two different grid cell sizes to investigate the grid sensitivity on the results compared to the reference model.

The results of the actual HRR and the mass inflow rate show small differences between using 10 cm grid cell size or 5 cm grid cell size. This means that using similar ratio for the grid cell size in the full-scale model is possible. Except the results of the neutral plane height are not similar. The results are even less accurate by using a finer grid cell size. The full-scale model is simulated with cellulose fire instead of propane fire so the results may give another empirical correlation than the empirical correlation of the reference model. Therefore a third new full-scale simulation models (with 10 cm grid cell size) is simulated with propane fire to investigate if the results of the actual HRR and the mass inflow rate will fit the empirical correlation of the scaled reference model. The results of the actual HRR and the mass inflow rate shows a deviation within 10% with the reference model by using propane fire instead of the cellulose fire. To investigate if a finer grid cell will result in a lower deviation with the results of the reference model a new simulation model with a lower grid cell size should be simulated.

1. Introduction

In high-rise apartment buildings, flames and smoke can travel through ductwork, between leaks in the interior wall and via elevator shafts and stairwells. One of the fastest ways of fire spread to other floors however is via external openings along the façade (Mammoser & Battaglia, 2002). This type of fire spread is dangerous because it is difficult to recognize by the building users. External combustion of unburned gases is caused by an enclosure with openings where a flashover stage is reached and the oxygen inside the enclosure becomes limited (Bengtsson, 2001). When unburned gases are mixed with new fresh air because of a limited oxygen concentration, as a result the fire release rate will increase. An increased heat release rate (HRR) will result in higher temperatures and heat fluxes. The emitted radiation from the enclosure fire will increase the façade heat fluxes by decreasing the distance. High façade heat fluxes lead to fire spread to other floors (compartments) through the opening parallel above. Besides fire spread through the external openings, cladding materials may burn at a specific heat flux which may result in a structure fracture. Therefore reducing external flaming is necessary to reduce the risk of fire spread to other fire compartments.

The determination on the risk of fire spread to other floors and to adjacent buildings in accordance with the Dutch building regulations is achieved by a simple calculation method. This calculation method is a rough approximation of the reality due to the input possibilities for special and complex compartment geometries. Not just the building geometry should be simplified, but also the fire location, fuel properties and fire development. As result of the simplified input parameters the output will show simplified results as well. Due to this, the output of this approximation method shows overpredicted risk for the fire spread to other fire compartments. Therefore a CFD simulation model with external flames will show more accurate results for the risk of fire spread.

To prevent and reduce fire spread to other floors via external openings Computational Fluid Dynamics (CFD) simulations with external flames should be investigated for understanding the behaviour and sensitivity of external flaming. It is possible to estimate the influence of different building and/or fire parameters on the external flaming behaviour by using CFD simulation models with external flames. Decreasing external flame height means a decreased façade heat flux and thus a lower risk for fire spread.

This is the second part of the graduation project at the Eindhoven University of Technology about numerical simulation of ventilation-controlled fires. The content of this report is as following. In chapter 2 a significant literature study is done which is needed in this research. To predict the influence on external flaming a CFD model with external flames is validated with experimental results (literature study), before using the CFD simulation for further investigation. In chapter 3 the method of this research is given. The results of the performed validation study including the grid sensitivity analyses (FDS 6.5.2, SMV 6.3.12), the sensitivity of different building and fire parameters and the results of a full-size fire compartment will be given in chapter 4. In chapter 5 and chapter 6 the discussion and the conclusion are given.

1.1 Aim & objectives

In the recent years, fire safety of high-rise building fires has attracted extensive attention. Especially in cases where flames are ejected from an enclosure and attached to an upper or opposite building's façade (Zhao, Beji, & Merci, 2015). External flames are the result of fire spread through external openings to upper floors. Because external flames are one of the fastest way for fire spread, the risk of fire through external flames can cause dangerous situations. Situations where the building users do not immediate recognize fire. Therefore more knowledge about external flames is needed to prevent and predict the effect of fire spread to other floors. Computational Fluid Dynamic (CFD) simulations can help predicting and understanding this phenomenon. Reducing the flame height of external flaming means a lower risk of fire spread to other compartments. So in this research the effects of different fire and building parameters on the flame characteristics outside the enclosure will be investigated.

An increased computer performance and research in the fire safety engineering has led to more CFD simulation studies to investigate different fire scenarios and its consequences. Fire CFD simulations are increasingly used for improvements in the fire protection and the fire safety engineering for reducing and preventing fire victims in the build environment. Although CFD calculations take a large computational time, fire in large scale models are more expensive especially for reproducing a variant study with adaptions. Before using CFD simulations in practice the model with its specific boundary conditions has to be validated with experimental results (cubic scale model) in order to be reliable and useful. Below the main- and sub-questions are given which will be answered in this master thesis.

Research question:

1. Which building or fire parameter will influence the external flame height most?

Sub-questions:

a. What is the accuracy of a CFD model with external flames (FDS 6.5.2)?
b. How to determine the external flame height from simulation results?
c. Is it possible to simulate a full-scale fire compartment by a scaled model?

1.2 Research relevance

From literature it can be concluded that most studies were done based on measurements or numerical simulations. A drawback is that the relation between measurements and CFD simulations are not clearly investigated for external flames. When a validated CFD model with external flames can be used for predicting the risk of external flames, the influence of different building and fire parameters can be accurately determined. This research will investigate the accuracy of using the CFD simulation software package FDS for predicting the external flames of ventilation-controlled fires.

1.3 Research limitations

This research is limited to a cubic (CFD) scale model with external flames as result of a ventilation-controlled enclosure fire. Only a ventilation-controlled cubic enclosure fire with one external opening is used for the validation study. The validated CFD scale model is only useful for compartment fires under similar boundary conditions. The validation of the simulated model is limited to the availability of well documented experimental results. The measurements of the heat release rate (HRR) inside the model, gas temperature at different heights (front corner) inside the model, neutral plane height, external flame height and façade heat flux are used for the validation study.

1.4 Research approach

To investigate the influence of several building and fire parameters on the external flaming behaviour, first a CFD model with external flames is validated with measurements based on the literature study. The validated CFD model with external flames is used as a reference model to investigate the influence of the building and fire parameters on the external flame behaviour (paragraph 3.4). In paragraph 3.3 the method of the validation study will be given.

At the end of this research the validated CFD model will be expanded to a real full-size fire compartment to investigate if a full-size model needs a finer grid cell size to reproduce accurate CFD results. Simulation model 3 from the sensitivity analyses study is used as a reference model for the full-size model (paragraph 3.5). All simulation models are performed with the CFD software package FDS 6.5.2. Below the schematic flow diagram of the research approach is given.

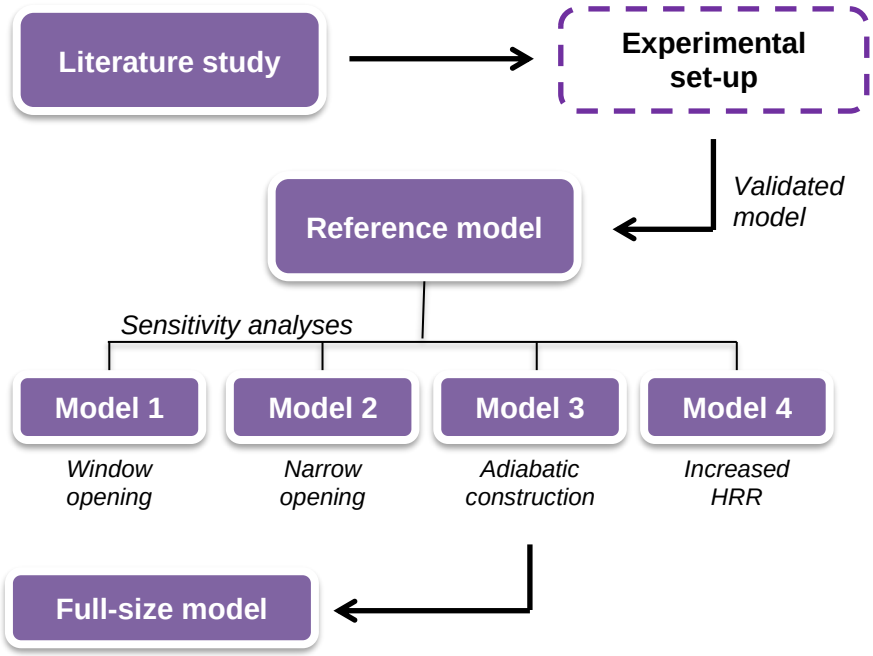

2. Literature study

2.1 Compartment fires in buildings

Before introducing the needed literature it is necessary to explain the typical compartment fire development and when an under-ventilated enclosure fire will occur. Usually, fire development in compartments or enclosures inside buildings is divided in four stages: the fire growth, flashover, fully-developed fire and the decay stage. Through these four time periods a local fire to a fully-developed fire compartment is developed. These four time periods are often divided in three different stages. The fire growth period is defined as the pre-flashover stage and the post-flashover stage includes the fully-developed fire and the decay period (Figure 1A).

The fire starts with the growth stage. When there is enough combustible fuel the Heat Release Rate (HRR) will increase. If the HRR rapidly increases a flashover stage will be reached which is a transition phase to a fully-developed compartment fire. If the flashover stage cannot be reached because of a low oxygen concentration or not enough fuel, the fire will extinguish (decay stage). If a flashover occurs the fire becomes a fully-developed compartment fire during the third stage. In the fully-developed fire stage all combustible fuels are involved. The HRR in the fire compartment is at its maximum in the third fire stage. Finally the decay stage occurs when all combustible fuels are burned. The HRR will decrease as well (Ingason, Li, & Lönnermark, 2015). When there is enough oxygen and fuel the HRR will increase during the growth stage, flashover and fully-developed fire stage. The decay stage is when there is not enough oxygen or fuel in a compartment.

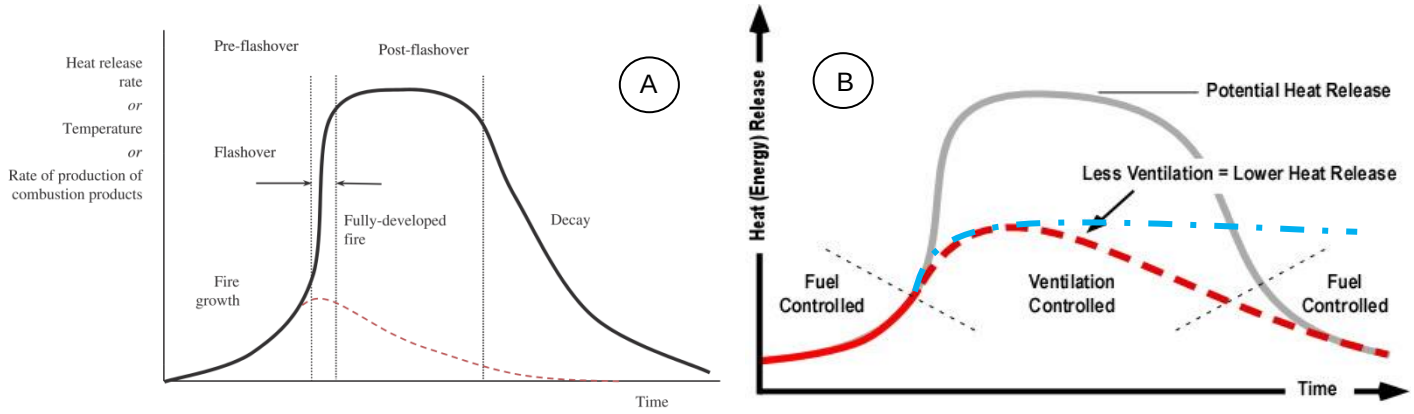

Figure 1: Phases of a typical compartment fire (Ingason, Li, & Lönnermark, 2015).

In fire compartments fire occurs differently than the standard fire curve because of different boundary conditions. In compartment fires two fire types are defined: fuel-controlled or ventilation-controlled fires. In the growth period or the pre-flashover stage of a compartment fire there is sufficient oxygen available for combustion and the fire growth is entirely dependent on the flammability and the fuel configuration. During this stage the fire is defined as fuel-controlled. The fire after the growth period can either continue to develop up to and beyond a point at which interaction with the compartment boundaries becomes significant (flashover) or it can start to decay (Figure 1B, red line). There are two factors in a fuel-controlled fire which influence the fire development. The first factor is a lack of fuel which will influence the produced HRR. The second factor is that the fire becomes a ventilation-controlled fire if there is enough fuel but the fire grows to a specific size which is determined by the inflow of fresh air through openings (Ingason, Li, & Lönnermark, 2015).

A ventilation-controlled fire or also called under-ventilated fire occurs when there is not enough oxygen available to combust all unburned gases inside the fire compartment. This can happen while there is a

certain air inflow from outside. The amount of oxygen through the opening is only enough during the first stage (ignition stage) but when the HRR inside increases the fire becomes ventilation-controlled because of limited oxygen. An external flame occurs as result of the limited oxygen concentration. Unburned combustion gases will burn further outside the compartment where there is enough oxygen, the HRR will then escape outside the enclosure. HRR inside the compartment is constant because all available oxygen inside is used for combustion (Figure 1B). During ventilation-controlled fire the outflow through the opening is always bigger than the inflow through the opening unless the HRR increases. This is because of the produced combustion gases which cannot be burned all inside the compartment (Shakerchi-Ritmeijer, 2016).

In under-ventilated fires the smoke yields and carbon monoxide are much higher than in a well-ventilated fire because of the limited oxygen concentration. Experimental research of the smoke development in an under-ventilated compartment shows that carbon monoxide (CO) and smoke yields increases during its development. The CO yield is increased by a factor of 5, whereas the smoke yield by a factor of 3 (Unkleja, Delichatsios, Delichatsios, & Lee, 2008). The most dangerous gas productions during fires in compartments are the unburned hydrocarbons (carbon dioxide (CO_2), carbon oxide (CO) and unburned carbons). In under-ventilated enclosures the unburned hydrocarbons very often are presented as result of the limited oxygen (Lönnermark & Björklund, 2008), (Gottuk & Lattimer, 2016). The production of these gases depends on the type and the amount of the fuel. The boundary conditions like the mass flow rate through openings and the oxygen concentration in the enclosure are determining factors for the combustion inside compartments.

External flames

External flames depend not only on the fuel surface and the size of external openings which influence the needed oxygen concentration in fire compartments. Below additional parameters which increase the risk of external flaming are given:

- Fuel composition (different HRR);
- Façade cladding material;
- Fire location;
- Wind direction.

Another important difference between a standard fire scenario and this experiment is the used fuel. Fires inside buildings are mostly assumed as cellulose (organic material) fires and not propane. This means that the theoretical HRR does not increase during the combustion time. The amount of the produced HRR inside the enclosure depends on the furniture and its auto-ignition temperature. Thus the duration of the fire depends on the fire load (Bengtsson, 2001). The burning time of a fire compartment increases the risk of external flaming by increasing the HRR. Using a low fire resistance façade cladding material will increase the fire spread to other floors. Because of the low auto-ignition temperature the façade cladding can be involved depending on the implementation. Then the actual HRR outside the compartment does not equal the produced actual HRR inside the fire compartment (furniture fire).
The location of fire inside compartments influences the fire development as well. If the fire is located under the air extraction then the fire will early extinguish because of the discharged combustion gases. If the fire is located at the corner more combustion gases will be produced because of the limited oxygen concentration.

The last and most important parameter is the wind direction outside during external flaming. Presence of wind inside or outside the compartment influences the fire exposure to the external structure. When wind blows through a burning compartment this will tend to reduce the fire exposure to the structure by reducing the fire duration and increasing the heat loss at the window (Law, Fire grading and fire behaviour, 1991). Increasing the wind means increasing the amount of oxygen which will allow a better combustion with less smoke production. An other advantage is that by mixing fresh air (with a higher

wind velocity) the direction of external flames may change with the wind direction. This may increase the fire safety of an upper compartment because of the lower temperatures and heat fluxes outside on the façade (Sugawa & Momita). When the wind conditions is unfavourable the risk of external flaming may be increased. In this research the wind conditions outside are not taken into account (no wind).

2.2 Experimental study

In the next paragraph the cubic scale model is described, which is used for the validation of the CFD model. The cubic scale model consists of a front face of 0.5 m x 0.5 m and depth of 0.5 m. All façades consist of fiberboard plates (0.025 m thick). To achieve an under-ventilated enclosure fire the room has one external opening. The (door-like) opening at the front façade is centered at the middle of the cubic scale model. The external opening at the front façade is designed to achieve an external flame as result of a limited oxygen concentration. The oxygen concentration inside the scale model is completely dependent on the inflow through the opening. In the middle of the scale model a rectangle propane burner (0.1 m x 0.2 m) with a maximum capacity of 50 kW is placed. In Figure 2 the experimental setup of the cubic scale model and the front façade with measurement devices is shown.

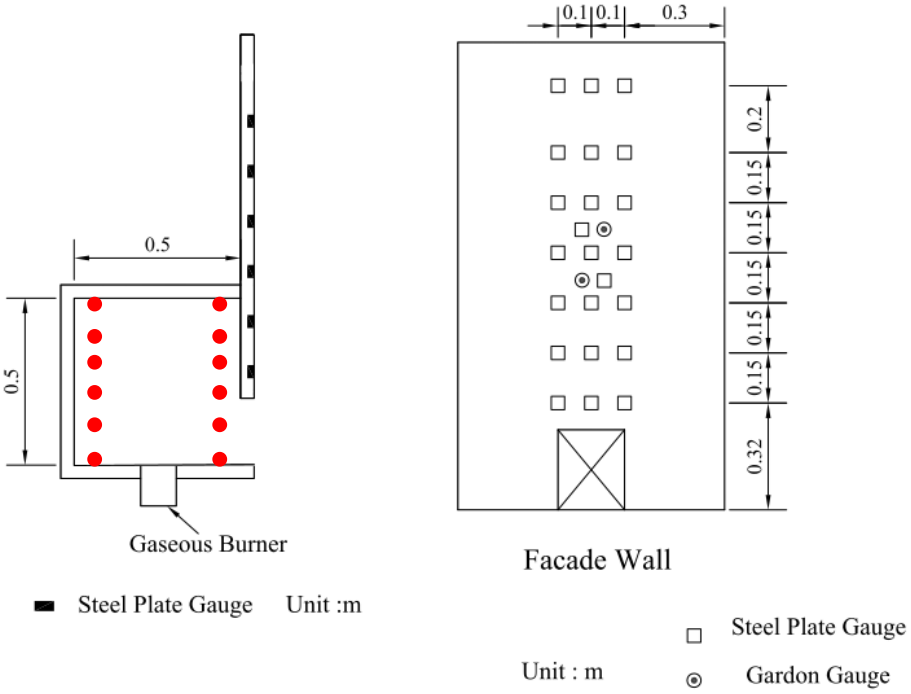

Figure 2: Left: the sketch of the experimental set-up, cross section cubic scale model.
Right: the front view of the facade wall with their instrumentation (Lee Y. , et al., 2007).

During the test several different variables were measured to investigate when external flames occur. The different variables measured in the cubic scale model which are needed for the validation study, are briefly described below. All variables were measured during the 20 minutes after the ignition stage. In appendix I a detailed description about the measurement procedure is given.

The following variables were measured:

- The heat release rate (HRR) inside the cubic scale model;
- The gas temperatures inside the cubic scale model (front and back corner);
- The flame height of external flames;
- The neutral plane height;
- The façade heat fluxes.

Below all measured variables which will be used for the validation study are presented. The actual HRR inside the cubic scale model and the theoretical HRR of the propane burner during the 20 minutes are shown in Figure 3. The results of the measured gas temperature distribution are given in Figure 4. The results of the flame height are given in Figure 5 and the results of the measured façade heat flux are given in Figure 6.

Heat release rate (HRR)

To mimic a real fire scenario where the gas temperature increases with time and can reach a quasi-steady state for fully developed fire conditions, the flow rate of the propane burner was increased by small steps of 1 minute until the designed steady maximum value was reached (theoretical HRR). Therefore the theoretical HRR shows a stepped line progression. The measured HRR inside the scale model (actual HRR) will increase by increasing the flow rate of the propane burner until a fully-developed enclosure fire was reached. In Figure 3 the history of the theoretical HRR (pink line) and the actual HRR (dark blue line) are given. The results show that the theoretical and actual HRR are the same before the intermediate plateau was reached. Before the plateau period was reached the flames exists only inside the cubic scale model. After approximately 8 minutes of ignition external flames will appear outside the cubic scale model and the actual HRR inside the cubic scale model equals 26.8 kW. After approximately 12 minutes the measured actual HRR inside the cubic scale model increases to the theoretical HRR (Figure 3) because of combustion inside the scale model. This means that only between approximately 8 and 12 minutes external flames appear. Thus after approximately 12 minutes there were no external flames.

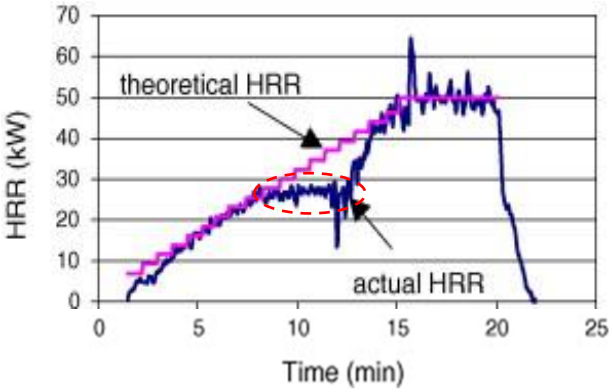

Figure 3: Theoretical and actual heat release rate history for the experiment having 0.2 m x 0.2 m opening. The intermediate plateau (red circle) indicates the heat released inside the cubic scale model (Lee, Delichatsios, & Silcock, 2007).

A lot of experiments have shown that the intermediate plateau in the actual HRR inside the cubic scale model can be determined by the inflow through the opening. It concerns the equation $1500\ A\sqrt{H}$, where A and H are the area and height of the opening expressed in meters. This equation was derived by multiplying the mass flow of air into the scale model ($0.5\ A\sqrt{H}$) by the heat of combustion per unit mass of air (3000 kJ/kg) which was completely consumed inside the scale model. The mass flow rate through the opening into the cubic scale model depends only on the opening size (Tang, Hu, Delichatsios, Lu, & Zhu, 2011). The measured inflow rate through the opening should be 0.00894 kg/s for this specific opening geometry.

Gas temperature

The measured gas temperature distribution at different heights inside the cubic scale model is shown in Figure 4. The gas temperature distribution is measured at the front and back corner inside the cubic scale model. Only the results of the gas temperature distribution at the front corner were shown. The results of the gas temperature distribution at the back corner were not shown in the publications.

The results of the gas temperature inside the scale model show a quite uniform gas temperature distribution from floor level to ceiling.

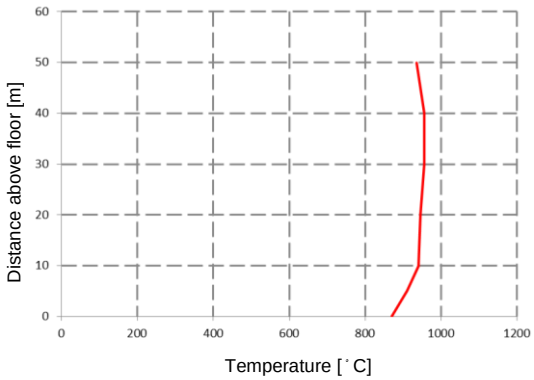

Figure 4: Vertical temperature distribution measured by the front corner thermocouple tree for the cubic fiberboard scale model (0.5 m x 0.5 m x 0.5 m) having opening size 0.2 m x 0.2 m with a propane burner (Lee, Delichatsios, & Silcock, 2007).

Flame heights and neutral plane

The flame height outside the cubic scale model, which was measured by using a CCD camera, is 0.59 m from the neutral plane and 0.67 m from the floor level. The height of the neutral plane under ventilation-controlled fire conditions was located at an approximated distance of 0.4H from the bottom of the opening (H stands for the total opening height). This equation was determined by a range of experiments which showed the same factor for the neutral plane from floor level. The calculated neutral plane is 0.08 m from floor level for this specific opening geometry.

Figure 5 shows the results of the flame height for propane external flames plotted against the theoretical HRR from the burner. The results of the mean flame height 50% at 50 kW propane fire for model 2A will be used for the validation study (chapter 7). The results for the external flame height are chosen for model 2A because all significant experimental results which were given by the scientific article, are shown for the cubic scale model with an opening of 0.2 m x 0.2 m.

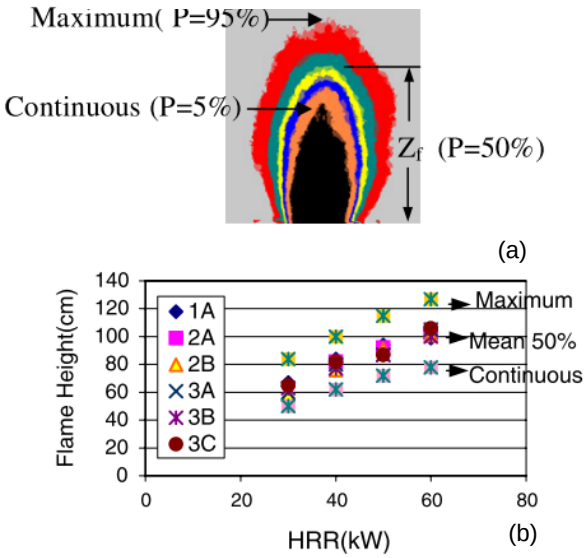

Figure 5: (a) A vertical cross section of the external flame with the probabilities. (b) The measured maximum, mean and minimum flame heights at different theoretical HRR. P represents the flame probability at 95%, 50% and 5% of the time (Lee, Delichatsios, & Silcock, 2007).

Three flame heights are shown in Figure 5: the 50% flame height, the minimum (solid flames) 5% presence of time and the maximum height 95% available. The flame height 50% means that this flame height appears 50% of the time. The results in Figure 5 shows that by increasing the theoretical HRR in the cubic scale model the maximum, minimum and mean flame height will increase as well.

Façade heat flux

Only the results of the measured heat flux along the centerline above the opening were publicized. Figure 6 shows the measured heat flux distribution along the centerline above the opening on the façade wall against the value of Z/Z_f for the experiment having an opening of 0.2 m x 0.2 m. Z and Z_f are the locations of the steel plate gauge (Figure 2) and the measured flame height (0.59 m). Both of them were measured from the position of the neutral plane which is 0.08 m (0.4H) above floor level. The measured heat flux at the façade decreases when the distance from the opening increases. This is because when the distance from the fire source increases the temperature and thus the heat flux will decrease. Because the results of the measured off-center heat flux distributions were not presented by the publications the heat flux at different heights along the centerline above the opening will be used for the validation study.

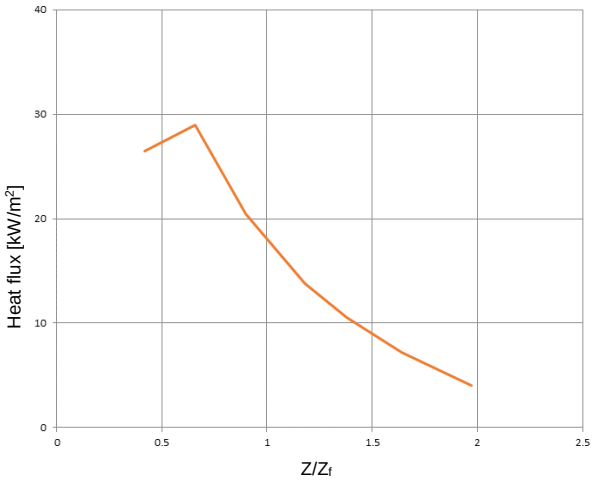

Figure 6: Heat flux distribution along the centreline above the opening (0.2 m x 0.2 m) on the facade wall (Lee Y. , et al., 2007).

2.3 Numerical study

In 2015 the cubic scale model with external flames was validated (Zhao, Beji, & Merci, 2015) by using the CFD simulation software package FDS 6.0.1 (Fire Dynamics Simulator) from NIST (National Institute of Standards and Technology). The CFD model with external flames was simulated with 4 cm, 2 cm and 1 cm grid cell size. The CFD results of the average temperature and horizontal air velocity at different heights along the opening during external flaming showed similar results by using 2 cm or 1 cm grid cell size. According to the grid sensitivity analyses it was concluded that using 2 cm grid cell size shows accurate CFD results compared to the experimental results. The simulation results by using 2 cm grid cell size were compared to the empirical correlation of the experimental results for the actual HRR, mass inflow rate and the neutral plane height.

The result of the actual HRR inside the simulated scale model however showed a deviation of 25% with the experiments. This resulted in a new empirical correlation that fits the simulated actual HRR ($1131\ A\sqrt{H}$) and differs from the correlation based on the experiments. The simulated mass inflow rate showed a deviation of 18% with the experimental results, resulting in a new empirical correlation for predicting the mass inflow rate through the opening during external flaming of $0.41\ A\sqrt{H}$. The simulated neutral plane height showed similar results as the empirical correlation of 0.4H from the experiments. Two methods, namely a temperature based method and a volumetric heat release rate based method were employed to define the flame height from the simulation results. The external flame height was over-predicted by these methods which were in line with the presumed under-prediction of the heat release rate inside the model and the mass flow rate through the opening. If the actual HRR and the mass inflow were under-predicted then there was relatively more excess fuel which leads to combustion outside the model. The flame height calculated with the time-averaged temperature distribution shows the lowest deviation with the experimental results (18%) (Zhao, Beji, & Merci, 2015).

In appendix II this numerical CFD research is reviewed. Through a lack of information it is difficult to judge if these results are suitable for predicting the external flames in ventilation-controlled fires. Therefore a new CFD validation study with a grid sensitivity analyses should be performed to investigate the behaviour of external flaming. The validated CFD scale model with external flames is used as reference model for the sensitivity analyses of several building and fire parameters.

3. Methodology

3.1 Numerical simulation of compartment fires

The use of computer based fire simulations has been developed over the year's in corporation with an increased computer performance. Fire simulations are increasingly used for improvements in fire protection and fire safety engineering to reduce and prevent fire victims in the building environment.
The risk of fire spread to other floors through external openings can be reduced by using CFD (Computational Fluid Dynamics) simulations with external flames. The risk of fire spread can be accurately solved by the used calculation method. Before using CFD simulations it is necessary to validate the used model with experimental results to investigate the accuracy of the used CFD simulation software package. The experiments should be similar to the investigated fire scenario (ventilation-controlled fire).

In general, there are two calculations methods to simulate fire inside fire compartments. The first fire simulation approach was the zone models (two-zone models) which consist of simplified plume models (Heskestad, Mccaffrey and Thomas). Two-zone models result in relatively low computer power requirements (Karlsson & G.Quintiere, 2000). The idea of two zone models is that a fire compartment consists of two zones, one hot upper layer and one cold lower layer (Figure 7). The gas temperature inside the enclosure is homogeneous at the upper and lower layer.
The more complex approach to simulate compartment fires is using CFD simulations. CFD is used in different areas but within the field of fire safety, smoke filling of enclosures is one of the most frequent used applications. Both are used for research and analytical fire safety design in buildings. Fire safety design consultants are frequent users of CFD-codes for smoke filling of enclosures. Therefore CFD is often used for the verification of analytical solutions for a buildings fire safety design.

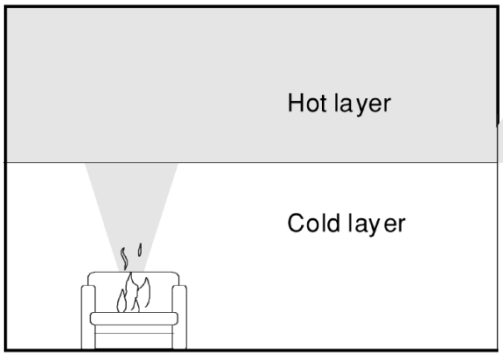

*Figure 7: Two-zone modelling of a fire in an enclosure (Karlsson & G.*Quintiere*, 2000).*

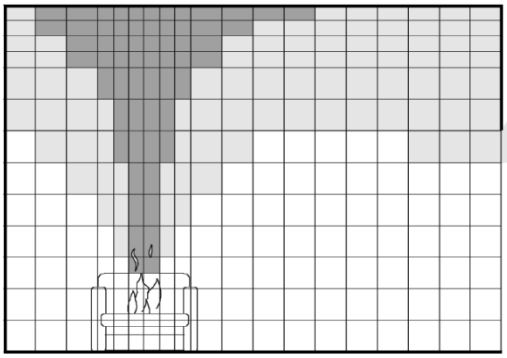

Figure 8: Computational fluid dynamics models divide the enclosure into large number of sub-volumes (Karlsson & G.Quintiere, 2000).

CFD simulations consist of three different approaches that can be used to simulate external flaming in reality. One of the disadvantages of using CFD models is the computational power which is needed. It is much higher than using the two-zone model calculation method. Previously, CFD modelling was mainly a tool in research projects. Traditionally the LES/DNS -type of CFD has been more applied to estimate the fire and smoke development in the building environment. This is due to the fact that increasing computer power now allows transient fire behaviour to be modelled by using CFD (Lönnermark & Björklund, 2008).

3.1.1 What is CFD?

Computational Fluid Dynamics is a method to numerically solve the governing equations of fluid dynamics. The solved equations are the set of Navier-Stokes equations governing continuity and conservation of energy, mass, velocity and species. The reason why the equations are solved numerically is that no analytical solution exists for the full Navier-Stokes equations.
In CFD programs a calculation domain is specified and divided into grid cells. It is in these cells that the conservation equations are solved (Figure 8). There are different kinds of approaches for solving the equations. The most common are DNS, LES and RANS as described below.

DNS

DNS stands for Direct Numerical Solution and is as the name implies a direct way to numerically solve the transport equations. This method solves the exact Navier-Stokes equations completely. All vortices or eddies are solved and nothing will be predicted. Because of the accuracy of this calculation method it is very time consuming and huge computational resources are needed. By decreasing the grid size a DNS turbulence prediction method can be achieved (Figure 10)

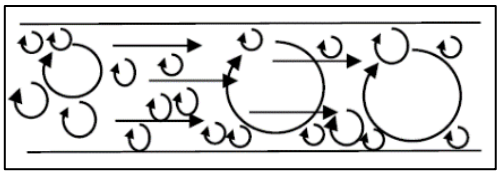

Figure 10: Direct Numerical Solution (DNS).

LES

Large Eddy Simulation (LES) is another turbulent flow prediction method which solves the filtered Navier-Stokes equations. This means small turbulent eddies (smaller than the used grid cell) will be predicted (not calculated). Only large eddies are solved (Figure 9). The LES calculation method is less computationally demanding compared to the DNS. If the grid is set fine enough LES converts to a DNS. Predictions of turbulence effects in the flow pattern are time dependent; therefore the time step is a limitation because every calculation result is based on the previous time step (Lönnermark & Björklund, 2008).

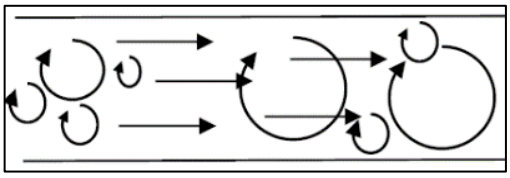

Figure 9: Large Eddy Simulation (LES).

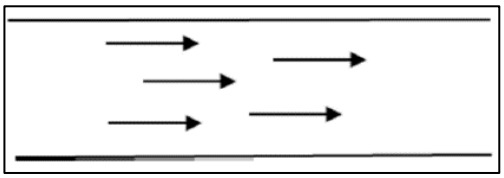

Figure 11: Reynolds Averaged Navier-Stokes (RANS).

RANS

The approach of RANS (Reynolds Averaged Navier-Stokes) is to decompose instantaneous values to a mean value with fluctuations (Figure 11). The RANS method is often used for steady state simulations because the solutions are independent of what has happened earlier (in time) in the simulation. Herewith it is the fastest and most inaccurate turbulent flow prediction method. Only the mean flow is solved, all eddies are predicted. The RANS turbulent flow prediction method is not useful for predicting the fire behavior in fire compartments.

<u>Application</u>

The CFD simulation software package which is used to simulate fire turbulence flow pattern predictions is FDS (Fire Dynamics Simulation). FDS is the first widely spread CFD code on transient fire driven flow. The program is developed by NIST, the National Institute of Standards and Technology (U.S. Department of Commerce). FDS is a dos-program and any visualization must be done in another (post-processing) program, in most cases the program Smokeview is used. FDS uses the LES and DNS turbulent flow prediction method. The Navier-Stokes equations will be solved for each cell size; therefore the simulation results are very dependent on the used grid cell size.

3.1.2 Verification and Validation

Verification is defined as the process of determining that a model implementation accurately represents the developer's conceptual description of the model and the solution to the model. Verification assessment examines if the computational models are the correct implementation of the conceptual models and if the resulting code can be properly used for an analyses. The strategy is to identify and quantify the errors in the model implementation and the solution. The two aspects of verification are the verification of a code and the verification of a calculation. Verification of a code involves error evaluation, which is looking for bugs, incorrect implementations of conceptual models, errors in input and other errors in the code and usage. Verification of a calculation involves error estimation, which is determining the accuracy of a single calculation and putting an error band on the final value (Slater J. W., Varification Assessment, 2008).
The verification of the used CFD simulation software package is done based on the technical reference guide of verification which is created by the NIST (McGrattan, et al., 2016). In this research it is assumed that CFD software package FDS 6.5.2 is already verified by the software developers.

Validation is defined as the process of determining the degree to which a model is an accurate representation of the real world from the perspective of the intended uses of the model. With other words solving the right equations in the right situation. One can only validate the code for a specific range of applications for which there is experimental data (Slater J. W., Validation Assesment, 2008). In other words word, validation of a model checks the results for a good representation of the reality.

In this research a CFD fire simulation model will be validated with experimental results from literature. A deviation between the fire simulation results and the reality will be shown. Not only CFD simulations have uncertainties and errors but experimental date as well. In comparing the CFD simulation results to experimental data one should discuss the experimental errors (Lönnermark & Björklund, 2008).

3.1.3 Uncertainty and Errors

This paragraph provides a classification of uncertainties and errors that are caused by CFD simulation results to differ from the true or exact values (Slater J. W., 2008). This is not only important for CFD simulations but all other computer simulation packages with use of grid and flow visualizers. In the validation the terms error and uncertainty are frequently used and the difference needs to be clarified.

Uncertainty

A potential deficiency in any phase or activity of the modeling process that is due to the lack of knowledge.

Error

A recognizable deficiency in any phase or activity of the modelling process that is due to the lack of knowledge (Data error, modelling error, implementation error, precision, absolute and relative errors, round-off error, truncation error and looping).

3.2 FDS combustion model

As mentioned previously, FDS uses sub-grid models to model phenomena which cannot be resolved by the largest eddy (grid cell). Herewith this tool is suitable for predicting the spread of heat and smoke in complex enclosures and generally predicting the 'far-field' conditions (i.e. conditions far from the flame region, like external flames). A default combustion model assumes a single step reaction with predestined products that occur infinitely fast. The combustion model is based on a mixed controlled model. Mixed controlled means that when fuel gases and oxygen mix they are immediately and completely burned. This is a good approximation for well-ventilated fires but a poor approximation for under-ventilated fires. For under-ventilated fires the HRR will be too high and burning will take place until the oxygen concentration inside is not enough to burn all HRR. To account for this, FDS uses a

simple empirical expression that describes whether or not the mix of fuel vapor and oxygen is allowed to burn (Lönnermark & Björklund, 2008).

Therefore a new extinction model is used in all simulation models. Different research shows that using this new extinction model shows a good agreement by FDS with the combustion in reality (Vidal, Wong, Rogers, & Mannan, 2005), (Vaari, Dloyd, & Mcdermott, 2011), (Quintiere & Rangwala, 2004). Figure 12 shows a graph of the flame gas temperature (x-axis) and the minimal needed oxygen concentration (y-axis) inside the enclosure. This graph shows when combustion inside a fire compartment occurs. This means that combustion will occur if the temperature lower flammability limit (LFL) and specific oxygen concentration is reached inside the enclosure. For example if the flame temperature is approximately 1700 K this means that combustion occurs until the oxygen concentration inside the enclosure is 0%. If the flame temperature is below 1700 K a higher oxygen concentration is needed for the ignition. In FDS the critical adiabatic flame temperature (CAFT) should be given, the limited oxygen concentration will then be automatically calculated based on the correlation in Figure 12. A flame temperature of 1700 K will be used for all CFD simulation models with external flames because the combustion in reality will always develop until the oxygen concentration is 0%. In most fire compartments the oxygen supply is not dependent on the inflow through external openings but through small air leaks. So there is always enough oxygen inside for the fire development although a limited amount.

Although this new flame extinction model shows a good prediction of the flame combustion model, it also has some disadvantages. The most important drawback is its grid dependence. The temperature of the flame is very dependent on the grid resolution. A fine mesh results in an increased flame temperature, because the flame is better modelled and more Navier-Stokes equations are solved per area. Using a course mesh means that the fire may early extinguish in time because of the minimal needed oxygen. The consequence is that in the simulation the fire will extinguish earlier while in reality it will burn further. Using a finer mesh (DNS) increases the calculation time, but will be more accurate.

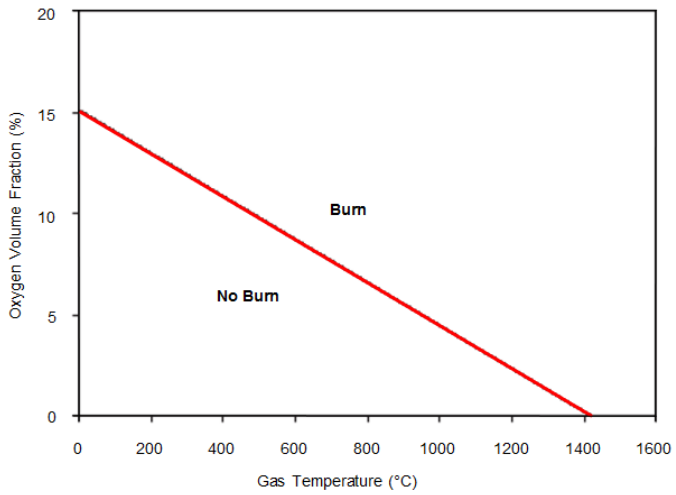

Figure 12: The correlation when fire will occur (Lönnermark & Björklund, 2008).

3.3 Validation study

This paragraph contains a new validation study of the cubic scale model with external flames. The simulated results will be compared with the experimental results as well (Lee Y. , et al., 2007), (Lee, Delichatsios, & Silcock, 2007), (Lee, Delichatsios, & Silcock, 2008), (Unkleja, Delichatsios, Delichatsios, & Lee, 2008). The CFD model with external flames from University of Ghent is in this paragraph further adapted and used for an own validation study by using FDS 6.5.2. In this research it is assumed that the simulation results calculated with FDS 6.0.1 are similar to the simulation results simulated with FDS 6.5.2. To determine which grid cell size shows a lower deviation with the experimental results the

simulation results of using 2 grid cell size and 1 cm grid cell size are compared with the measurements (paragraph 2.2).

The aim of this validation is to study how a CFD software package (in this case FDS 6.5.2 and SMV 6.3.12) deals with external flames of ventilation-controlled compartment fire scenarios. Therefore, the CFD simulation model with external flames will be compared with measurements.

3.3.1 Simulation model

The simulated CFD model should corresponds to the experimental set-up (Lee Y. , et al., 2007), (Lee, Delichatsios, & Silcock, 2007), (Lee, Delichatsios, & Silcock, 2008). The simulated CFD model consists of the dimensions of 0.5 m x 0.5 m x 0.5 m with one opening. The external opening is 0.2 m wide by 0.2 m height. All external walls consist of fiberboard plates. The following material properties of the fiberboard plates were assumed: density of 350 kg/m^3, thermal conductivity of 0.3 W/m.K, emissivity 0.9 and a heat capacity of 1700 J/kg.K (Zhao, Beji, & Merci, 2015). In Figure 13 a schematic overview of the simulated model is given. At the middle of the model a 0.1 m x 0.2 m propane burner with a maximum HRR of 50 kW is modelled (Figure 14). The actual HRR inside the model should depends on the oxygen concentration which enters through the opening, to create a ventilation-controlled fire scenario.

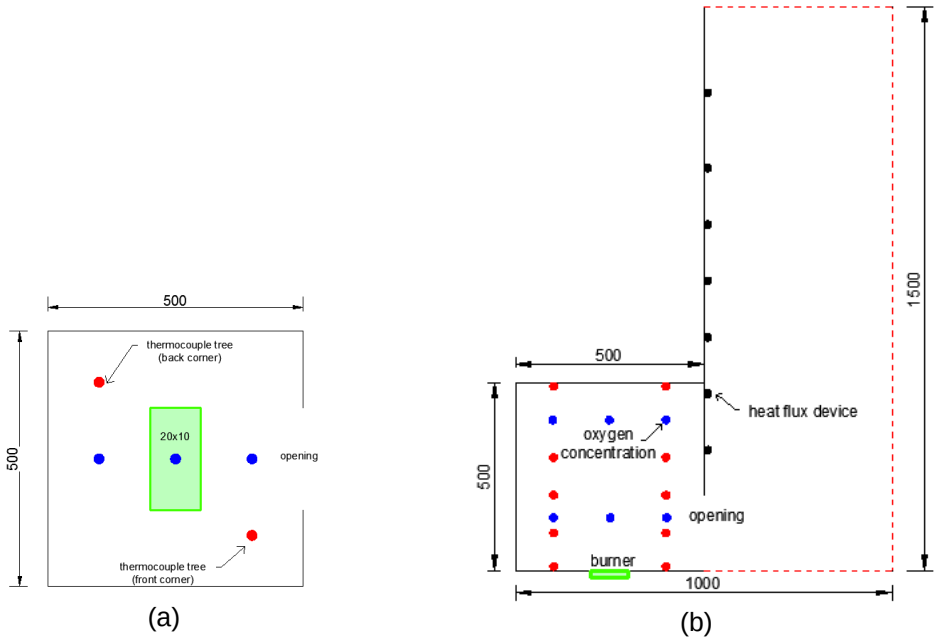

Figure 13: Sketch of the experimental set-up and location measurement devices (temperature, oxygen concentration and heat flux). (a) Top view of the enclosure. (b) Side view of the enclosure.

The simulated CFD model is divided in two domains (Figure 15). In Figure 15 grid cells in the x, y and z direction are given. Two mesh domains are used to exclude the flow pattern from behind the upper floor façade. Domain 1 covers the inside of the model and the lower part of the outside and domain 2 covers the upper part of the outside. The computational domain has been extended by 0.5 m outside the model. The 0.5 m outside domain is modelled in order to limit the influences of the 'open' boundary condition on the external flame, see Figure 16. Because in this research the external flames are simulated as result of the ventilation-controlled fire inside the model, both mesh

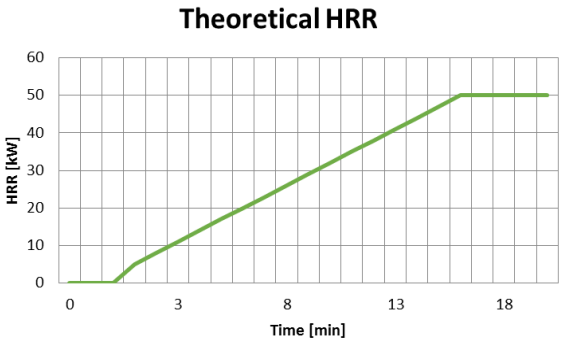

Figure 14: Theoretical HRR of the propane burner obtained from experimental research (Lee, Delichatsios, & Silcock, 2007).

domains have similar grid cell size. Both mesh domains have the same grid cell size in order to increase the accuracy of the simulation results between different grid cell sizes. Using a coarse grid cell for the fire inside and a finer grid cell for the outside domain this will affect the external flaming as well. This can over-predict or under-predict the external flaming duo to the fineness grid cell size inside the model. The obstructions in the simulated model are made of at least one grid cell thick.

From the literature study it can be concluded that CFD simulation results are sensitive to the grid cell size because of the used extinction model which depends on the critical flame temperature (T_{LFL}), see paragraph 3.2. A smaller grid cell size is generally preferred for more accurate simulation results. In a finer grid cell size the Navier-Stokes equations will be solved for every small volume. One of the important disadvantages of increasing the grid cells is the increased calculation time. For this reason using fine grid cell size in simulations will be avoided.

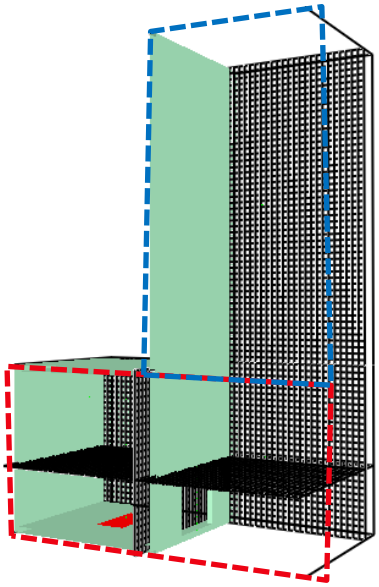

Figure 15: FDS fire enclosure model with grid cells in the x, y and z direction. Red: domain 1. Blue: domain 2.

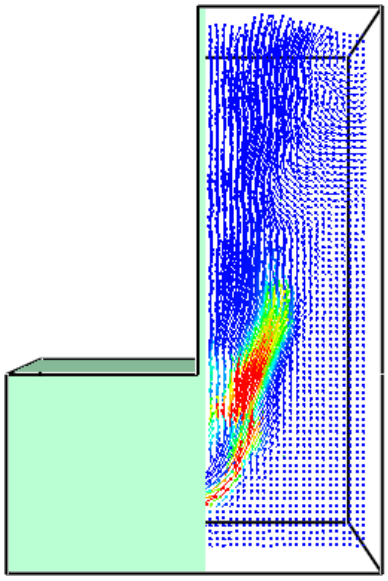

Figure 16: An example of the flow field in the 'open' boundary outside the fire enclosure when external flaming occurs.

From a previous validation study (Zhao, Beji, & Merci, 2015) it can be concluded that using 2 cm grid cell size and lower provides the most accurate simulation results. For that reason in this research 2 cm grid cell size will be used to validate the simulation results. To investigate which grid cell size is needed for an acceptable accurate CFD simulation results a grid sensitivity analyses is performed. Therefore besides validating the simulation results of 2 cm grid cell size simulation results of 1 cm grid cell size will be validated as well. Based on the deviation with the experimental results the grid cell size with accurate results will be determined.

Only two different grid cell sizes are simulated because of the increased computing time. The computing time of using 2 cm grid cell size takes approximately 4 days in total while simulating the cubic scale model by 1 cm grid cell size takes approximately 32 days of computing time. Off course, the computing time depends on the computer performance (Used PC: Intel Xeon CPU E5-2650 v2 @ 2.6 Ghz, 5.98 GB RAM).

3.3.2 Simulation variables

All mentioned measured variables (paragraph 2.2) are simulated by a CFD model and validated with experimental measurements (Lee Y. , et al., 2007), (Lee, Delichatsios, & Silcock, 2007), (Lee, Delichatsios, & Silcock, 2008). A lot of measurement devices are simulated to compare simulation results with the experimental results. Below all simulated measurement variables are given:

- The actual HRR inside the model;
- The mass in- and outflow rate;
- The oxygen concentration inside the model;
- The gas temperature inside the model (front corner);
- The air velocity (opening);
- The gas temperature (opening);
- The façade heat flux;
- The external flame height.

3.3.3 Boundary conditions and settings

The turbulence model is based on Large Eddy Simulation (LES). The used extinction model is based on a critical flame temperature value (T_{LFL}). Extinction model 2 is used instead of the FDS default extinction model. As mentioned in paragraph 3.2 the extinction model influences the combustion model of the simulated fire source. If the simulated gas temperature of the flame drops below the given critical flame temperature (T_{LFL}), combustion of fire will extinguish (Figure 12). The fire development inside the model depends on the critical flame temperature of the fire. If the critical flame temperature is below 1700 K the oxygen concentration inside the model will not decrease to zero oxygen concentration inside.

To simulate a ventilation-controlled fire with external flames the oxygen concentration inside the model should be zero when external flaming occurs. Using a critical flame temperature below 1700 K external flames will occur earlier than a higher fixed critical flame temperature, because the limited oxygen concentration inside the model will be reached earlier. In other words combustion inside the model is influenced by the oxygen concentration inside the model which is needed for the combustion under certain conditions. A critical flame temperature of 1700 K has been used in this validation study (McGrattan k. , et al., Fire dynamics simulator user's guide , 2016). The simulated fire inside the CFD model becomes ventilation-controlled when the oxygen concentration becomes zero.

A radiative fraction of 0.35 for propane fire is prescribed as a lower bound in order to limit the uncertainties in the radiation calculation which is induced by uncertainties in the temperature field (McGrattan k. , et al., Fire dynamics simulator user's guide , 2016). Heat losses to the walls are calculated by solving the 1-D Fourier's equation for conduction. For the validation study the default soot yield value of 0.01 kg soot/kg fuel of propane is used. The soot yield is a parameter which influences the amount of unburned gases during combustion process. This value represents an average value of outside combustion as well (McGrattan k. , et al., Fire dynamics simulator technical reference guide Volume 1: Mathematical model , 2016).

Actual HRR

The actual HRR inside the simulated model has been determined by integrating the HRR of the inside volume ("HRR") included the façades. To compare if the theoretical HRR equals the total HRR of all domains together ($Q_{in}=Q_{out}$) the HRR at different domains is simulated by FDS during 20 minutes. In theory there will be no energy loss between the different mesh domains. The simulated total HRR on the model will be automatically generated by FDS 6.5.2 and saved in the CHID_hrr.csv file. Each column represents the time history of the different integrals (see, equation (1)).

$$\text{Q\_ENTH} = \text{Q\_CONV} + \text{Q\_COND} + \text{Q\_DIFF} + \text{Q\_RADI} + \text{HRR} + \text{Q\_PRES} + \text{Q\_PART} \quad \text{[kW]} \quad (1)$$

In this research the average actual HRR inside the model during external flaming simulated with both grid cell sizes will be compared with the empirical correlation which is determined from several measurements ($1500\ A\sqrt{H}$).

Mass in- and outflow

The mass inflow and outflow rate through the opening is fixed by two simulation variables at doorway level (opening surface) called “MASS FLOW -” and “MASS FLOW +”. These two devices calculate the positive mass flow rate and the negative mass flow rate which stands for the inflow and outflow of air through the opening. The results of the mass flow device are calculated conform equation (2).

$$\dot{m} = \int \rho u \,.\, dS \qquad \text{[kg/s]} \quad (2)$$

In this research the simulated average mass inflow rate through the opening during external flaming will be validated with the measured mass inflow rate ($0.5\ A\sqrt{H}$). The average mass outflow rate during external flaming will be not validated.

Oxygen concentration

To investigate when a ventilation-controlled fire in an enclosure with openings occurs the oxygen concentration at different heights is simulated. The oxygen concentration (“oxygen”) inside the simulated model is determined at 6 different positions (X= -0.25 m, -0.40 m and -0.1 m, Z= 0.14 m and 0.40 m), see Figure 13 (blue dots).

Gas temperature

The gas temperature (“THERMOCOUPLE”) inside the simulated model is determined at 10 cm from the front corner at 7 different heights from the floor level (Z= 0.01, 0.05, 0.10, 0.20, 0.30, 0.40, 0.49 m), see Figure 13 (red dots). In FDS 6.5.2 are two different devices which can be used to calculate the gas temperature: “THERMOCOUPLE” and “TEMPERATURE” simulation device. The temperature device is to simulate the gas temperature but the quantity thermocouple is the temperature of a modelled thermocouple. The temperature simulated by a thermocouple lags the true gas temperature by its bead size. A thermocouple quantity acts like a physical thermocouple bead which takes radiation losses and thermal lag as the bead heats up into account. Thermocouple devices should therefore be used by comparing FDS to experimental thermocouple devices. The result of the temperature and thermocouple device should shows at the end of the simulation the same simulated temperature. The difference between using a temperature or thermocouple device is the progress of the temperature before it stabilized. A thermocouple increases slowly to the temperature at the end of the simulation, this is partly due to the heat losses of the thermocouple.

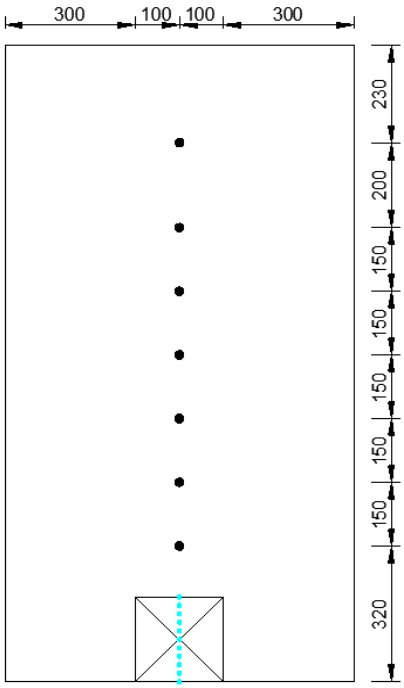

Figure 17: A sketch of the facade with heat flux (black dots), temperature, pressure and velocity (cyan dots) measurements.

A temperature simulation device (“TEMPERATURE”) is used to simulate the average gas temperature at the neutral plane height during external flaming. The simulated gas temperature at different heights (Z= 0.00, 0.02, 0.04, 0.06, 0.08, 0.10, 0.12, 0.14, 0.16, 0.18, 0.20 m) along the opening centerline will be simulated every 2 cm. A temperature device instead of a thermocouple device is used because the average gas temperature is not measured before and therefore it is not comparable with measurements.

Air velocity

To indicate the neutral plane height at the opening the average horizontal air velocity ("U-VELOCITY") at different heights is simulated (Z= 0.00, 0.02, 0.04, 0.06, 0.08, 0.10, 0.12, 0.14, 0.16, 0.18, 0.20 m). As mentioned before the neutral plane height is when there is no mass in- and outflow rate. This means that the average horizontal air velocity is zero at this height. Figure 17 shows in cyan the dots simulated at different positions through the opening. In this research the average horizontal air velocity is calculated during external flaming. Based on the average horizontal air velocity the neutral plane height is determined.

Façade heat flux

The actual HRR inside the scale model increases during the simulation time from the ignition phase until external flaming occurs. By increasing the actual HRR inside the scale model the gas temperature inside will increase. When external flaming occurs the gas temperature outside will increase as a result of the increased HRR inside the scale model. High gas temperatures outside mean that received radiation may influence ignition of surrounding materials. Thus calculating the heat flux on the façade depends on the emitted radiation by external flaming (Quintiere J. G., 2002). A high heat flux on the façade may ignite the exterior cladding of upper façades or opposite buildings. Ignition of the second item is possible if the material receives a heat flux higher than its critical flux for ignition. For remote (at distance) ignition under auto ignition conditions, direct flame heating is small or zero. So the critical compartment temperature needs to be greater than or equal to the auto ignition temperature (approximately 400-600 ˚C). The auto ignition temperature of the cladding depends on the material properties. A material which is less resistance to high temperatures and heat flux may ignite at a lower temperature which will increase the risk of fire spread to other compartments via external openings. In general the heat flux at the façade increases by decreasing the distance to the fire source. Increasing the distance from the fire source results in a decreased façade heat flux. This means a lower façade heat flux prevents fire spread to upper floors. Therefore, the façade heat flux should be validated as well to investigate the deviation of the façade heat flux with the measurements.

In this research the façade heat flux caused by external flaming is simulated above the opening at different heights (Figure 17).The heat flux at the façade is calculated by FDS conform equation (3). The used heat flux simulation device is the "GAUGE HEAT FLUX". This heat flux device is designed to compare the measured heat flux from experiments. In total 7 heat flux devices are simulated and compared with the experimental results (Z= 0.32, 0.47, 0.62, 0.77, 0.92, 1.07 and 1.27 m).

$$\dot{q}''_{gauge} = \varepsilon_{gauge}\left(\dot{q}''_{inc,rad} - \sigma T^4_{gauge}\right) + h\,(T_{gas} - T_{gauge}) \qquad [kW/m^2] \quad (3)$$

The heat fluxes at the façade will be determined for only one grid cell size. This is due to the fact that external flames and thus the façade heat fluxes are influenced by the fire development inside the model. Therefore the grid sensitivity analyses is performed only for the actual HRR, mass inflow rate, gas temperature and the neutral plane height. The grid cell size with the lowest deviation with the measurement results (actual HRR, mass inflow rate, gas temperature and the neutral plane height) will be used to determine the deviation of the façade heat flux with the measurements.

External flame height

The mean flame height was visually measured by a CCD camera. The measured flame height appears 50% of the time. The validated model with external flames should be used to determine the flame height which exist 50% of the simulation time. In a previous validation study (Zhao, Beji, & Merci, 2015) the mean flame height is obtained only from the average temperature distribution. The standard deviation of the flame during external flaming is given in Figure 18. The flames show big differences from the average temperature distribution. The standard deviation shows which temperatures deviate from the mean temperature value. Figure 18 shows that the flame temperature deviates a lot from the mean temperature during external flaming. This means that averaged flame results do not represent the flame

height which appears 50% of the time. Therefore a new calculation method to determine the external flame height is investigated.

The relation between the flame visibility and flame temperature (and flame heat release) was investigated by experiments. Different researches show that the flame height of external flames can be determined by two different ways. From the temperature (°C) and the heat release rate per unit area (Mw/m³) a visible flame can be obtained (Heskestad, 1999) (Orloff & Ris, 1982) (Cox, 1995). Based on a minimum temperature and a minimum heat release the flame visibility was described. A visible flame is when the flame temperature decreases below 500 °C or the heat release rate decreases below 0.5 MW/m³ or 1.2 MW/m³. In fact increasing the flame temperature outside influences the flame HRR outside as well.

Therefore in this research the flame visibility is determined by only the simulated flame temperature distribution. So the flame height will be predicted when the flame is visible and the flame tip reaches a flame temperature of 500 °C. This temperature is almost the temperature of a blue flame.

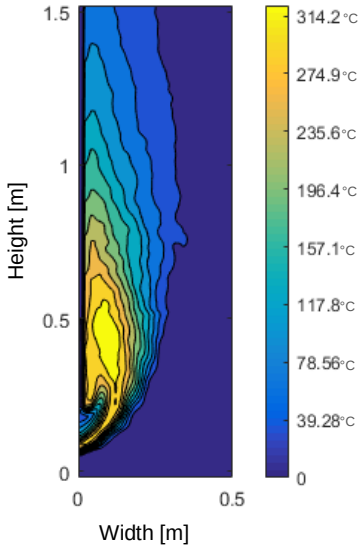

Figure 18: The flame standard deviation during external flaming. Big flame fluctuations are shown outside the model.

Two calculation methods are designed to calculate and validate the results with the experiments (appendix II). Both calculation methods predict the mean flame height of external flames, see appendix III-a and appendix III-b. These calculation methods are based on the flame temperature distribution (y=0).To investigate the mean flame height like in the experiments the temperature distribution per second has been viewed in Matlab R2016b (appendix IV-a and appendix IV-b). External flames occur when there is a limited oxygen concentration inside the model. The flame temperature distribution is only used between 8 minutes and 20 minutes ($\Delta t = 720\ s$) to calculate the flame height which appears 50% of the time during external flaming.

To determine which flame height during 50% of the simulation time occurs, the results of the temperature are divided into a boxplot. A boxplot method is a simplified but very useful, representation of the distribution of the simulated temperature data outside the model. All results will be ranked from low to high. The median or also called the second quartile (Q2) is the value which separates the higher half of the data samples from the lower half samples. The median value shows that 50% of the samples are below the median and that 50% of the samples are above the median. In contrast to averaged values the median value is not influenced by extreme values like the maximum and minimum temperature differences (Hoffmann, 1981). The mean (averaged) value of the samples depends on how often the maximum and minimum data occurs. The mean value will increase when a lot of maximum values are recorded (for example the external flames at the end of the simulation time). The mean value will decrease when a lot of minimum values are recorded. This is one of the reasons why a median value is often used for understanding statistics instead of averages values.

The boxplot is a quick way of examining one or more sets of data graphically. Boxplots are particularly useful for comparing distributions between several groups or sets of data. The boxplot can be compared against the probability density function for a normal distribution which helps understanding the boxplot (Figure 19). To reproduce a boxplot only five values are needed: the minimum, the first quartile (Q1), the median (or second quartile Q2), the third quartile (Q3) and the maximum.

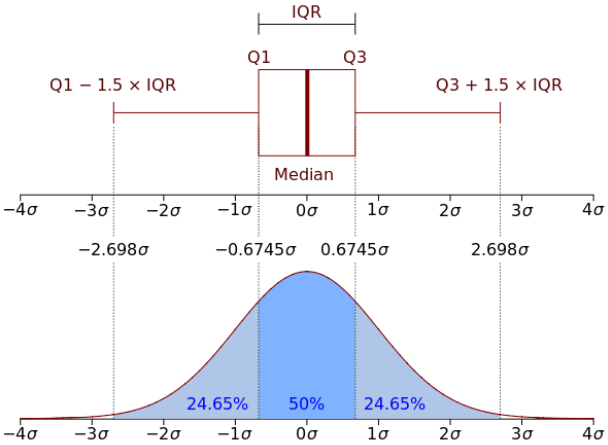

Figure 19: Boxplot and a probability density function of a normal distribution (Maggio, 2011).

The median is not enough to estimate the flame height which occurs 50% of the time. To determine the measured mean flame height the first quartile (Q1) and the third quartile (Q3) should be calculated. The median of the data set between the second quartile and the minimum value (lower half of the data set) is the first quartile (Q1). The median of the data set between the second quartile and the maximum value (upper half of the data set) is the third quartile (Q3). The mean of the data set between Q1 and Q3 shows the data set which occurs 50% of the time. The data set which has been put into increasing order is divided into four quartiles. Each part in the boxplot shows 25% of the data set. This means the data set from the first quartile until the third quartile shows 50% of the data set which exist 50% of the time. This data set eliminates the maximum and minimum values of the data. Both calculation methods are based on a ranked data set (boxplot). The results of both calculation methods will be compared with the experimental results. The best selected calculation method will be used to determine the external flame height which occurs 50% of the time.

The results of both calculation methods will be compared to the measured external flame height (paragraph 2.2). For the external flame height is one grid cell size used as well. Based on the gird sensitivity analyses the grid cell size with a lower deviation for the actual HRR, mass inflow rate, gas temperature and the neutral plane height with the measurements. This grid cell size will be used to investigate which calculation method shows a better agreement with the measured external flame height.

3.4 Sensitivity of building and fire parameters

A sensitivity analyses will be performed after the validation study of the CFD model with external flames in ventilation-controlled enclosure fires. A sensitivity analyses will investigate the influence of different parameters on the neutral plane height and the external flame height. The actual HRR inside the model and the mass inflow rate through the opening of different simulation models will be compared to the new empirical correlation of the validated CFD model. The results of the CFD simulation models will be absolute and relative compared to the results of the validated CFD model (reference model).

Three design parameters and one fire parameter will be adjusted from the validated CFD model with external flames. The validated CFD model simulated with 2 cm or 1 cm grid cell size is called the reference model for the comparison of the different sensitivity parameters (Figure 20):

- Simulation model 1: a window-like opening instead of a door-like model;
- Simulation model 2: narrowing the opening geometry;
- Simulation model 3: using adiabatic construction instead of fiberboard;
- Simulation model 4: increasing the fire release rate inside the model.

If changing different parameters in the validated CFD model shows similar deviation between a 2 cm and 1 cm grid cell size then a 2 cm grid cell size can be used to predict the influence on the neutral plane height and the external flame height. This can results in a decreased calculation time. Besides the influence on the neutral plane and the external flame height, the results of the actual HRR and the mass inflow rate of the different simulation models will be compared to the linear correlation of the reference model.

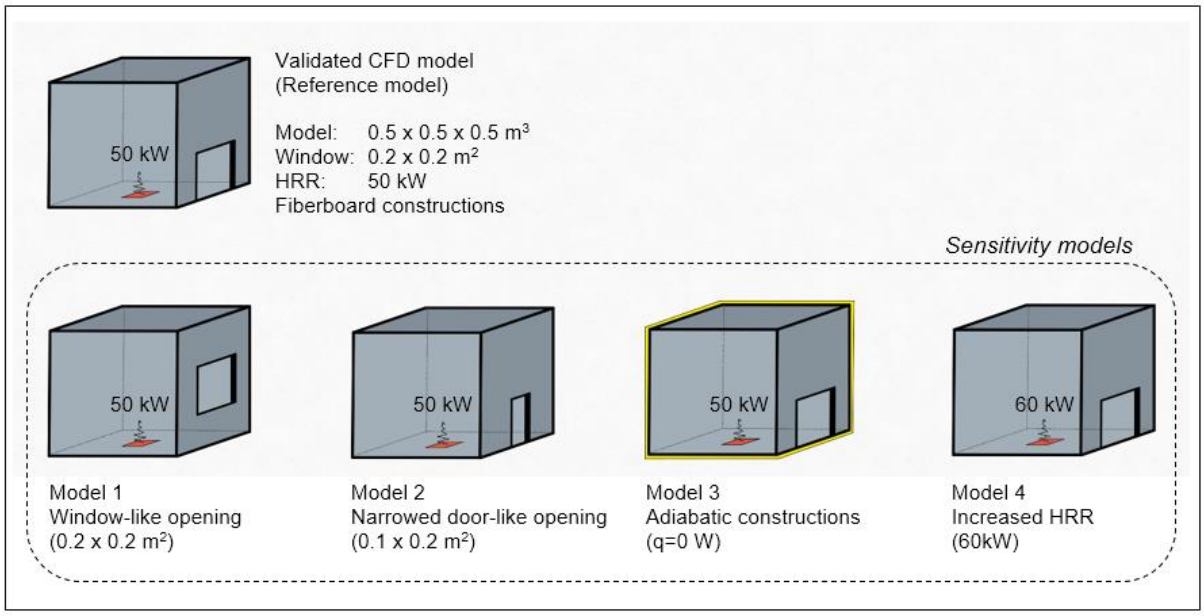

Figure 20: The reference model and the four simulation models for the sensitivity of different building and fire parameters.

From the literature study it can be concluded that shifting the opening from door-like opening to a window-like opening, using an adiabatic construction or increasing the fire release rate (burner) inside the model should all not affect the actual HRR inside the model during external flaming, because the actual HRR inside the model and the mass inflow rate through the opening are determined by the opening surface and the opening height. The actual HRR and the mass inflow rate during external flaming should always be similar to the validated actual HRR and the validated mass inflow rate. When the opening surface will be changed the actual HRR inside the model does not equal the validated actual HRR and the validated mass inflow rate. The actual HRR inside the model is expressed in terms of the empirical correlation $C.A\sqrt{H}$ which translates the actual HRR inside the model by the opening

height and the opening area. This means that the actual HRR inside the model depends on the opening geometry. If the actual HRR inside the model will not be affected unless the opening geometry will be changed, the mass inflow rate through the opening will not be influenced unless the opening geometry will be changed as well. For predicting the average mass inflow rate the empirical correlation of $C.A\sqrt{H}$ is used.

3.4.1 Simulation models

In this paragraph four simulation models will be explained. The reference model is a validated CFD model with external flames (paragraph 3.3). Based on the validation study the used grid cell size will be determined.

Simulation model 1: window-like model

In simulation model 1 the door-like opening is shifted to the middle of the front façade like a window opening. The opening size is remained like in the reference model (0.2 m x 0.2 m). Inside the model at the center a propane burner is placed with a theoretical HRR of a maximum fire release rate of 50 kW. All façades are designed from 0.02 m of fiberboard. Figure 21 shows simulation model 1 with a window-like opening.

Simulation model 2: narrowed opening model

In simulation model 2 the opening geometry of 0.2 m x 0.2 m which is used in the validation study is adjusted to 0.1 m x 0.2 m at the center of the front façade. The location of the door-like opening will be remained like in the validated CFD model. Inside the model at the center a propane burner is placed with a theoretical HRR of a maximum fire release rate of 50 kW. All façades are designed from 0.02 m of fiberboard. Figure 22 shows simulation model 2 with a door-like opening geometry of 0.1 m x 0.2 m.

Simulation model 3: adiabatic construction model

In simulation model 3 is the door-like opening geometry of 0.2 m x 0.2 m remained like the validated CFD model. Inside the model at the center a propane burner is placed with a theoretical HRR of a maximum fire release rate of 50 kW. All facades are adjusted from 0.02 m fiberboard to 0.02 m of adiabatic construction. Adiabatic construction are walls which do not allow heat to pass across the construction. An adiabatic construction is similar to an infinitely isolated wall. The actual HRR inside the model will be at maximum when the heat losses through the walls are very small.

Simulation model 4: increased theoretical HRR

In simulation model 4 the door-like opening of the reference model is remained. Inside the model at the center a propane burner is placed with a theoretical HRR of a maximum fire release rate of 60 kW instead of a maximum fire release rate of 50 kW, see Figure 24. Figure 25 shows the difference between the theoretical HRR as used in the reference model and the new theoretical HRR of simulation model 4 with a maximum of 60 kW.

The results of the all simulation models (Table 3.4.1.1) will be compared to the results of the reference model.

Table 3.4.1.1: All simulated variants.

Model name	simulation models				
	1	2	3	4	0
propane fire	√	√	√	√	√
fibreboard construction	√	√	-	√	√
door-like opening	-	√	√	√	√
window-like opening	√	-	-	-	-
narrowed opening	-	√	-	-	-
adiabatic construction	-	-	v	-	-
theoretical HRR (kW)	50	50	50	60	50

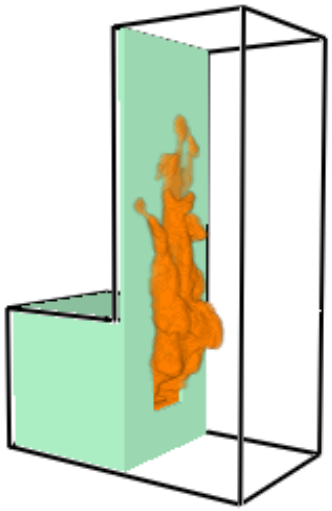

Figure 21: A screenshot of simulation model 1 with a window-like opening of 0.2 m x 0.2 m at the middle of the front façade.

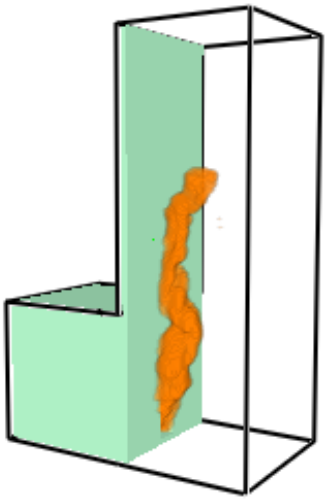

Figure 22: A screenshot of simulation model 2 with a door-like opening of 0.1 m x 0.2 m (narrowed opening geometry).

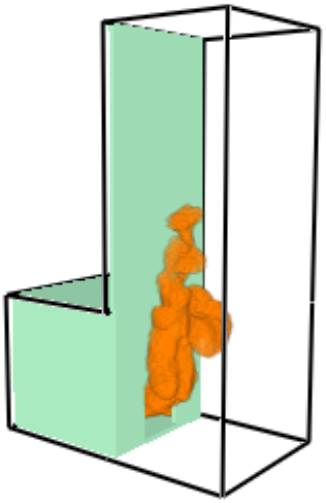

Figure 23: A screenshot of simulation model 3 with adiabatic construction instead of fibreboard construction.

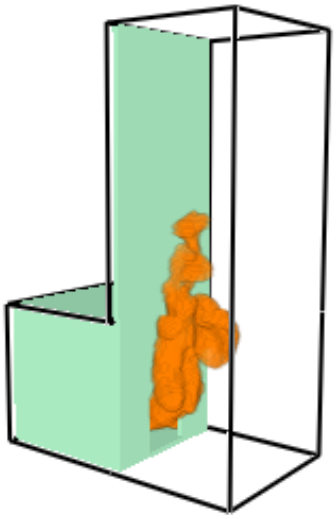

Figure 24: A screenshot of simulation model 4 with an increased theoretical HRR (60 kW).

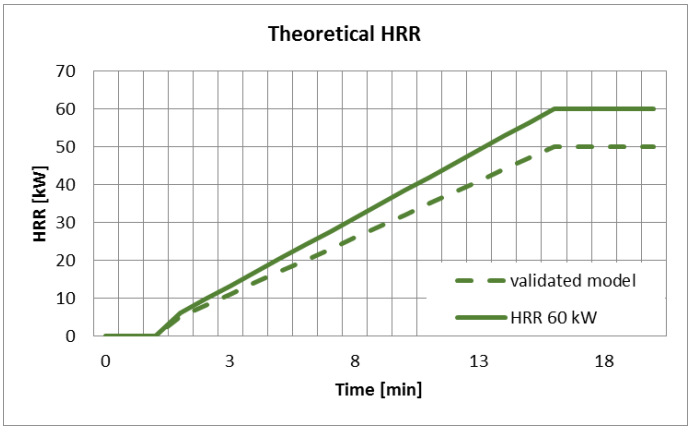

Figure 25: The dashed line shows the theoretical HRR which is used in the validation CFD study (50 kW). The continuous line shows the adjusted theoretical HRR (60 kW) of simulation model 4.

3.4.2 Simulation variables

All variables are simulated during 20 minutes from the ignition. Below all calculations are shown which are performed for each simulation model. These calculations are done to investigate the influence of the different parameters on the neutral plane height and the external flame height.

- The actual HRR inside and outside the model;
- The sum of the actual HRR of different areas;
- The mass inflow rate through the opening;
- The neutral plane height from floor level;
- The external flame height.

To investigate the influence of different parameters on the risk of fire spread to other floors, the validated simulation model is adjusted with different parameters and compared to the results of the validated CFD model. Two grid cell sizes are used (2 cm and 1 cm grid cell size) to investigate if using a 2 cm grid cell size shows for each different simulation model similar deviation as with 1 cm grid cell size.

Actual HRR

Each simulation model is divided in 3 different areas (inside / outside lower part / outside upper part). The average actual HRR calculated in each model will be compared to the average actual HRR of the reference model. The sum of all actual HRR at different areas should equal the theoretical HRR which is produced by the propane burner inside the model.

Mass inflow rate

The average mass inflow rate through the opening will be calculated during external flaming and will be compared with the average mass inflow rate of the reference model. The

Neutral plane

The neutral plane height is determined from the average horizontal air velocity at different heights at the opening centerline. Per height the average horizontal air velocity is calculated during external flaming. The neutral plane height is when the average horizontal air velocity becomes nearly zero, there is no in- and outflow of air.

Flame height

The external flame height which occurs 50% of the time will be determined by a new calculation method based on simulation results. The flame height is calculated based on the temperature distribution outside the model. The external flame height which occurs 50% of the time is determined from the temperature distribution between the data set from the first quartile (Q1) to the third quartile (Q3) (boxplot method).

3.5 Full-scale fire compartment

Modelling fire in fire compartments is mostly simplified through a CFD model with an opening in the façade for the inflow. And thus the oxygen concentration which is needed for the ignition process inside a fire compartment. Fire inside fire compartments does not depend on the inflow rate through the external opening during the ignition, because during the ignition stage the temperature inside the enclosure is not high enough to break the glass. At the ignition stage the fire will develop through the available oxygen concentration inside the compartment. Other flows like the air supply and small cracks inside the enclosure provides enough oxygen concentration for the fire ignition. When external flames occur these mass flows are too small and that is why they are ignored in this research. Because the fire inside the compartment depends on the big mass flow differences through the external opening. Fire inside the enclosure will develop during the flashover stage to a fully-developed stage when there is more oxygen involved (e.g. via the external openings). Because external flames occur when the fire

inside is well developed (after flashover stage) and thus high temperatures occur inside the fire compartments, the CFD models are modelled when the glass is already broken.

A drawback of using CFD simulations is the long calculation time. For a cubic scale model with external flames 32 days for the calculation time are needed (Intel Xeon CPU E5-2650 v2 @ 2.6 Ghz, 5.98 GB RAM). This will be a limitation for modelling a real fire compartments. Modelling a full-scale model will increase the amount of grid cells by using 2 cm or 1 cm grid cell size. If it is possible to simulate a real fire compartment with a lower amount of grid cells, then the calculation time will decrease by increasing the grid cell size. To investigate if a lower amount of grid cells can be used for modelling a fire compartment with external flames, the validated cubic scale model is scaled to a real fire compartment (factor 10 bigger than the cubic scale model).
If the model is scaled to a full-scale fire compartment this means that the amount of gird cells will increase by using similar grid cell size. Therefore a longer calculation time is needed to solve the Navier-stokes equations. To investigate if by scaling the validated CFD model with a factor 10 the grid cell size may also be scaled by this factor to generate accurate CFD results (10 cm grid cell size), a simulation is performed and compared to a scaled validated model (reference model: simulation model 3).

3.5.1 Simulation model

The validated CFD model will be expanded by a factor of 10. The new cubic real fire compartment consists of the dimensions of 5.0 m by 5.0 m and 5.0 m high with one side a door-like opening. The opening geometry is 2.0 m wide and 2.0 m high. All external walls are adiabatic to decrease the calculation time. Using adiabatic constructions will decrease the uncertainty of different material properties which occur in practice, because the interaction of an adiabatic construction will be not taken into account. Due to this a model with an adiabatic construction predicts the fire development without a specific material.

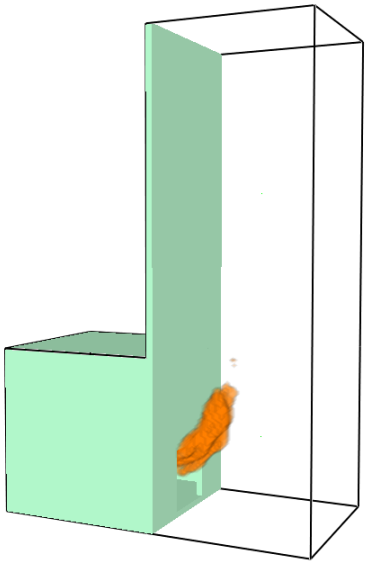

Figure 26: A screenshot of the CFD model with external flames (real fire compartment.

Because in real buildings cellulose fire ($C_4H_6O_3$) occurs most of the time, a new fire source with cellulose is modelled instead of propane. In this research it is assumed that the differences between using a cellulose fire and a propane fire is too small to influence the simulation results. According to the empirical correlation of the experimental study (paragraph 2.2) the actual HRR inside the model and the mass inflow rate do not depend on the theoretical HRR and the fuel properties. Therefore in the reference model a cubic scale model with a propane fire is modelled and compared with a real (full-scale) compartment fire which consist of cellulose fire. To investigate if modelling propane fire and cellulose fire shows small differences on the actual HRR and the mass inflow rate a third full-scale model with propane fire is simulated. Figure 26 shows an illustration of the model of a real fire compartment (appendix V). To decrease the calculation time all simulation models will be stationary calculated. This means that the external flames occur after a few seconds.

The new simulation model is divided in two domains as well. Domain 1 covers the inside of the model and the lower part of the outside and domain 2 covers the outside upper part. The computational domain has been extended by 5.0 m outside the model. The 5.0 m outside domain is modelled in order to limit the influences of the ‘open’ boundary condition on the external flaming. Two mesh domains are used to exclude the flow pattern from behind the upper floor façade. Because the reference model is scaled by factor 10 the grid cell size is increased by a factor of 10 as well. This means that the amount of grid cells equals the scaled reference model with external flames. To investigate if using a finer grid cell size shows more accurate results a 5 cm grid cell size will be compared to the simulation results of the 10

cm grid cell size (cellulose fire). Using 10 cm grid cell size result in 589680 cells ((104x54x54)+(52x54x102)) while using 5 cm grid cell size result in 4717440 cells ((208x108x108)+(104x108x204)). To exclude the uncertain factor of the fuel property (propane vs cellulose) a third model with propane fire and 10 cm grid cell size is compared to the results of the cellulose fire simulated with 10 cm grid cell size.

3.5.2 Simulation variables

The variables actual HRR and mass inflow rate will be simulated until a (constant) steady-state conditions are reached. The results of both grid cell sizes (10 cm and 5 cm) should be compared to the empirical correlation which is determined based on the results of the reference model (paragraph 3.4: simulation model 3).

- The actual HRR inside the model;
- The mass inflow rate through the opening;
- The neutral plane height from floor level.

Actual HRR

The actual HRR calculated inside the model during external flaming will be compared to the reference model with adiabatic construction which is simulated by 1 cm grid cell size. A maximum theoretical HRR of 10000 kW will be available during the simulation period. The actual HRR inside the model during external flaming will be used after it is stabilized.

Mass inflow rate

The mass inflow rate through the opening will be simulated and compared with the mass inflow rate which is obtained from the reference model with adiabatic construction (paragraph 3.4). The average mass inflow rate is calculated during external flaming and is compared to the linear correlation of the reference model.

Neutral plane

The neutral plane height is determined from the average horizontal air velocity at different heights at the opening centerline. Per height the average horizontal air velocity is calculated. The neutral plane height is when the average horizontal air velocity becomes nearly zero then there is no in- and outflow of air. The calculated neutral plane height will be compared to the neutral plane height of the reference model with adiabatic construction.

To investigate if using similar amount of grid cells in a full-scale CFD model shows similar results as the reference cubic scale model only the actual HRR inside the model, the mass inflow rate through the opening and the neutral plane height are compared during external flaming by two different grid cell sizes. The result of the external flame height is not compared with the flame height of the reference model. This is because the external flame height depends largely on the theoretical HRR inside the compartment. Therefore comparing the external flame height is not important in this part of the research.

4. Research results

4.1 Validation study

CFD simulation results are often dependent on the grid cell size. In this paragraph a grid sensitivity analyses will be discussed by comparing the simulation results with experimental results. Using a finer grid cell size will increase the calculation time but may show minimum differences with a coarser grid cell size. Therefore a grid sensitivity analyses is performed to investigate if the deviation with the measured variables decreases by using a finer grid cell size. Not only the differences between two different grid cell sizes are important but the grid cell size that imitates the reality (experimental results). Based on the grid sensitivity analyses a grid cell size with the most adequate simulation results will be chosen for further investigation. The grid sensitivity analyses is done for only the measured variables inside the model (actual HRR, mass inflow rate, gas temperature and the neutral plane height).

Actual HRR

The actual HRR is simulated at three different domain areas. One area inside the model and two areas outside the model (upper and lower outside part). In Figure 27, Figure 28 and Figure 29 the results of the different areas by two different grid cell sizes are given. The simulated actual HRR outside the model is divided in two areas for each grid cell size. With two different areas the fire heat release is clearly defined when external flames appear outside the model and when external flames reach the upper floor level. The fire heat release at the upper floor façade determines the risk of fire spread to upper floors compartments.

In Figure 27 the actual HRR inside the model is simulated by a 2 cm and 1 cm grid cell size. The actual HRR inside the model simulated with 2 cm grid cell size is lower than the HRR inside the model simulated with 1 cm grid cell size. The actual HRR inside the model increases until external flames occur. External flames occur when the actual HRR inside the model is stabilized. The actual HRR inside the model simulated with 2 cm grid cell size stabilizes after approximately 7 minutes while the actual HRR inside the model simulated with 1 cm grid cell size stabilizes after approximately 8 minutes after the ignition. In Figure 28 and Figure 29 the actual HRR outside the model is given. The graphs of both outside areas show external flaming. Figure 28 shows that external flames occur when the actual HRR inside the model is stabilized. External flames at the outside lower part show a small difference between using 2 cm or 1 cm grid cell size. The actual HRR outside the model at the upper part shows when flames reach the upper floor. This is after approximately 9 minutes simulated with 2 cm grid cell size while using 1 cm grid cell size external flames occurs after approximately 11 minutes at the upper floor. Figure 29 shows that external flames simulated with 2 cm grid cell size consist of a higher HRR while the simulated external flames by 1 cm grid cell size consist of a lower HRR. An increased actual HRR inside the model means that the fire is better developed. Through an increased actual HRR inside the model the actual HRR of the outside domain will decrease. This is because the simulated actual HRR of all different areas together should equal the theoretical HRR of the propane burner.

The simulated actual HRR of all areas together should equal in both grid cell sizes the theoretical HRR of the propane burner. The difference between these two grid cell sizes is the distribution of the actual HRR over the three different areas. The actual HRR in Figure 28 and Figure 29 shows significant results of external flaming. The actual HRR in the outside lower part shows no differences between 2 cm gird cell size and 1 cm grid cell size after 16 minutes (Figure 28). The actual HRR in the outside upper part simulated with 1 cm grid cell size shows an over-predicted external flame because of the increased HRR (Figure 29). The HRR differences between using 2 cm and 1 cm grid cell size of all areas are given in Figure 30. The difference between using 2 cm grid cell size and 1 cm grid cell size inside the model increases after approximately 6 minutes. The difference of the actual HRR outside (lower part)

the model increases after approximately 6 minutes as well. After approximately 12 minutes the difference between using 2 cm grid cell size or 1 cm grid cell size decreases. The difference of the actual HRR outside (upper part) increases after approximately 8 minutes.

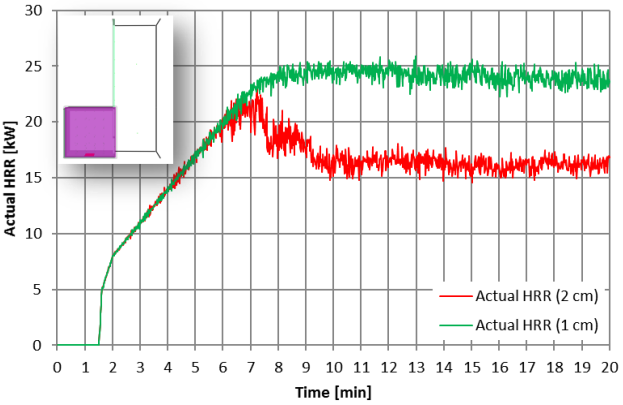

Figure 27: Cell size effect on the simulated actual HRR inside the model with ventilation-controlled propane fire.

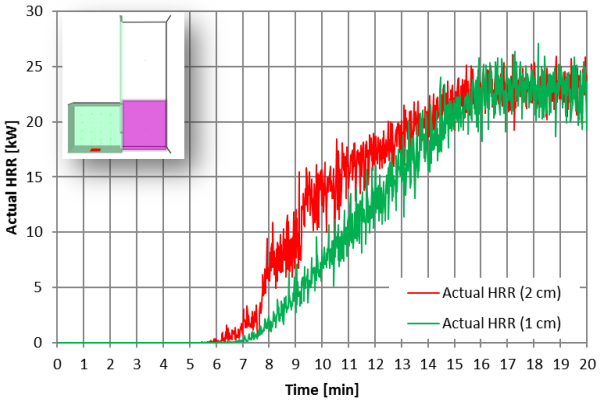

Figure 28: Cell size effect on the simulated actual HRR outside (lower part) when external flaming occurs.

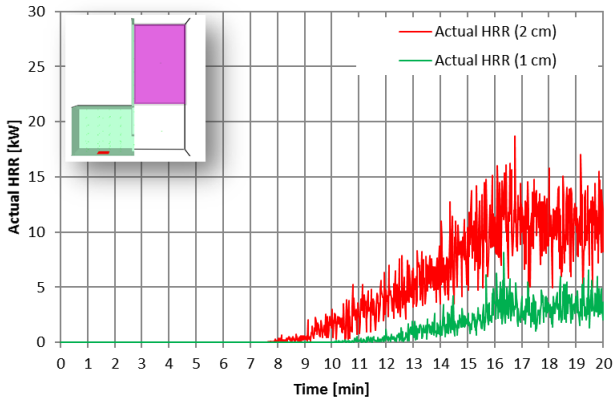

Figure 29: Cell size effect on the simulated actual HRR outside (upper part) when external flaming occurs.

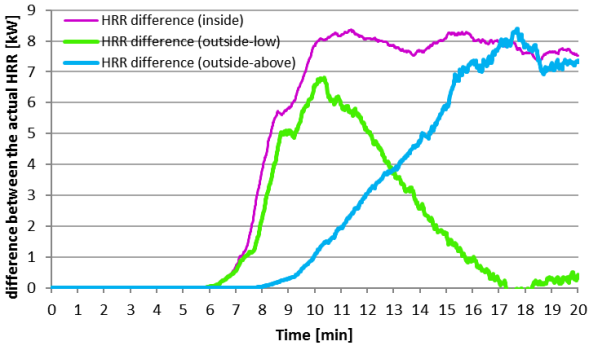

Figure 30: The difference in kW between the simulated actual HRR of the different areas together using 2 cm grid cell size and 1 cm grid cell size.

From the simulated oxygen concentration inside the model can be determined when external flaming occurs. The oxygen concentration inside the model is simulated at 6 different positions. In Figure 32 and Figure 31 the results of the oxygen concentration are simulated by 2 cm grid cell size and 1 cm grid cell size. The oxygen concentration inside the model decreases by increasing the actual HRR inside the model (Figure 27). The oxygen concentration decreases to zero when the inflow of fresh air is totally involved with the fire. When the oxygen concentration inside the model decreases the fire becomes ventilation-controlled by the limited oxygen. The oxygen concentration inside can be compared to the actual HRR inside the model. When external flames occurs the oxygen concentration inside the model is zero and the fire is limited through the limited oxygen.

From the results of the oxygen concentration inside the model it can be concluded that external flames occur after approximately 7 minutes with 2 cm grid cell size (Figure 32) while using 1 cm grid cell size external flames occur after approximately 8 minutes (Figure 31). The results of the oxygen concentration show that when external flames appear the fire inside the model becomes ventilation-controlled.

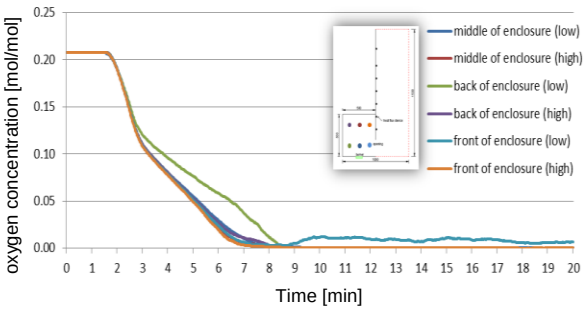

Figure 31: The oxygen concentration at different heights inside the model with 2 cm grid cell size during 20 minutes.

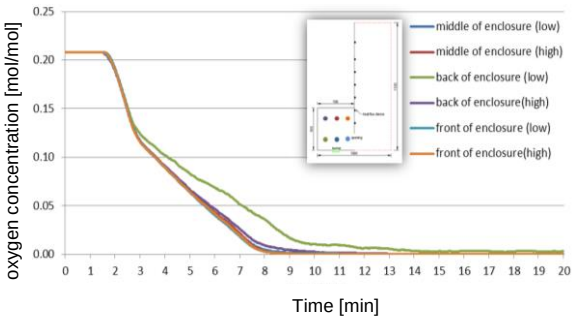

Figure 32: The oxygen concentration at different heights inside the model with 1 cm grid cell size during 20 minutes

The results of the simulated actual HRR inside the model and the measured actual HRR inside the cubic scale model are shown in Figure 33. The simulated actual HRR inside the model calculated with 2 cm and 1 cm grid cell size are both lower than the measured actual HRR inside the scale model when external flaming occurs (Table 4.1.1). In Table 4.1.1 the deviation in percentage is given from the experimental results and empirical correlations. Using a 2 cm grid cell size shows a deviation between approximately 23% at the begin of external flaming and a deviation of 40% at the end of the simulation with the experimental results, while using a 1 cm grid cell size shows a deviation of 10% with the experimental results during external flaming. The steady-state intermediate plateau at the measured actual HRR inside the scale model shows a good agreement with the empirical correlation for the actual HRR inside an under-ventilated enclosure with one external opening. The measured actual HRR of different experiments results shows an empirical correlation of $1500\ A\sqrt{H}$. Because the simulated actual HRR inside the model deviates from this empirical correlation a new correlation based on the deviation of 2 cm and 1 cm grid cell size is given in Table 4.1.1.

Table 4.1.1: The deviation of using 2 cm or 1 cm grid cell size with the experimental results given by the empirical correlation.

	Experiments	Simulations 2 cm grid cell size	Deviation	Simulations 1 cm grid cell size	Deviation
Empirical correlation	$1500\ A\sqrt{H}$	$1150\ A\sqrt{H}$ $900\ A\sqrt{H}$	23% - 40%	$1350\ A\sqrt{H}$	10%
Actual HRR inside	26.8 kW	20.6 kW 16.1 kW		24.1 kW	

From this results it can be concluded that the actual HRR simulated with FDS 6.5.2 (Figure 33, green line) is lower when the steady-state conditions are reached compared to when the measured actual HRR reaches the steady-state plateau (Figure 33, dark blue line). The simulated actual HRR inside the model simulated with 1 cm grid cell size is approximately 10% lower than the measured actual HRR inside the scale model. This means that using 1 cm grid cell size shows sufficiently accurate simulation results with the experiments.

The simulated actual HRR with 1 cm grid cell size and the measured actual HRR inside the cubic scale model are similar the first 8 minutes of burning. The simulated and measured actual HRR show after approximately 8 minutes of the ignition that the fire inside the enclosure becomes ventilation-controlled and external flames occur. A ventilation-controlled fire occurs mostly in fire compartments when the fire becomes out of oxygen and the combustion is entirely dependent on the availability of fresh air (through openings). The oxygen concentration will drop until zero at the moment of external flaming (ventilation-controlled). Figure 32 shows that the oxygen concentration inside the model at different height decreases to zero after approximately 8 minutes of combustion. This means after approximately 8 minutes unburned gases will burn further outside the enclosure with unlimited oxygen concentration.

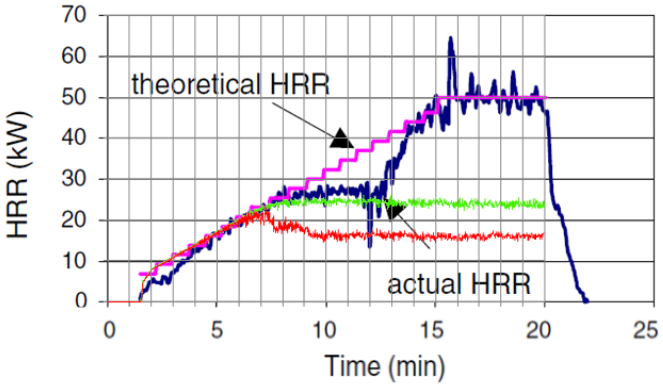

Figure 33: Simulated (red and green line) and measured (dark blue line) actual HRR inside the model with 50 kW propane burner. The theoretical HRR is the HRR which is produced by a 0.1 m x 0.2 m propane burner (pink line). Simulation results of 1 cm grid cell size show a lower deviation with the experimental results.

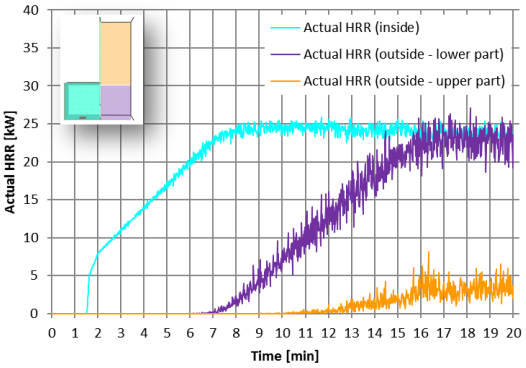

Figure 34: The actual HRR inside and outside the model are simulated with 1 cm grid cell size during 20 minutes. The total HRR without energy loss of all domains should equal the theoretical HRR with a maximum of 50 kW.

When outside combustion of unburned gases occurs, a steady-state plateau will be reached inside the model. The measured actual HRR steady-state plateau occurs only between 8 minutes and 12 minutes. The simulated actual HRR shows a steady-state progression after 8 minutes until 20 minutes after ignition. In the measurements the actual HRR inside the cubic scale model increases after 12 minutes of ignition. An increased actual HRR inside the scale model means that there are no external flames. The simulated actual HRR outside the model will increase during the simulation time until a steady-state flame is reached. The flames outside the model will be stabilized when the maximum theoretical HRR inside the model is reached. The maximum fire heat release will be reached after 16 minutes of the ignition (Figure 34). In appendix VI-a the HRRPUV inside and outside the cubic scale model calculated with 1 cm grid cell size are given for each 2 minutes after the ignition.

Mass in- and outflow

The simulated mass in- and outflow rate of 2 cm and 1 cm grid cell size are compared in Figure 35 and Figure 36. Results show a lower inflow and outflow rate through the opening by using 2 cm grid cell size. This is not surprisingly an increased inflow and outflow rate through the opening with grid cell size 1 cm because the actual HRR inside the simulated model increases as well. The influence of an increased mass in- and outflow through openings is due to the increased actual HRR inside the simulated model. Increasing the pressure differences between inside and outside the model results in an increased actual HRR inside (Figure 27). When the HRR inside increases the mass inflow and outflow rate through the opening will increase as well.

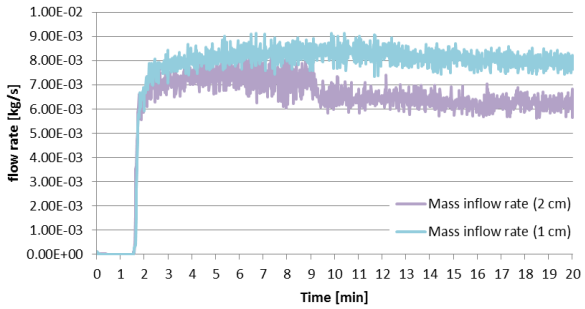

Figure 35: Cell size effect on the simulated mass inflow rate through the external opening (0.2 m x 0.2 m).

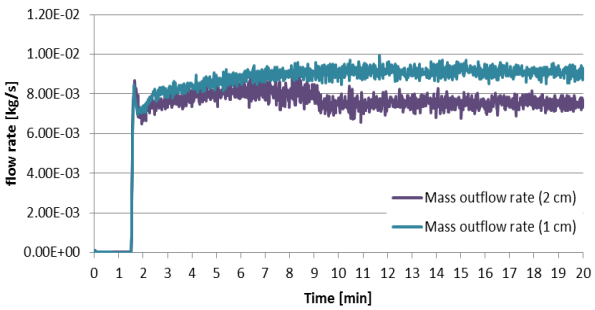

Figure 36: Cell size effect on the simulated mass outflow rate through the external opening (0.2 m x 0.2 m).

From the simulated in- and outflow rate can be concluded that the mass flow rate calculated with 1 cm grid cell size is higher, because of the increased actual HRR inside the model. The in- and outflow through the opening simulated with 1 cm grid cell size reaches a steady state condition although the in- and outflow simulated with 2 cm grid cell size is before external flaming higher than the mass flow rate after external flaming (see, Figure 37).

Only the simulated mass inflow rate through the external opening can be validated with the measured mass inflow rate. Table 4.1.2 shows the results of the mass inflow rate simulated by using 2 cm grid cell size and 1 cm grid cell size. From these results it can be concluded that using 1 cm grid cell size shows a lower deviation (6%) with the experimental results. Using 2 cm grid cell size shows a deviation between 8% and 28% during the simulation time. The mass inflow rate simulated with 2 cm grid cell size shows before external flaming a lower deviation with the experimental results. This deviation increases by decreasing the actual HRR inside the model. In fact the amount of air flow through the opening should be constant during the simulation period.

Table 4.1.2: The deviation of the mass inflow rate with experimental results is given by empirical correlations.

	Experiments	Simulations 2 cm grid cell size	Deviation	Simulations 1 cm grid cell size	Deviation
Empirical correlation	$0.5\ A\sqrt{H}$	$0.41\ A\sqrt{H}$ $0.36\ A\sqrt{H}$	18% - 28%	$0.47\ A\sqrt{H}$	6%
Mass inflow rate	0.0089 kg/s	0.0073 kg/s 0.0064 kg/s		0.0084 kg/s	

The measured mass inflow rate into the scale model is expressed by the empirical correlation $0.5\ A\sqrt{H}$ which is developed for ventilation-controlled compartment fires with one opening. This means that the simulated mass inflow rate should be 0.0089 kg/s for this specific opening geometry. The simulated average mass inflow rate is 0.0084 kg/s calculated with 1 cm grid cell size. These results are not surprising because the mass inflow rate depends on the actual HRR inside the scale model. If the actual HRR inside the scale model is low the mass inflow rate through the opening is low as well. So if the simulated actual HRR inside the model shows a deviation with the measured results, the simulated mass inflow rate will undoubtedly deviate with the measured mass inflow rate.
The temperature differences between the enclosure and its surroundings create a pressure difference which causes the flow through the opening. The pressure difference of the upper layer (hot) in a fire compartment is always bigger than the lower layer (cold) because of the temperature differences with ambient conditions. Production of combustion gases ensures a bigger mass outflow rate than the mass inflow rate.

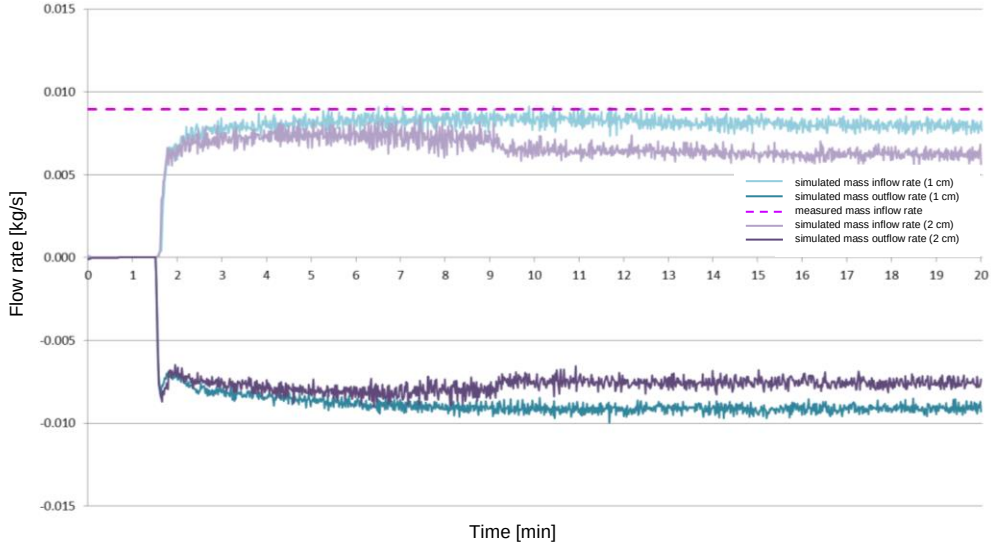

Figure 37: The mass in- and outflow rate through the external opening simulated with 2 cm and 1 cm grid cell size. The average mass inflow rate is compared to empirical correlation of the inflow rate in ventilation-controlled fire compartments with one opening.

In Figure 37 the mass in- and outflow rate through the opening simulated with 2 cm and 1 cm grid cell size are given. The light-colored lines show the simulated inflow rate of fresh air through the opening. The dark-colored lines show the simulated outflow rate of combustion gases. The pink dashed line shows the measured average inflow rate of fresh air. This graph shows that using 1 cm grid cell size presents more accurate results for the mass inflow rate than using 2 cm grid cell size.

Gas temperature

The gas temperature inside the model at the front corner is simulated with 2 cm and 1 cm grid cell size. The results of the gas temperature progression are shown at different heights during 20 minutes, see Figure 38 and Figure 39. In Figure 38 the gas temperature distribution is simulated with 2 cm grid cell size. In Figure 39 the gas temperature distribution is simulated with 1 cm grid cell size.

To compare the simulated results with the experimental results the gas temperature distribution is simulated by one thermocouple tree (front corner). Before external flames appear the increasement of the gas temperature distribution of all heights is at maximum. After external flames occur the gas temperature increscent decreases until a semi steady-state gas temperature is reached. The gas temperature inside the model will not stabilize after the external flames occur because of the steady-state actual HRR and mass inflow rate through the openings.

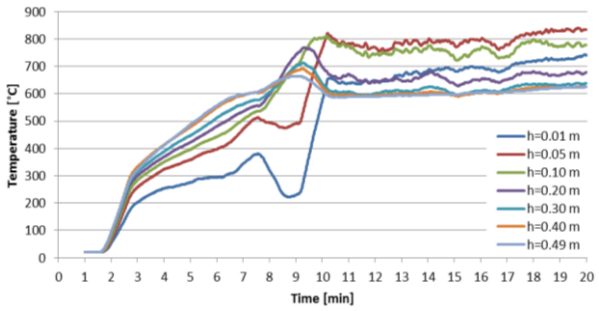

Figure 38: Simulated temperature distribution inside the model (front corner) at several heights during 20 minutes with 2 cm grid cell size.

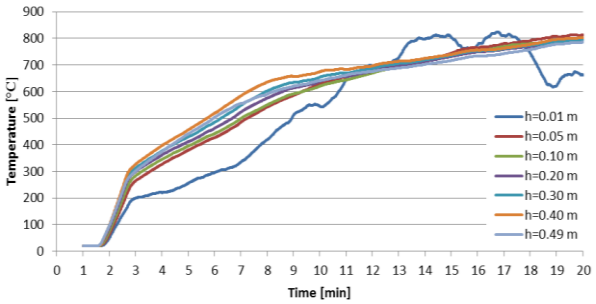

Figure 39: Simulated temperature distribution inside the model (front corner) at several heights during 20 minutes with 1 cm grid cell size.

The gas temperature distribution simulated by 2 cm grid cell size is after approximately 11 minutes stabilized whereas the gas temperature distribution simulated by 1 cm grid cell size will stabilize at the end of the simulation (after 20 minutes). Because the simulated gas temperature distribution constantly increases only the gas temperature at the end is compared with the experimental results.

Table 4.1.3 show the gas temperature at the end of the simulation for 2 cm and 1 cm grid cell size. The third column of the table represents the deviation at each height between using 2 cm grid cell size and 1 cm grid cell size. From Table 4.1.3 it can be concluded that the gas temperature shows a deviation between simulated result of 2 cm grid cell size and 1 cm grid cell size. The deviation in the upper layer (hot zone) is bigger than the deviation in the lower layer (cold zone). The gas temperature at floor level simulated by 2 cm grid cell size is higher than the gas temperature simulated by 1 cm grid cell size. From 0.10 m from floor level the gas temperature which is simulated by 1 cm grid cell size is higher than the gas temperature simulated by 2 cm grid cell size. This means that the gas temperature difference between using 2 cm and 1 cm grid cell size is bigger by increasing the height from floor level. The gas temperature inside the model is simulated with both grid cell sizes at different heights. The simulated gas temperature distribution is validated with experimental results. Because of experimental lack of information, only the gas temperature distribution at the front corner is compared with the experimental results.

Table 4.1. 3: The simulated gas temperature deviation of both grid cell sizes at the front corner.

Height [m]	Temperature [ºC] 2 cm grid cell size	Temperature [ºC] 1 cm grid cell size	Deviation [%]
0.00	740.4	662.8	10.4
0.05	832.8	812.2	2.4
0.10	777.2	800.0	2.8
0.20	677.4	788.4	14.1
0.30	637.9	795.1	19.8
0.40	626.2	802.3	21.9
0.50	624.5	785.6	20.5

Table 4.1.4: The gas temperature deviation of both grid cell sizes compared with the experimental results.

Height [m]	Measured temperature [ºC]	Simulated temperature [ºC] (2 cm grid cell size)	Deviation [%]	Simulated temperature [ºC] (1 cm grid cell size)	Deviation [%]
0.00	870	740	14.9	682	21.7
0.05	910	833	8.5	803	11.8
0.10	940	777	17.3	806	14.2
0.20	945	677	28.4	792	16.2
0.30	955	638	33.2	798	16.5
0.40	955	626	34.5	803	15.9
0.50	935	624	33.3	789	15.6

The average gas temperature simulated with 2 cm grid cell size deviates 24% from experimental results while the average gas temperature simulated with 1 cm grid cell size shows a deviation of 16% (Table 4.1.4). This means that using 1 cm grid cell size gives a lower deviation with the experimental results. In Figure 40 the simulated and measured gas temperature distributions are compared together. The gas temperature distribution simulated with 2 cm and 1 cm grid cell sizes are both lower than the measured gas temperature distribution inside the scale model. The gas temperature distribution simulated with 1 cm grid cell size shows a similar gradient with the experimental results than the gas temperature distribution simulated with 2 cm grid cell size. In appendix VI-b the gas temperature inside and outside the cubic scale model simulated with 1 cm grid cell size are given for each 2 minutes after the ignition.

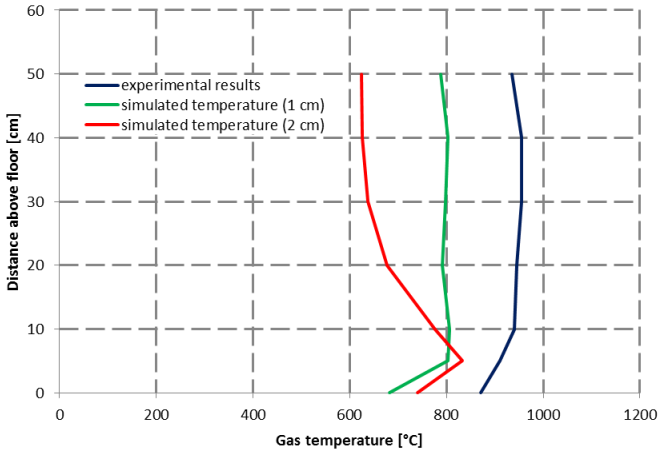

Figure 40: The measured and simulated (2 cm and 1 cm) gas temperature distribution at different heights inside at the front corner.

Neutral plane

The neutral plane height is the height where there is no inflow and outflow of air through the opening. At this height the air velocity through the opening is zero. This height separates the inflow of fresh air and the outflow of combustion gases. The neutral plane height is important for the validation of the external flaming with experimental results. To determine the accurate neutral plane height a grid sensitivity analyses is performed. In Figure 41 the air velocity at different heights along the opening surface is shown. The air velocity at different heights (once every 2 cm) is simulated during 20 minutes. Because the fire development inside the model is transient, the air velocity through the opening will be transient as well. Therefore the average air velocity at different heights is calculated in the period of external flaming. Thus average air velocity with 2 cm and 1 cm grid cell size is simulated during external flaming (approximately after 8 minutes until 20 minutes). In Figure 42 the average gas temperature at the same period and height is given.

The results show that the neutral plane simulated by 2 cm grid cell size is lower than the neutral plane simulated by 1 cm grid cell size. The neutral plane simulated with 2 cm grid cell size is 0.06 m while the neutral plane simulated with 1 cm grid cell size is 0.08 m. This means using 2 cm grid cell size simulates a bigger outflow with combustion gases than using 1 cm grid cell size.

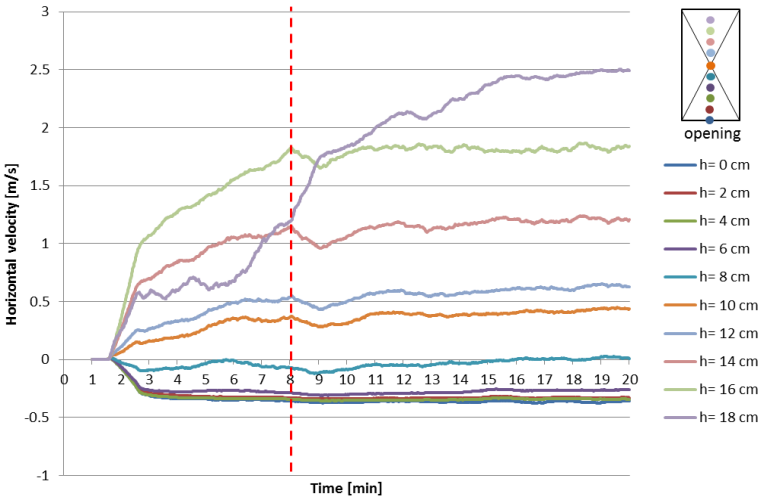

Figure 41: The simulated air velocity at different heights along the opening centreline during 20 minutes are given. The heights with a positive air velocity determines the outflow region. The heights with a negative air velocity determines the inflow region.

The line of the horizontal air velocity simulated by 2 cm grid cell size does not show a smooth line progression. The average horizontal air velocity shows a negative velocity at 0.08 m (inflow) height while the horizontal air velocity at 0.06 m height shows the neutral plane where there is no inflow and outflow. Other research shows that the air flow under the neutral plane height should be negative (inflow) and the air flow above the neutral plane height should be positive (outflow). The development of the average air velocity per height simulated with 1 cm grid cell size shows below the neutral plane height a negative air velocity and above the neutral plane height a positive air velocity. The average air velocity using 2 cm grid cell size does not show a good estimation of the inflow and outflow through the external opening.

The lines in Figure 42 show the average gas temperature at different height through the opening simulated with 2 cm and 1 cm grid cell size. The average gas temperature below the 0.06 m shows small differences between using 2 cm grid cell size or 1 cm grid cell size. The differences between using 2 cm and 1 cm grid cell size increases by increasing the height. This means that high differences are shown in the outside hot layer with combustion gases. The gas temperature at different heights

simulated with 1 cm grid cell size shows a smooth line progression in comparison with the simulated gas temperature by using 2 cm grid cell size. Figure 42 shows that the average gas temperature at the neutral plane height (0.08 m) is 300 ˚C.
Figure 41 shows the simulated air velocity at different heights with 1 cm grid cell size during 20 minutes. The simulated air velocity along the opening centerline will increase by increasing the actual HRR inside the model. The simulated negative air velocity shows the heights located in the inflow region (h= 0.0, 2.0, 4.0 and 6.0 cm). The simulated positive air velocity shows the heights located in the outflow region (h= 10.0, 12.0, 14.0, 16.0 and 18.0 cm). The results of the simulated air velocity will be stabilized when the fire inside the model becomes ventilation-controlled after approximately 8 minutes.

The neutral plane at the opening centerline was determined by a CCD camera. Measurements of different experiments with external flames shows that the neutral plane height can be obtained by the empirical correlation 0.4H (H is the opening height). Experimental results show that the neutral plane height along the opening is 0.08 m from the floor level. Results of the sensitivity analyses show that using 2 cm grid cell size gives a neutral plane height of 0.06 m height while using 1 cm grid cell size gives a neutral plane height of 0.08 m. This means using 1 cm grid cell size shows no deviation with the experimental results. This means that using 1 cm grid cell size provides accurate simulation results. In appendix IV-c the horizontal air velocity inside and outside the cubic scale model simulated with 1 cm grid cell size are given for each 2 minutes after the ignition.

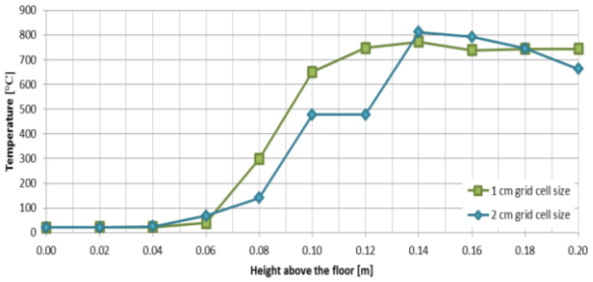

Figure 42: The average gas temperature at different heights through the external opening simulated by 2 cm grid cell size and 1 cm grid cell size.

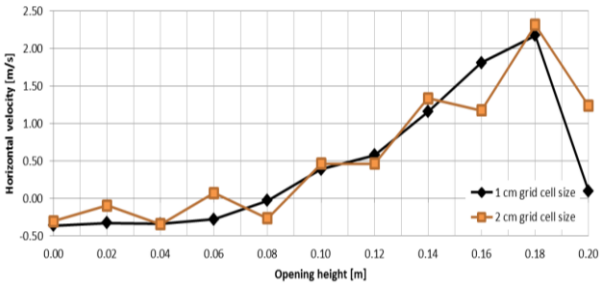

Figure 43: The average air velocity through the external opening at different heights simulated by 2 cm grid cell size and 1 cm grid cell size.

Façade heat flux

The façade heat flux is simulated with 1 cm grid cell size based on the grid sensitivity of the actual HRR, mass inflow rate, gas temperature distribution and the neutral plane height. The most important parameters for predicting the external flame are: the actual HRR inside the model, inflow rate through the opening and the neutral plane height. If these variables are simulated with a minimal deviation from the experimental results then it means that the façade heat flux shows a good prediction.
The façade heat flux is measured with 1 cm grid cell size at 7 different heights above the opening centerline. The simulated maximum heat flux at different heights with 1 cm grid cell size is given in Figure 44: the green line shows measured heat flux, the yellow line shows the simulated maximum heat flux (Figure 45) and the red line shows the simulated maximum heat flux of averaged data

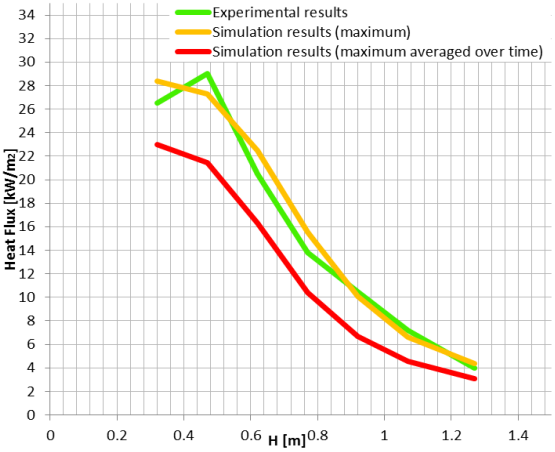

Figure 44: The simulated and measured facade heat flux at different heights.

(Figure 46). Simulation results of the maximum heat flux (yellow line) show good agreement with the measured heat flux (green line). The simulated maximum heat flux at different heights is higher than the simulated maximum heat flux of the averaged data (Figure 45) because of the simulated heat flux peak values (Figure 46). In Table 4.1.5 the heat flux at different height deviations with experimental results are given. The maximum heat flux shows an average deviation of 8% with the experimental results while the averaged maximum heat flux shows an average deviation of 25% (Table 4.1.5).This means that the maximum peak values beneficially influence the simulated results.

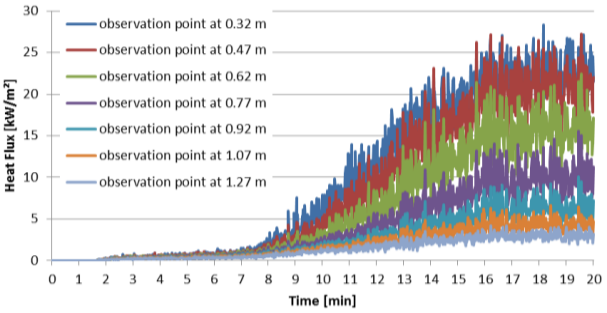

Figure 45: The simulated facade heat flux with 1 cm grid cell size at different heights during 20 minutes.

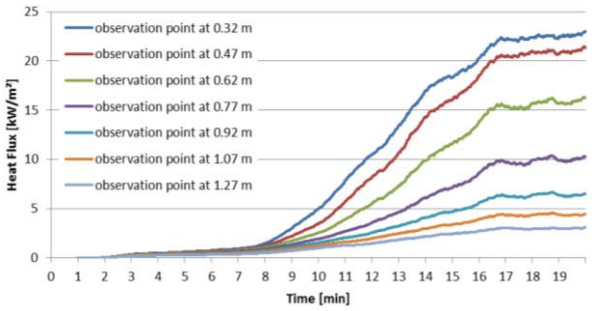

Figure 46: The simulated average facade heat flux with 1 cm grid cell size at different heights during 20 minutes.

Table 4.1. 5: The heat flux deviation with experimental results is per height given.

Height [m]	Measured heat flux [kW/m²]	Simulated heat flux [kW/m] (Figure 45)	Deviation [%]	Simulated heat flux [kW/m] (Figure 46)	Deviation [%]
0.32	26.5	28.4	7.1	23.0	13.2
0.47	29.0	27.3	5.9	21.5	26.0
0.62	20.5	22.5	9.6	16.3	20.3
0.77	13.8	15.6	12.7	10.4	24.7
0.92	10.5	10.1	3.7	6.7	36.5
1.07	7.2	6.6	8.1	4.6	36.8
1.27	4.0	4.4	9.2	3.1	23.2

External flame height

The actual HRR outside the model increases during the simulation time. If the actual HRR outside increases this means that external flames occur as result of ventilation-controlled fire. Because of an increased actual HRR the flame height outside the model will increase as well. Appendix VI-d represents the soot fraction, the HRRPUV and the external flame height each 2 minutes after the ignition.

The results of all medians, minimum and maximum flame height of both calculation methods are shown. The calculated medians, minimum and maximum show an indication of the boxplot distribution, see Table 4.1.6 and Figure 47. Table 4.1.6 shows that the flame heights calculated by method 2 differ from the flame heights calculated by method 1. The results show that the minimum and the maximum flame height calculated with method 2 approximately equal the minimum and maximum flame height calculated with method 1. All other averages and medians show big differences in flame height between using calculation method 1 or calculation method 2.
The measured flame height which appears 50% of the time is 0.68 m from floor level. The median flame height calculated by method 1 under-predicts the measured flame height. Using the median flame height calculated by method 2 over-predicts the measured flame height. The calculated flame height shows a lower flame height by using calculation method 1 than calculation method 2. Basically the flame height results calculated by method 1 agree better with the measured flame height. Therefore calculation method 1 is used to determine the flame height which exists 50% of the time.

Table 4.1. 6: The flame height calculated by calculation method 1 and calculation method 2 and the deviation between using calculation method 1 and calculation method 2 with experimental results is given.

	Flame height (method 1)	Flame height (method 2)	Deviation
Minimum	0.18 m	0.18 m	0.0 %
Median Q1	0.33 m	0.54 m	63.6 %
Median Q2 (Figure 48)	0.57 m	0.80 m	40.4 %
Median Q3 (Figure 49)	0.79 m	1.00 m	26.6 %
Maximum	1.52 m	1.52 m	0.0 %
Average Q1-Q3 (Figure 53)	0.58 m	0.79 m	36.2 %
Average Q2-Q3 (Figure 52)	0.68 m	0.90 m	32.4 %
Average (Figure 50)	0.61 m	0.78 m	27.9 %

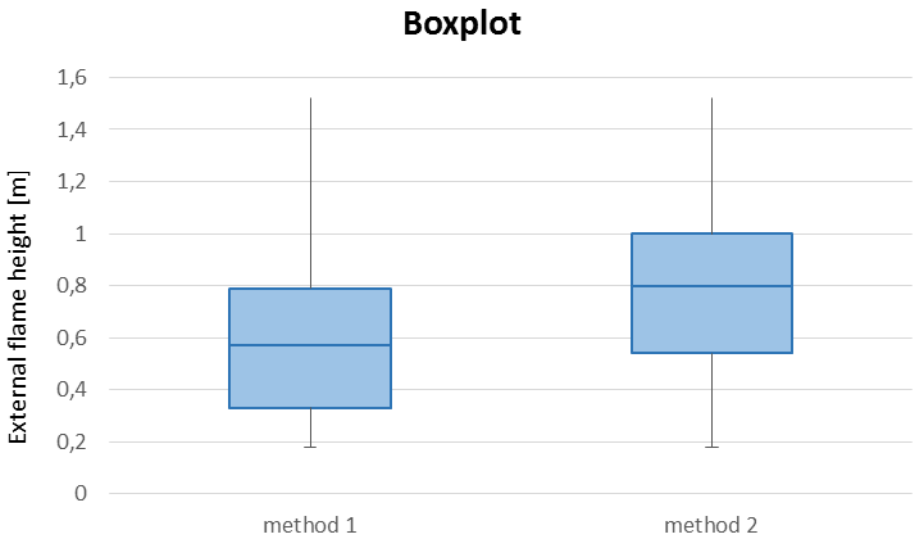

Figure 47: A Visualization of using method 1 and method 2 by the boxplot given. This graph shows the distribution of the dataset of using method 1 and method 2.

In fact using the median flame height (from calculation method 1) does not define the flame height which exists 50% of the time. The average temperature distribution between median Q1 and Q3 of the data set determines a virtual temperature distribution which appears 50% of the simulation time. The median Q1 and Q3 of the data set show a deviation of approximately15% with the experimental results. The average between median Q1 and Q3 flame height is 0.58 m while the average between median Q2 and Q3 shows a flame height of 0.68 m. Using the average temperature distribution between median Q2 and Q3 shows a pessimistic flame height which occurs 25% of the simulation time.

Using the average flame height calculated by calculation method 1 shows a better agreement with the experimental results than using the average between Q1 and Q3. This is because of the maximum flame height at the end of the simulation time. The average flame height calculated with calculation method 1 deviates approximately10% from the measured flame height, see Figure 48, Figure 49, Figure 50, Figure 51, Figure 52 and Figure 53. The calculated external flame temperature distribution is visualized. All calculated temperature distribution results show an indication of the external flame height. The colors are divided in 8 regions of 100 ˚C from 20 ˚C (ambient temperature) until a maximum temperature of 820 ˚C. A visible flame temperature is given by the region from 420 ˚C to 520 ˚C (green). From these results it can be concluded that using calculation method 1 gives equivalent flame heights. Therefore calculation method 1 will be used for all other simulations to determine the flame height which occurs 50% of the time.

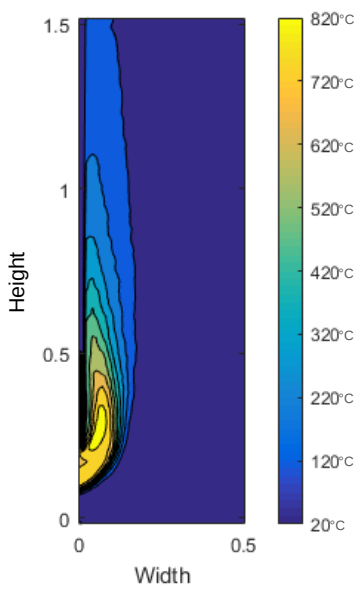

Figure 48: The median (Q2) flame height determined by calculation method 1. A visible flame is when a minimum flame temperature of 520 ˚C is reached.

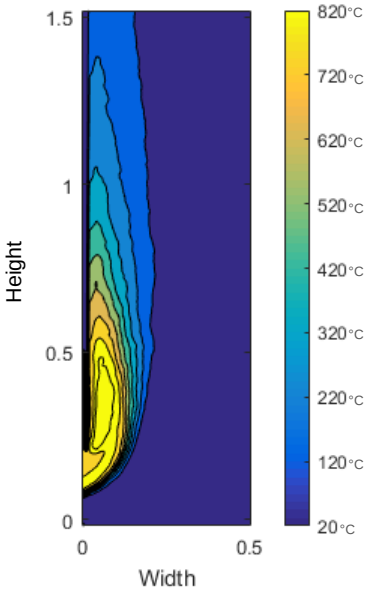

Figure 49: The median (Q3) flame height determined by calculation method 1. A visible flame is when a minimum flame temperature of 520 ˚C is reached.

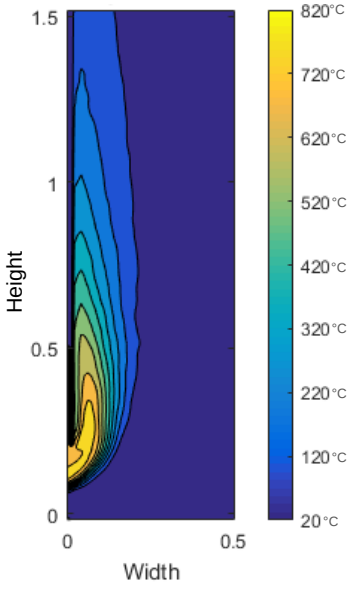

Figure 50: The average flame height determined by calculation method 1. A visible flame is when a minimum flame temperature of 520 ˚C is reached.

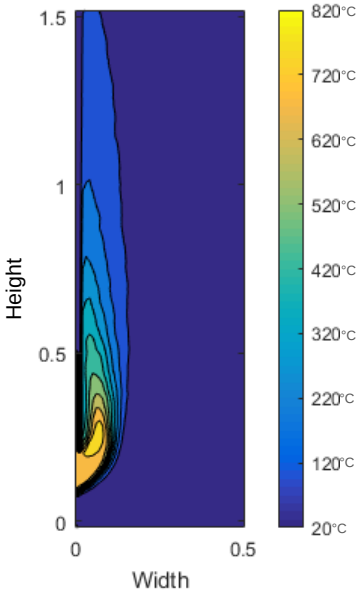

Figure 51: The average flame height between median (Q1) and median (Q2) determined by calculation method 1. A visible flame is when a minimum flame temperature of 520 ˚C is reached.

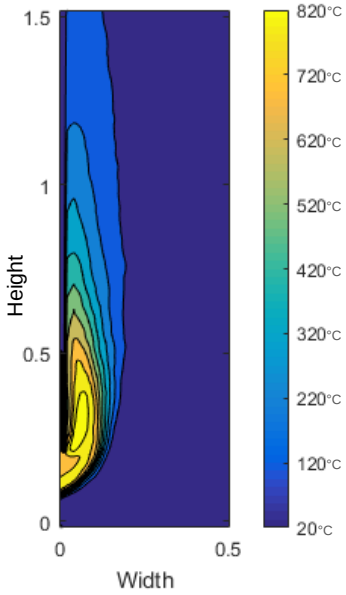

Figure 52: The average flame height between median (Q2) and median (Q3) determined by calculation method 1. A visible flame is when a minimum flame temperature of 520 ˚C is reached.

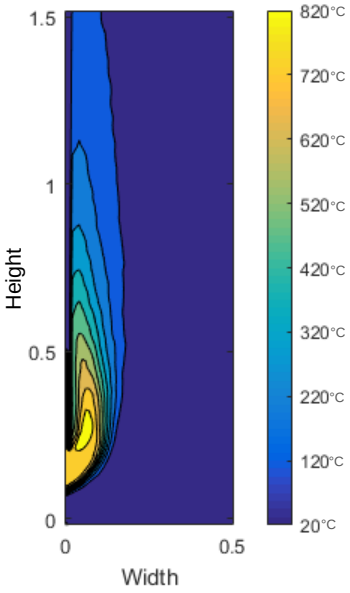

Figure 53: The average flame height between median (Q1) and median (Q3) determined by calculation method 1. A visible flame is when a minimum flame temperature of 520 ˚C is reached.

4.2 Sensitivity of building and fire parameters

In this paragraph the results of the sensitivity analyses will be compared. The results of the actual HRR, the mass inflow rate, the neutral plane height and the external flame height simulated with both grid cell sizes will be compared to the results (absolute values) of the reference model (validated CFD model) simulated with both grid cell sizes. In appendix VII-a the results are given for the comparison between both grid cells (absolute values).
The results of the actual HRR, the mass inflow rate and the neutral plane height of the different simulation models are relatively compared to the (validated) reference model, to investigate the influence on the external flame height.

Results absolute comparison

The deviation of the actual HRR and the mass inflow rate simulated by 2 cm and 1 cm grid cell size is not relatively the same as the deviation between the results of the reference model simulated by 2 cm and 1 cm grid cell size. Except the simulation model with an increased theoretical HRR shows identical results for the actual HRR and the mass inflow rate. From the theory it is concluded that the actual HRR and the mass inflow rate should by shifting the door-like opening and increasing the theoretical HRR equal the actual HRR and the mass inflow rate of the reference model. Using adiabatic constructions and changing the opening surface shows logically different results than the results of the reference model.

The deviation between the reference model and the adjusted simulation models simulated by 2 cm grid cell size is not relatively the same as between the reference model and the adjusted models simulated by 1 cm grid cell size. Using 1 cm grid cell size shows a lower deviation with the results of the reference model. Therefore using 2 cm grid cell size is not useful to predict the effect on external flaming by changing different parameters. The neutral plane height of all simulation models simulated with 1 cm grid cell size shows a deviation within 5% with the neutral plane height of the reference model.
In most of the simulated models using 2 cm grid cell size shows flow discontinuities. This means that the simulated actual HRR of the different domains together does not equal the theoretical HRR of the fire source, while results of the actual HRR of all different domains together result in the theoretical HRR of the fire. Hereby using 1 cm grid cell size shows accurate results where there are no heat losses.
All simulation models show an increased external flame height simulated with 1 cm grid cell size compared to the external flame height calculated with 2 cm grid cell size. The actual HRR at the outside upper part is higher by using 2 cm grid cell size instead of 1 cm grid cell size. Although the actual HRR at the outside is higher than simulated with 1 cm grid cell size, determining the external flame height by using 2 cm grid cell size will under-predict the risk for fire spread to other floors. This means a finer grid will result in an increased external flame height compared to a coarser grid.

Results relative comparison

In Figure 54, Figure 55, Figure 56 and Figure 57 the results of the actual HRR, the mass inflow rate, the neutral plane height and the calculated external flame height are compared with the reference model. All simulation results shows an increased external flame height compared to the reference model. The results of the shifted opening from a door-like to a window-like model show a huge increasement for the external flame height of approximately 41%. The results show that an increased or decreased actual HRR compared to the reference model results in an increased external flame height. The neutral plane height of different simulation models show small differences with the neutral plane height of the reference model. The results of the actual HRR inside the model and the mass flow rate through the opening show identical differences in relation with the validated simulation model. The results show that when the mass inflow rate increases or decreases the actual HRR will be influenced as well (Figure 54 and Figure 55).

To investigate if the obtained correlation is useful to predict the actual HRR and the mass inflow rate of other simulation models, the actual HRR and the mass inflow rate should show a deviation within 10%

from the linear correlation (reference model). To illustrate if all simulation models show an agreement with the validated correlation for predicting the actual HRR inside the model (1350 $A\sqrt{H}$) and the validated correlation for predicting the actual mass inflow rate through the opening (0.47 $A\sqrt{H}$) the results of the adjusted simulation models are compared to the linear correlation from the validation study. For the neutral plane height the empirical correlation of 0.4H is used to predict the neutral plane height of different adjusted simulation models.

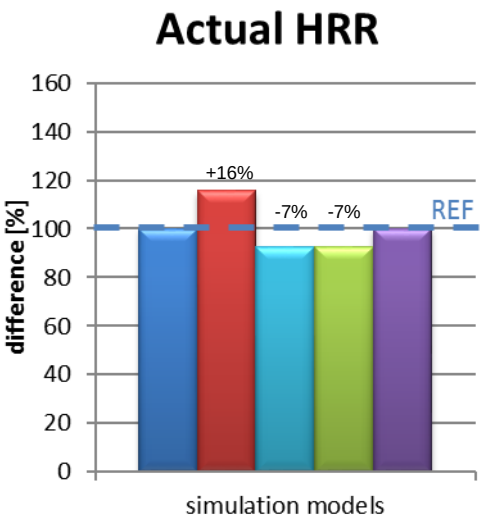

Figure 54: The influence of different parameters on the actual HRR inside the model simulated with 1 cm grid cell size. The actual HRR inside the model of different simulation models is relatively compared to the reference model.

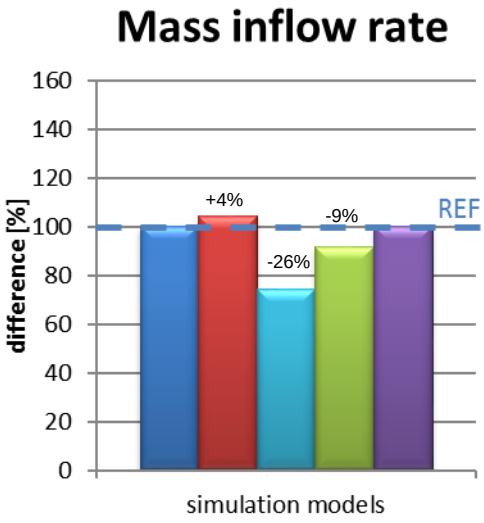

Figure 55: The influence of different parameters on the mass inflow rate through the opening simulated with 1 cm grid cell size. The mass inflow rate through the opening of different simulation models is relatively compared to the reference model.

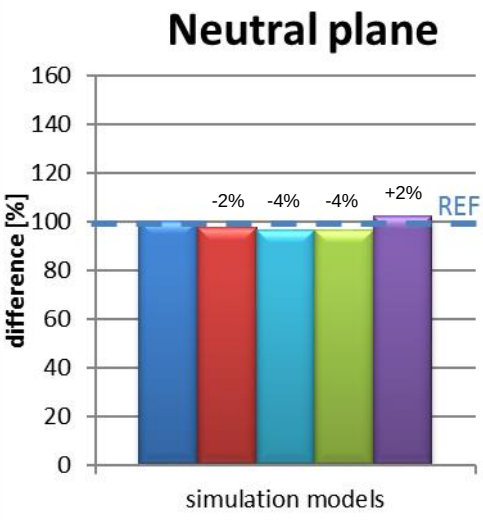

Figure 56: The influence of different parameters on the neutral flame height simulated with 1 cm grid cell size. The neutral plane height of different simulation models is relatively compared to the reference model.

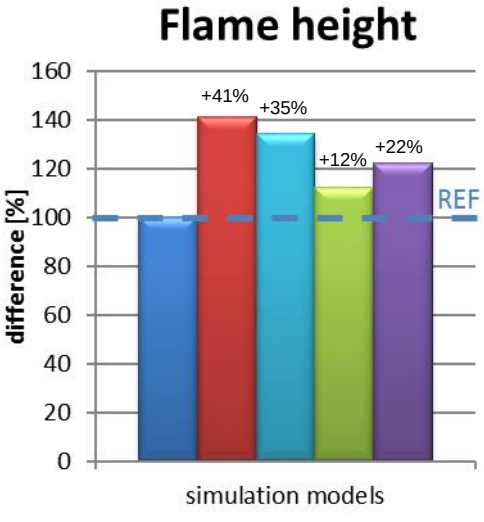

Figure 57: The influence of different parameters on the external flame height simulated with 1 cm grid cell size. The external flame height of different simulation models is relatively compared to the reference model.

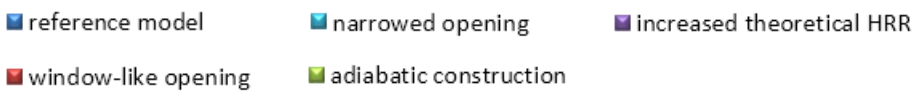

All simulation results show a deviation within 10% from the linear correlation for the actual HRR inside the model (appendix VII-b). The narrowed opening model shows a deviation of more than 10% from the validated correlation for the mass inflow rate (appendix VII-b). The mass inflow rate of the narrowed opening model should be higher according to the validated linear correlation. The rest of the simulations show for the mass inflow rate a deviation with the linear correlation within 10%. The neutral plane height of all simulation models show a deviation within 10% from the empirical correlation which is determined by the experiments.

4.3 Full-scale fire compartment

The results and differences between both grid cell sizes of a full-scale fire compartment is given in this paragraph. The results of the actual HRR inside the enclosure of both grid cell sizes for a cellulose fire are shown in Figure 58. Both simulation models with different grid cell size are compared to the empirical correlation which is determined by the reference model with adiabatic constructions. When external flames occur the actual HRR according to the (full-size) reference model should equal 7070 kW ($1250\ A\sqrt{H}$). The results of the actual HRR of the simulation model with cellulose fire simulated with 10 cm grid cell size shows a deviation of approximately 11% from the actual HRR of the theoretical model (7070 kW). The results of the actual HRR of the simulation model with cellulose fire simulated with 5 cm grid cell size shows a deviation of approximately 10% from the actual HRR of the reference model. While the results of the actual HRR of the simulation model with propane fire simulated with 10 cm grid cell size shows a deviation of approximately 4% from the actual HRR of the reference model.

The results of the mass inflow rate through the opening simulated by 10 cm and 5 cm grid cell size during external flaming are given in Figure 59. According to the reference model when external flames occur the mass inflow rate should be 2.43 kg/s ($0.43\ A\sqrt{H}$) for a propane fire. The results of the mass inflow rate during external flaming of the simulation model with cellulose fire simulated by 10 cm grid cell size shows a deviation of approximately 7% from the mass inflow rate calculated by the reference model. The results of the mass inflow rate of the simulation model with cellulose fire simulated with 5 cm grid cell size shows a deviation of approximately 6% from the mass inflow rate calculated by the reference model. While the results of the mass inflow rate of the simulation model with propane fire simulated with 10 cm grid cell size shows a deviation of approximately 5% from the mass inflow rate determined in the reference model.

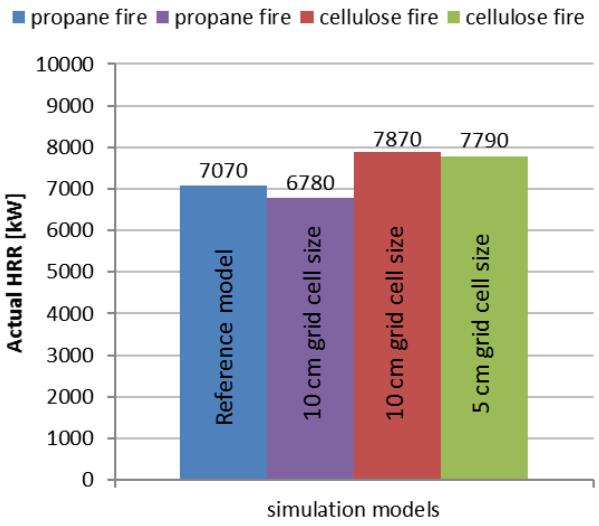

Figure 58: The results of the actual HRR inside a real fire compartment simulated by 10 cm and 5 cm grid cell size compared to the actual HRR inside the reference model.

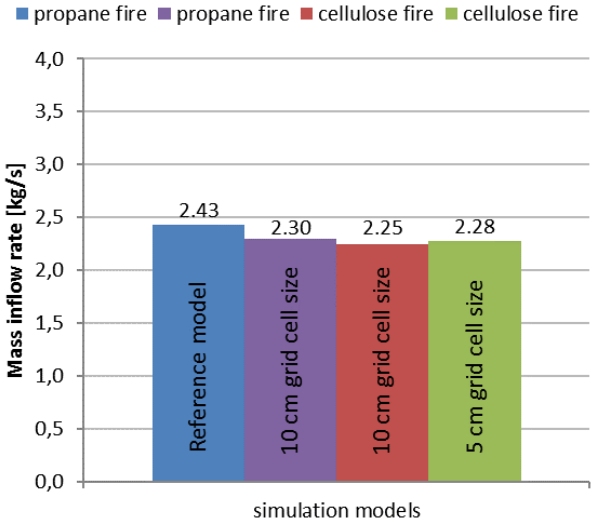

Figure 59: The results of the mass inflow rate through the opening of a real fire compartment simulated by 10 cm and 5 cm grid cell size compared to the mass inflow rate of the reference model.

The results of the neutral plane height simulated by 10 cm and 5 cm grid cell size are shown in Figure 60. The results of the neutral plane height show a lower deviation with the empirical correlation of the reference model by using 10 cm grid cell size (cellulose fire). In general the results of the neutral plane height should be equal to the empirical correlation of 0.4H by using 5 cm grid cell size. The results of the neutral plane height should show a lower deviation with the results of the reference model simulated with 5 cm grid cell size (cellulose fire). The results of the neutral plane height of the simulation model with propane fire shows a deviation of 10% from the results of the reference model.

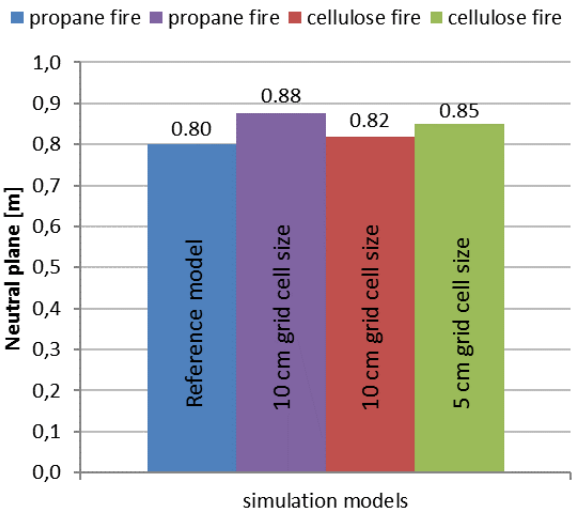

Figure 60:The results of the neutral plane height of a real fire compartment simulated by 10 cm and 5 cm grid cell size compared to the neutral plane height of the reference model.

Although using a finer grid cell size (5 cm) it shows a lower deviation with the results of the reference model for the actual HRR and the mass inflow rate. The differences between using 10 cm or 5 cm grid cell sizes are small (Figure 58 and Figure 59: cellulose fire). Except the result of the neutral plane height that shows a higher deviation with the results of the reference model by using a finer grid cell size.

With other words using a finer grid cell size does not result in a better fitted neutral plane height. All simulation results show a deviation within the 10% with the results of the reference model. The results of the simulation model with propane fire with 10 cm grid cell size shows a lower deviation with the results of the actual HRR and the mass inflow rate of the reference model. These results shows that using cellulose or propane fire will influence the results of the actual HRR and the mass inflow rate of a fire compartment.

5. Discussion

5.1 Experimental study

In this paragraph the use ability of this experimental research (Lee Y. , et al., 2007) is compared to the external flames of a ventilation controlled fire scenario in reality. Because the fire in the cubic scale experiment is completely dependent on the big mass inflow of the oxygen through the opening, this experimental study is well suited to be used for the validation of external flames in ventilation controlled fires with FDS 6.5.2. Through these big mass flows the small mass flows inside a fire compartment will be ignored in case of fire. Therefore the fire will not develop if there is no external opening in the cubic scale model. In all cases where external flames occur, it is assumed that the glass is already broken due to the high temperatures and thus high pressures.

As mentioned before in the cubic scale model the inflow of air is completely dependent on the inflow through the external opening. In fact in real compartment fires glass will break at a certain temperature and until this happens the inflow of air during the ignition stage is not determined by the inflow through the external opening. Thus the mass flow of air which is involved in the combustion is determined by other parameters, like by the air supply and air leaks in constructions. When fire occurs in an enclosure, most of the time the doors are open and there are several airflow differences in the fire compartment. This means the fire is not trapped in one area whereby external flames occur at a later stage. Not only the inflow of air determines the fire development but the fuel properties, amount of openings, location of opening, geometry of opening, fuel composition, façade cladding material, fire location and the wind direction.

Through lack of information not all measured variables are available or well documented and thus cannot be used for the validation study. Below the documented experimental results are given:

- Only the actual HRR inside the cubic scale model is given. The actual HRR outside the model is not shown. Therefore the actual HRR outside the model (HRR external flames) will be assumed as the difference between the theoretical HRR of the burner and the actual HRR inside the cubic scale model;
- The mass outflow rate through the external opening as result of the measured mass inflow rate was not measured during the experiments. Even the mass inflow rate is not shown by a graph during the experiments. Only the average mass inflow rate is given by the a empirical correlation during external flaming;
- The results of the measured gas temperature distribution at different heights is only given for the front corner. The results of the measured gas temperature distribution at the back corner is not shown;
- The neutral plane height and the external flame height are not visualized, only the results are given;
- The results for the façade heat flux is shown for only 7 locations instead of 21 locations;
- The material properties of fiberboard were not presented.

Although the mentioned poor documented results above, this cubic scale model can be used for the validation of a CFD model with external flames. The measured actual HRR outside the cubic model can be assumed as the difference between the theoretical HRR minus the measured actual HRR inside the cubic scale model. The missing measured mass outflow rate does not mean that the simulated mass outflow cannot be compared to the mass outflow rate of the experiments. If the simulated mass inflow rate shows similar results as the measured mass inflow rate it can assumed that the balance between inflow and outflow is similar as the experimental results. One measured thermocouple tree (front corner)

is enough to compare the simulated gas temperature with the measured gas temperature at different heights. For comparing the simulated neutral plane height and the external flame height only the measured heights are needed. A visualization will be unnecessary. The results of the simulated heat flux on the façade will be therefore compared to the results of the measured heat flux (7 locations). For the simulation model standard material properties of fiberboard can be assumed.

5.2 Validation study

For the validation study only well documented experimental results are simulated with both 2 cm and 1 cm grid cell size, like the actual HRR inside the scale model, the gas temperature at different heights (front corner), the average mass inflow rate through the opening and the neutral plane height. The measured façade heat flux and flame height are compared only with 1 cm grid cell size results, because the façade heat flux and thus the external flame height depends on the modelled actual HRR inside the model and the mass flow rate through the opening. If using 1 cm grid cell size shows a better agreement with the experimental results then the façade heat flux and the external flame should be simulated with 1 cm grid cell size as well.
For a grid sensitivity analyses without experimental results mostly three different grid cell sizes have to be simulated to investigate the differences. When the simulation results between two different grid cell sizes show small differences then the used grid cell size shows the most accurate simulation results. This is because the used finest grid cell size (1 cm) shows for the actual heat release rate, the mass inflow rate and the neutral plane height a deviation within 10%. Due to the fact that a finer grid cell size increases the computing time only two grid cell sizes are compared with the experimental results.

Model simplifications

Through lack of information the material properties (the used fiberboard) are assumed in the model. For all façades standard fiberboard plates properties are used. The material properties do not influence the actual HRR inside the model because the actual HRR inside will be simulated including the façades. Fiberboard plates of 0.020 m thickness are modelled while all facades consist of 0.025 m thick fiberboard plates in the experiments. A lower wall thickness in the model is used in accordance with the performed grid (restriction of the CFD package). Flow through objects with a minimum mesh resolution of 1 cm will be solved by FDS. Walls with 2.5 cm thickness difference will not be taken into account by using 1 cm grid cell size.

In the experiments one side is insulated (insulation board) at the outside of the façade in order to secure the steel plate gauge (heat flux sensor). This insulation board will not affect the actual HRR inside the scale model but the actual HRR outside the model will be different and thus the external flame. Because the measured actual HRR inside the scale model is determined based on the actual HRR outside the scale model the effect of the insulation board is taken into account. The insulation board is ignored outside the model.
Another measure aid in the experiments is the use of a horizontal fiberboard plate above the opening. The horizontal fiberboard plate is used to prevent heat transfer from flames to the steel plate gauge located above the opening centerline. The horizontal fiberboard plate is not simulated in the CFD model because the heat flux devices in FDS calculate the heat flux at a specific time. Heating up the heat flux sensor will not be taken into account by FDS.
One important simplification is that the airflow is completely determined by the external opening. No air leakage is included in the simulations. In reality air leakage often exist in the form of small cracks which will be smaller than the finest grid size in the simulation model. Air leakages in the experiment are extremely reduced so the influence is minimalized.

Measurement uncertainties

The measured actual HRR (Figure 33) shows an unpredictable progression when external flaming occurs. The measured actual HRR inside the scale model increases after the intermediate plateau. After approximately 4 minutes of external flaming the actual HRR inside the scale model increases to

the maximum HRR (50 kW). Increasing the actual HRR inside the scale model can only be obtained when unburned gases will burn inside the scale model. Experimental results show that external flames occur only during 4 minutes. After approximately 12 minutes there are no external flames outside the scale model. This unexpected behaviour of the actual HRR is strange because of the increased actual HRR inside the scale model. It seems that the HRR is captured inside the scale model.

The actual HRR outside the scale model is measured by a calorimeter hood but is not presented in the publications. If the actual HRR outside the scale model is presented by graphs the actual HRR inside and outside the scale model will be clearly compared with the simulated actual HRR. Because the simulated actual HRR outside the model is based on the simulated actual HRR inside the model. Despite these unpredictable actual HRR behaviour the results of the actual HRR during external flaming are well predicted by the use of CFD simulation software FDS.

Only the gas temperature distribution at the front corner is compared with the experimental results. Because the simulated gas temperature increases during the simulation time the gas temperature per height is taken at the end of the simulation time. These heights are compared with the measured gas temperature, although the presented gas temperature is the average gas temperature during external flaming. In the measurements the gas temperature per height is stabilized while the gas temperature from the simulations increases during the simulation time. Somehow comparing the simulated gas temperature with the measured gas temperature is not the best way. Because when the actual HRR inside the cubic scale model increases the measured gas temperature will increase as well. So this is why the measured gas temperature will not agree the simulated gas temperature distribution.

A CCD camera is used to determine the flame height during external flaming. The flame height is obtained based on the flame visibility. The boundary for a visible or non-visible flame is difficult to assign because it depends on human visibility. Previous research investigates the existence when visible flames occur. The visibility of the flame can be measured by the temperature or the HRR of the flame. Experimental results show which minimal flame temperature or minimal flame HRR is needed for a visible flame. Determination of the flame height which appears 50% of the time are until now not investigated. No literature is found about how to determine the flame height from simulated data. Two new methods are proposed in this master thesis to determine the flame height that appears 50% of the time, obtained from simulation results. These calculation methods should be validated with the measured external flame height. It is difficult to determine the best calculation method for the flame height while the results are compared with only one experiment.

5.3 Sensitivity of building and fire parameters

It is not surprisingly that the external flame height increases by shifting the door-like model to a window-like model, narrowing the opening and by increasing the theoretical HRR inside the model. Shifting the door-like model to a window-like model will increase the external flame most and thus the risk for fire spread to other floors because of the smaller distance to the upper floor. Decreasing the opening surface means a lower mass inflow rate through the opening which will result in a lower actual HRR. Therefore the external flame height will increase as well. Increasing the theoretical HRR will show an increased external flame height because of the increased actual HRR at the outside lower and upper part.

The results of the simulation model of the shifted door-like opening to a window-like opening increases the external flame height approximately 41% from the door-like opening model (reference model). Other parameters like using adiabatic constructions, narrowing the opening and increasing the theoretical HRR inside the model increases relatively the external flame from the validated external flame height. This increasement is the result of the decreased actual HRR inside the simulated models.
From the results of the sensitivity of building and fire parameter it can be concluded that predicting the actual HRR, mass inflow rate and the neutral plane height is possible by using the validated (new) linear

correlation for the opening geometry 0.2 m x 0.2 m. The simulation model with a narrowed opening size is not enough to investigate if this new linear correlation is useful for all other opening geometries. More simulations are needed to investigate if this new linear correlation can be helpful to predict the actual HRR and the mass inflow rate.

5.4 Full-scale fire compartment

Expanding the model to a full-scaled fire compartments needs to be verified and validated as well. In this research a CFD model with external flames is validated, so this model is used as a reference model with adiabatic construction. This reference model consists of a door-like opening instead of a window-like opening. Because the door-like opening model is simulated with adiabatic construction and therefore it is used as a reference model. Although in reality external flames occur through a window-like opening it will not affect the simulation results to answer the research sub-question.

The results show that using propane fire result in a lower deviation with the reference model (factor 10) compared to a cellulose fire source. However the deviation shows results within 10% from the reference model. A third model with finer grid cell should be modelled to investigate if using a smaller grid cell size will decrease the deviation with the reference model.

With the empirical correlation of the cubic scale model (propane fire) a cellulose fire in a full-scale compartment fire can not be predicted unless the cubic scale model will be simulated with a cellulose fire source as well. Because this cubic scale model is well validated with the experimental results it can be assumed that the results of the full-scaled fire compartment will result in accurate simulation results. Using a scale model will decrease the calculation time and will result in more accurate results. This has been proven by the results of the full-scale simulation model with propane fire (simulated by 10 cm grid cell size) which shows by similar amount of grid cells a higher deviation than calculated by the cubic scale model (simulated with 1 cm grid cell size). Depending on the fire scenario a scaled model can be used instead of a full-scale model for simulating the actual HRR inside the model, mass inflow rate and neutral plane height. For determining the external flame height a real fire compartment can not be scaled.

6. Conclusions

This master thesis is performed for the department Building Physics and Services at the University of Technology Eindhoven. The aim is to investigate the influence of different fire and building parameters on the external flame behaviour. The main research question and additional questions are answered below:

Which building or fire parameter will influence the external flame height most?
To answer this question the following results are simulated by a validated CFD model (FDS 6.5.2): the actual HRR, the mass inflow rate, the neutral plane height and the external flame height. All investigated fire and building parameters have influence on the external flame height. Below the investigated parameters are shown with their result from high influence (a) till low influence (d) on the external flame height (see, Table 6.1).

Table 6.1: The influence of different building and fire parameters on the external flame height.

	Parameter	**Influence on external flame height**	
a	window-like opening	↑41%	++++
b	narrowed door-like opening	↑35%	+++
c	increased theoretical HRR	↑22%	++
d	adiabatic constructions	↑12%	+

The external flame height of the simulation model with a window-like opening (simulation model 1) increases the external flame height by approximately 41% compared to the reference model (validated model). Other parameters like narrowing the opening (simulation model 2), using adiabatic constructions (simulation model 3) and increasing the theoretical HRR inside the model (simulation model 4) increases the external flame height as well but less compared to the window-like opening (simulation model 1).

How to determine the external flame height from simulation results?
To determine the external flame height from the simulation results two new calculation methods are proposed in this master thesis. The results show that using calculation method 1 a good agreement with the measured flame height is obtained. For calculation method 1 the flame temperature distribution per second is needed when external flames occur. The date set of the flame temperature per grid cell during the time is ranked by the boxplot method. Therefore a virtual flame is produced from all date sets of the temperature distribution.

What is the accuracy of a CFD model with external flames (FDS 6.5.2)?
The accuracy of the simulation results is validated by experimental results based on the literature study of a cubic scale model with external flames. From the validation study it is concluded that the results of the actual HRR, the mass inflow rate and the neutral plane height simulated with 1 cm grid cell size show an accuracy with a deviation within 10% compared to the measurements. The simulated gas temperature inside the model shows an average deviation of approximately 16% with the measurements. This is because of the increased actual heat release rate inside the scale model after approximately 12 minutes of ignition. This increase will influence the gas temperature inside at different heights. The other investigated variables are not affected by the increased actual heat release rate inside the cubic scale model. The simulated external flame height deviates 15% (calculation method 1) from the measured flame height. This is because the flame height in the experiment is measured based on the visibility and there is no fixed temperature which indicates a visible flame height.

From this validation study it can be concluded that a finer grid cell size is needed to determine the accuracy of external flames than the grid cell which is needed for flames inside compartment fires, see appendix II.

Is it possible to simulate a full-scale fire compartment by a scaled model?
From the simulation results the following can be concluded. Depending on the fire scenario a scaled model can be used instead of a full-scale model for simulating the actual HRR inside the model, mass inflow rate and neutral plane height. For determining the external flame height a real fire compartment can not be scaled.

Further research is needed to investigate a full-size fire compartment with propane fire and cellulose fire and a finer grid cell size. However these proposed simulations will require a long calculation time, depending on the computer performance and therefore not achievable for this master thesis. Further research is needed to conclude the reliability of a full-size model compared to a scale model.

Bibliografie

Bengtsson, L. G. (2001). *Enclosure fires.* Sweden: swidish rescue services agency.

Cox, G. (1995). Basic considerations in combustion fundamentals of fire. *Academic Press*, 1-30.

Gottuk, D. T., & Lattimer, B. Y. (2016). Effect of combustion conditions on species production. *SFPE Handbook of fire protection engineering*(5th), 486-527.

Heskestad, G. (1999). Flame heights of fuel arrays with combustion in depth. *Fire safety science-proceedings of the fifth international symposium*, 427-438.

Hoffmann, R. (1981). *Box Plot: Display of Distribution*. Opgehaald van Physics: http://www.physics.csbsju.edu/stats/box2.html

Ingason, H., Li, Y. Z., & Lönnermark, A. (2015). Fuel and ventilation controlled fires. In H. Ingason, Y. Z. Li, & A. Lönnermark, *Tunnel Fire dynamics* (pp. 23-32). New York: Springer.

Karlsson, B., & G.Quintiere, J. (2000). *Enclosure fire dynamics.* USA: CRC Press.

Law, M. (1991). Fire grading and fire behaviour. *Fire safety Journal 17*, 147-153.

Lee, Y., Delichatsios, M., Ohmiya, Y., Wakatsuki, K., Yanagisawa, A., & Goto, D. (2007). Flame heights and heat fluxes on a builing facade and an opposite building wall by flames emerging from an opening. *International Association for fire safety science*, 202-210.

Lee, Y.-P., Delichatsios, M. A., & Silcock, G. (2007). Heat fluxes and flame heights infacades from fires in enclosures of varying geometry. *Proceedings of the combustion institute 31*, 2521-2528.

Lee, Y.-p., Delichatsios, M. A., & Silcock, G. (2008). Heat flux distribution and flame shapes on the inert facade. *International association for fire safety science*, 193-204.

Lönnermark, A., & Björklund, A. (2008). *Smoke spread and gas temperatures during fires in retail premises- Experiments and CFD simulations.* SP Technical Research Institute of Sweden.

Maggio, M. (2011, august 26). *Maggie Maggio*. Opgehaald van Fire II: color and temperature: http://maggiemaggio.com/color/2011/08/fire-ii-color-and-temperature/

Mammoser, J. H., & Battaglia, F. (2002). A computational study on the use of balconies to reduce flame spread in high-rise apartment fires. *Fire Safety journal 39*, 277-296.

McGrattan, k., Hostikka, S., McDermott, R., Floyd, J., Weinschenk, C., & overholt, K. (2016). *Fire dynamics simulator technical reference guide Volume 1: Mathematical model .* USA: National institute of standards and technology NIST.

McGrattan, K., Hostikka, S., McDermott, R., Floyd, J., Weinschenk, C., & Overholt, K. (2016). *Fire Dynamics Simulator Technical References Guide Volume 2: Verification.* USA: National Institure of standards and technology NIST.

McGrattan, k., Hostikka, S., McDermott, R., Floyd, J., Weinschenk, C., & overholt, K. (2016). *Fire dynamics simulator user's guide .* USA: National institute of standards and technology NIST.

Orloff, L., & Ris, J. d. (1982). Froude modelling of pool fires. *Nineteenth symposium (international) on combustion/ the combustion institute*, 885-895.

Quintiere, J. G. (2002). Fire behavior in building compartments. *Proceedings of the combustion institute, volume 29*, 181-193.

Quintiere, J., & Rangwala, A. (2004). A Theory for flame extinction based on flame temperature. *University of Maryland, fire protection engineering*, 387-402.

Shakerchi-Ritmeijer, R. (2016). *Numerical simulation of external flames in under-ventilated fires-Literature study.* Eindhoven: FELLOW/fse.

Slater, J. W. (2008, Juli 17). *Uncertainty and error in CFD simulations*. Opgehaald van NPARC Alliance CFD verification and validation: https://www.grc.nasa.gov/WWW/wind/valid/tutorial/errors.html

Slater, J. W. (2008, Juli 17). *Validation Assesment*. Opgehaald van NPARC Alliance CFD verification and validation: https://www.grc.nasa.gov/WWW/wind/valid/tutorial/valassess.html

Slater, J. W. (2008, Juli 17). *Varification Assessment*. Opgehaald van NPARC Alliance CFD verification and validation: https://www.grc.nasa.gov/WWW/wind/valid/tutorial/verassess.html

Sugawa, O., & Momita, D. (sd). Flow Behavior of Ejected Fire Flame/plume from an Opening Effected by Bexternal Side Wind. *Fire Safety Science*, 249-260.

Tang, F., Hu, L., Delichatsios, M., Lu, K., & Zhu, W. (2011). Experimental study on flame height and temperature profile of buoyant window spill plume from an under-ventilated compartment fire. *International Journal of Heat and Mass transfer*, 93-101.

Unkleja, S., Delichatsios, M. A., Delichatsios, M. M., & Lee, Y.-p. (2008). Carbon monoxide and smoke production downstream of a compartment for under-ventilated fires. *International association for fire safety science*, 849-860.

Vaari, J., Dloyd, J., & Mcdermott, R. (2011). CFD simulations on extinction of co-flow diffusion flames. *VTT Technical Research Centre of Finland*, 781-793.

Vidal, M., Wong, W., Rogers, W., & Mannan, M. (2005). Evaluation of lower flammability limits of fuel air diluent mixtures using calculated adiabatic flame temperatures. *University of Texas, chemical engineering*, 21-27.

Zhao, G., Beji, T., & Merci, B. (2015). Application of FDS to Under-ventilated enclosure fires with external flaming. *Fire Technology*, 2117-2142.

Technische Universiteit
Eindhoven
University of Technology

Department of the Built Environment
Building Physics and Services

Den Dolech 2, 5612 AZ Eindhoven
P.O. Box 513, 5600 MB Eindhoven
The Netherlands
www.tue.nl

Numerical simulation of external flames in ventilation-controlled fires

Annexes

Supervisors:
prof. ir. W. (Wim) Zeiler
ir. R.A.P. (Ruud) van Herpen FIFireE
ir. I.M.M.M.C. (Ingrid) Naus

Author
ing. R (Reem) Shakerchi-Ritmeijer
0863348

Date
April 2017

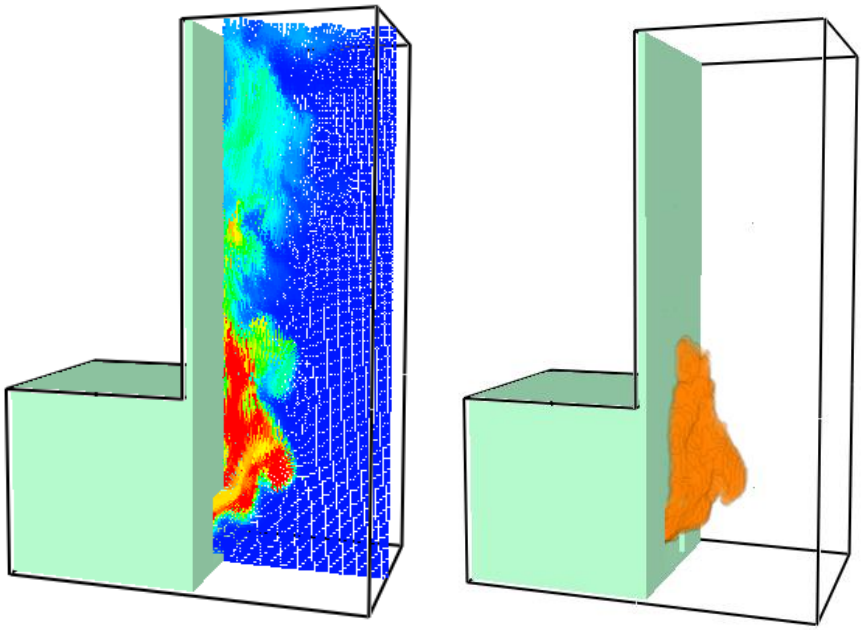

FELLOW/fse Stichting Fellowship FSE WO² Eindhoven
DPA Cauberg-Huygen

Appendix I: experimental study

Appendix I: experimental study - procedure

Below a detailed description about the experimental procedure is given.

The experimental procedure was designed to establish a steady state condition inside the scale model. To establish this steady state some adjustments were made, such as increasing the flow rate of the fuel (or increasing the HRR) at a fixed rate after its ignition until the desired flow is reached and the gas temperature in the scale model reaches a horizontal plateau. This procedure took approximately 15 minutes. To deflect the flames and thereby prevent the flames from impinging on the facade and imposing a heat flux on the steel plate gauges (heat flux sensor), a horizontal ceramic fiberboard plate was placed over the opening when flames start to appear outside of the opening. The horizontal ceramic fiberboard plate was removed after quasi-steady conditions were established inside the cubic scale model. After that the flames were attached to the façade exposing the façade heat flux gauges. This is done to measure the received heat flux on the façade which is caused by the external flames (Lee, Delichatsios, & Silcock, 2008).

Heat release rate

The actual HRR inside the scale model including the facades is measured by placing the model under a calorimeter hood meter which analyse the produced combustion gases (Figure 1). The rate of heat release in a fire enclosure can be estimated with measurements of the flow of the air through external openings and the concentration of oxygen in the exhaust stream (Huggett, 1980). Based on the measured actual HRR outside the cubic scale model the actual HRR inside the cubic scale model (including the facades) can be determined. The actual HRR inside the cubic scale model is the theoretical HRR which is produced by the propane burner minus the measured actual HRR outside the cubic scale model. This means that the sum of the measured actual HRR should equal the theoretical HRR of the propane burner.

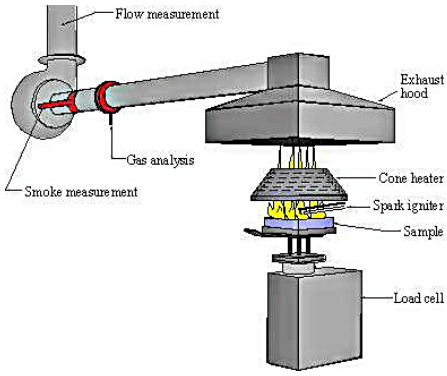

Figure 1: An example of the used calorimeter hood which measures the actual HRR outside cubic scale model.

Gas temperatures

Gas temperatures inside the cubic scale model were measured with two thermocouple trees at two diagonal corners having 6x 1.5 mm Type K thermocouple (Figure 2). The gas temperature inside the cubic scale model is measured at 6 different heights. The thermocouple tree is positioned 10 cm from the corners (front and back) as indicated with red dots in the cross section of Figure 5 (Lee, Delichatsios, & Silcock, 2008).

Figure 2: An example of a thermocouple tree with temperature sensors.

Flame heights and neutral plane

A CCD camera and an image-processing technique (Figure 3) were employed to map flame presence probability and to determine the extent of external combustion. The image processing technique (CDD camera) is used to determine flame height probability of 50% of the time and the neutral plane height during external flaming (Lee, Delichatsios, & Silcock, 2008). The neutral plane height is the height where there is no inflow and outflow through the external opening. This height indicates the hot layer (outflow) and cold layer (inflow) through the opening.

Façade heat flux

A steel plate gauge (heat flux sensor) was placed at the façade to measure the heat fluxes above the opening (Figure 4). When external flames occur this will influence the heat flux on the façade above the opening. Therefore the steel plate gauge is used to measure the façade heat flux at 21 different locations. Each three heat flux sensors are placed at the same height above the opening.

Because using a steel plate gauge is cheaper than using a Gardon gauge, heat fluxes with a steel plate gauge were calibrated with the Gardon gauge. The deviation between using a steel plate gauge instead of using Gardon gauge is less than 2%. Herewith it can be concluded that using a steel plate gauge instead of the Gardon gauge does not matter for the measured façade heat fluxes. In Figure 5 the steel plate gauge above the opening at 7 different heights on the front façade are shown (Lee, Delichatsios, & Silcock, 2008).

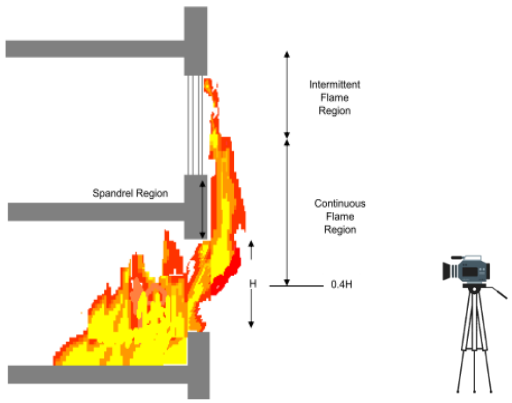

Figure 3: A schematic overview of the measurement procedure of determining the neutral plane height and flame height which appears 50% of the time.

Figure 4: An example of the used heat flux sensor on the façade.

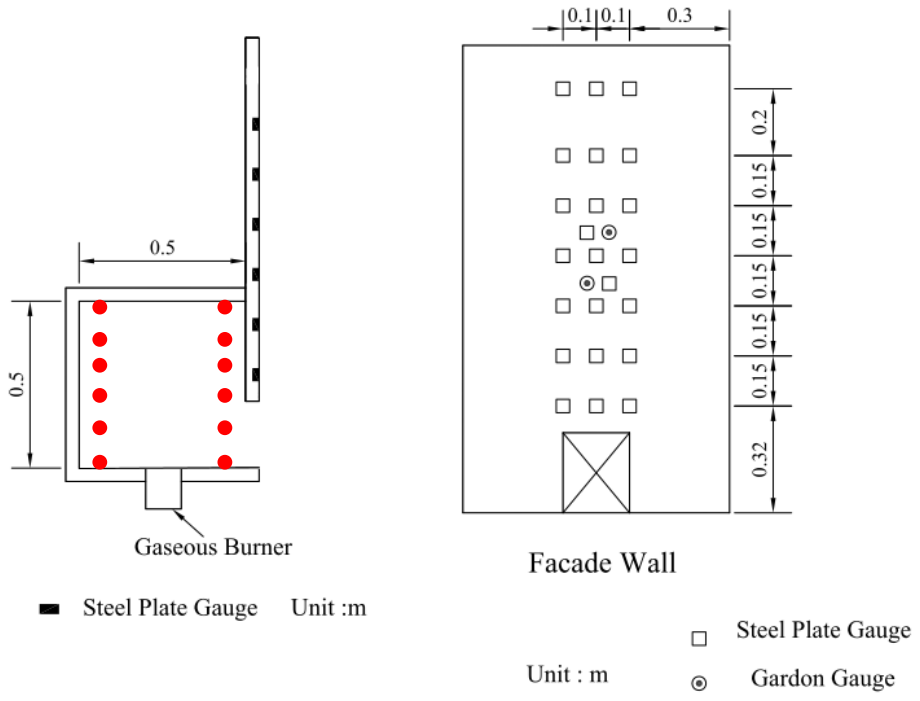

Figure 5: Left- the sketch of the experimental set-up, cross section cubic scale model. Right- the front view of the facade wall with their instrumentation (Lee Y. , et al., 2007).

Appendix II: article review

Appendix II: article review – University Ghent

In this appendix a validation study is performed with similar experimental results from literature. The CFD simulation results of the University of Ghent are compared to the measurement results. A new empirical correlation is designed based on the CFD simulation results. Below is a literature review given about the CFD results of this article.

Simulation model

The set-up in the modelling corresponds to the previously discussed experiments. The simulation model dimensions were 0.5 m x 0.5 m x 0.5 m. All facades consist of fiberboard plate (0.025 m). Below the material properties of the used fiberboard plate are given:

- Density of 350 kg/m³;
- Thermal conductivity of 0.3 W/m.K;
- Emissivity of 0.9;
- Heat capacity of 1700 J/kg.K.

By setting various widths and heights of the opening an under-ventilated condition has been obtained inside the simulation models. A 0.1 m x 0.2 m propane burner provides a fire source with a specific theoretical HRR inside the model. For each opening configuration different theoretical HRR are used (Figure 6a). In all simulation models a propane burner as fire source is located at the center of the models. Four different opening geometries are considered: 0.1 m x 0.2 m, 0.2 m x 0.2 m, 0.2 m x 0.3 m and 0.3 m x 0.3 m. In total 32 different models were simulated with FDS 6.0.1 (Table 1).

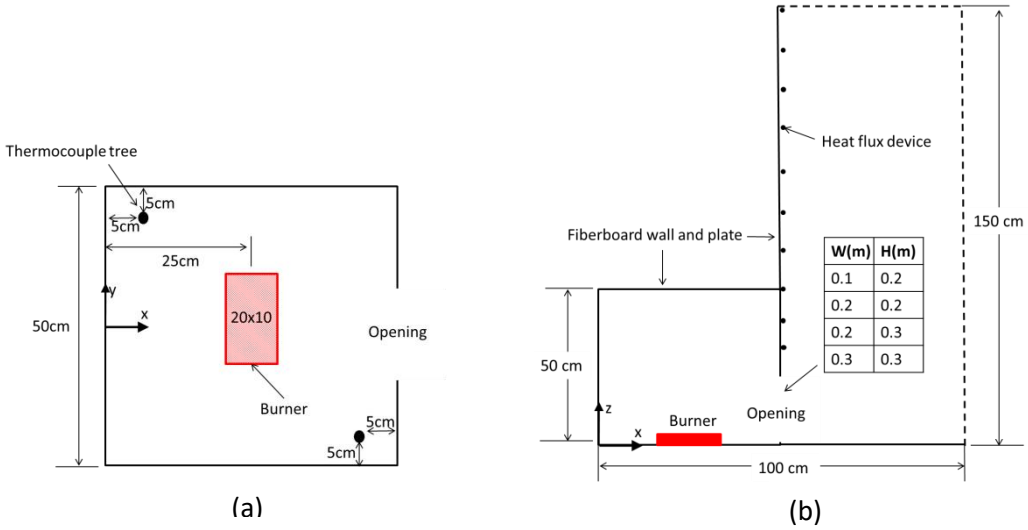

Figure 6: Sketch of the experimental set-up (Zhao, Beji, & Merci, 2015)
(a) Top view of the enclosure. (b) Side view of the enclosure.

The computational domain has been extended by 50 cm outside the model, as shown in Figure 6b, in order to limit the influence of the 'open' boundary condition on the flow field. Two meshes were used within the simulation domain. The first mesh contains inside the model and the lower part of the outdoor domain. The second mesh covers the rest of the domain (Figure 7b). The obstructions in the FDS model were made at least one grid cell thick. Most of studies show that FDS simulation results are sensitive to grid cell size. Smaller grid cells are generally preferred for more accurate simulations. However, such simulations will also be more expensive in terms of computational cost and storage requirement. Therefore, it is necessary to discuss the required grid resolution for the present study. In case of enclosure fires with external flaming, both the fire source and the vent flow need careful consideration. For the fire source a characteristic length scale D^* is related to the total heat release rate $\dot{Q}$ by the following relation:

$$D^* = \left[\frac{\dot{Q}}{\rho_\infty C_\infty T_\infty \sqrt{g}} \right]^{2/5} \quad (1)$$

In equation (1) $\dot{Q}$, ρ_∞ , C_∞ , T_∞ and g are respectively the total heat release rate (kW), the density at atmosphere gas (kg/m³), the specific heat of air (kJ/kg.K), the atmosphere temperature (K) and the gravity acceleration (m/s²). McGrattan suggested a cell size of 10% of the plume characteristic length D* as adequate resolution, based on careful comparisons with plume correlations. Based on this '10% criterion' the required cell size for a HRR between 30 kW and 90 kW is in the range of 2.3 cm to 3.6 cm. Besides the length scale concerning the fire source, it is also necessary to examine other length scales, concerning the accurate simulation of the flow through the opening. However, this length scale has not been considered systematically in a lot of numerical studies.

Table 1: List of simulations (Zhao, Beji, & Merci, 2015).

Opening geometry		$\dot{Q}_{in}$	Fire source	Grid	
W (m)	H (m)	(kW)	HRR $\dot{Q}$ (kW)	size (cm)	Case no.
0.1	0.2	13.42	30	4,2,1	1–3
0.1	0.2	13.42	40	4,2,1	4–6
0.2	0.2	26.83	50	4,2,1	7–9
0.2	0.2	26.83	60	4,2,1	10–12
0.2	0.2	26.83	70	4,2,1	13–15
0.2	0.3	49.30	60	4,2,1	16–18
0.2	0.3	49.30	70	4,2,1	19–21
0.2	0.3	49.30	80	4,2,1	22–24
0.3	0.3	73.94	80	4,2,1	25–27
0.3	0.3	73.94	90	4,2,1	28–30
0.2	0.2	26.83	30,40	1	31,32

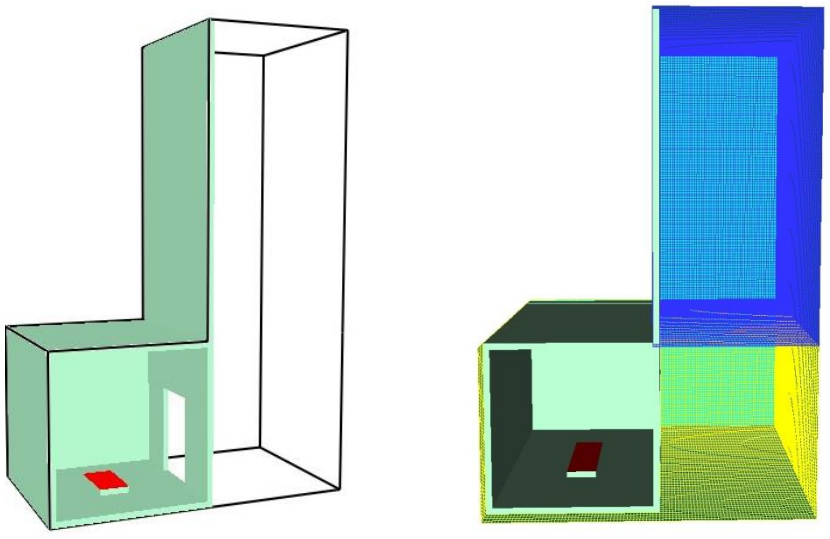

(a) (b)

Figure 7: Snapshots of the simulation domain and meshes (Zhao, Beji, & Merci, 2015)
(a) Model simulated by FDS 6.0.1. (b) Model with two mesh domains.

In this study 4 cm, 2 cm and 1 cm grid cell size are used for each simulation model. In order to get under-ventilated conditions all the HRR of the burner are set to be larger than the value of $1500\ A\sqrt{H}$ (Table 6.1.1). Using 1 cm grid cell size means that each cell has dimensions of 0.01 m x 0.01 m x 0.01 m and the total number of cells in the computational domain is 630 000 ((102x60x54)+(50x60x100)).

The total simulation time is 20 minutes from the ignition stage. The steady-state conditions compared to the experimental data should be reached after 8 minutes to 12 minutes. The simulation results which will be discussed in the following paragraph are mean values averaged during the steady-state conditions from 500 to 1200 seconds.

Simulated variables

During the simulation several variables are calculated with FDS. All measured variables are simulated during the 20 minutes from the ignition stage. Below the simulated variables are given:

- The actual HRR inside the model;
- The mass in- and outflow rate;
- The gas temperature inside the model (front and back corner);
- The gas temperature (opening);
- The air velocity (opening);
- The external flame height.

Procedure

In FDS version 6.0.1 the Navier-Stokes equations are solved by using a second order finite difference numerical scheme with a low-Mach number formulation. The turbulence model is based on Large Eddy Simulation (LES). Four models can be chosen for the sub grid-scale turbulent viscosity. FDS uses a combustion model based on the mixing scalar quantities that represent a mixture of species. A simple extinction model has been implemented in FDS which is based on a critical flame temperature (LFL). In cells where the temperature drops below this temperature LFL value combustion does not continue since the released energy cannot raise the temperature above the value for combustion to occur. A critical flame temperature of 1700 K has been used in the present study with a propane burner according to the experimental research.
A radiation fraction of 0.35 is prescribed as a lower bound in order to limit the uncertainties in the radiation calculation induced by uncertainties in the temperature field. Heat losses to the walls are calculated by solving the 1-D Fourier's equation for conduction. In the present study the default models and constants in FDS are applied.

Actual HRR

The actual HRR inside the model is calculated with FDS by integrating the HRR per unit volume "HRRPUV". The actual HRR inside the model including the facades will be calculated per second during 20 minutes. To investigate when external flames occur the actual HRR of the outside area is calculated as well. The sum of all calculated actual HRR should be the same as the input of the propane burner.

Mass in- and outflow

The mass inflow and outflow rates through the opening are simulated with FDS by two measurement devices at the level of the doorway called "Mass Flow +" and "Mass Flow -". These two measurements simulate only the inflow and outflow through the total external opening surface.

Gas temperature

The gas temperature at different heights is simulated for two purposes. The first purpose is to validate the simulated gas temperature inside the model with the experiments. The gas temperature inside the model is determined by a "THERMOCOUPLE" at different heights in two opposite corners (Figure 6). The simulated gas temperature is determined from floor level (Z= 0.04 m, 0.09 m, 0.14 m, 0.19 m, 0.24 m, 0.29 m, 0.34 m, 0.39 m, 0.44 m and 0.49 m).
The second purpose is to measure the average gas temperature through the opening during external flaming. The average gas temperature during external flaming is only simulated and therefore a "TEMPERATURE" device is used at different heights. It depends on the grid size which gas temperature heights are simulated through the opening. By using 2 cm grid cell size the average gas temperature is

determined between each 2 cm. If 1 cm grid cell size is used then the average gas temperature is determined between each 1 cm.

Air velocity

The average air velocity at different heights through the opening is determined by a "U-VELOCITY" device. The average horizontal air velocity is simulated during external flaming to determine the neutral plane height through the opening cross section. The neutral plane is when the air velocity is zero. This means there is no in- and outflow of air through this specific height. So the neutral plane can be determined when the air velocity through the opening is zero.

External flame height

In this study two different methods have been considered to determine the flame height of the ejected flames. The first method uses a temperature reference value to define when flames are visible. For the flame tip a minimum temperature reference value of TΔ= 500 ˚C is determined by Heskestad (Heskestad, 1999). The flame tip position is taken as the highest location outside the model where the time-averaged mean temperature is T= 520 ˚C (y= 0). In Figure 8 the time-averaged temperature distribution is given. All flame heights are determined from the neutral plane height.

In the second method the flame tip is determined from the heat release rate per unit volume (HRRPUV) of the external flame cross section. For this method two reference values of the HRRPUV are considered namely 0.5 MW/m³ (Cox, 1995) and 1.2 MW/m³ (Orloff & Ris, 1982). This means that if the simulated HRRPUV exceeds 0.5 MW/m³ or 1.2 MW/m³ a flame is supposed to be present.

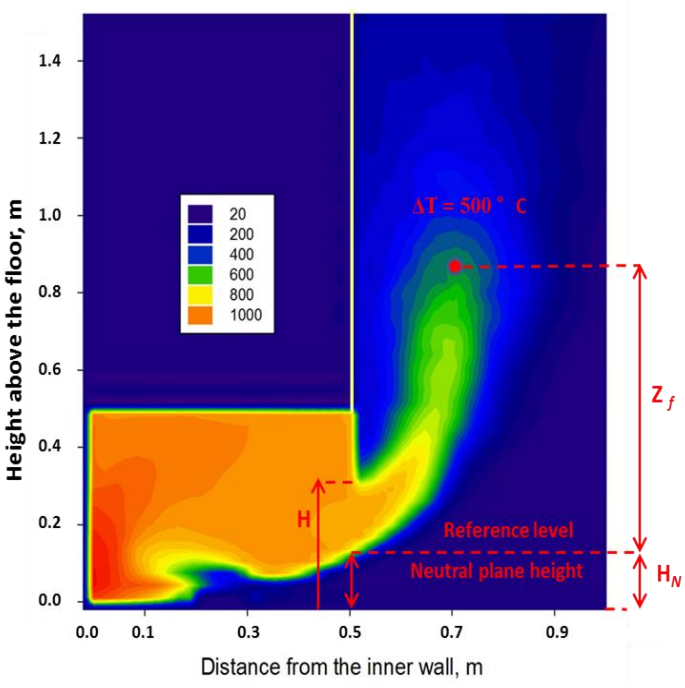

Figure 8: Time-averaged temperature contour plot showing the flame tip position and the neutral plane height (Zhao, Beji, & Merci, 2015).

Simulation results

In this paragraph all published simulation results are discussed. To determine which grid cell size shows the most accurate simulation results a grid sensitivity analysis is performed. The results of the grid sensitivity analysis are determined from the simulated averaged gas temperature and the simulated averaged air velocity at different heights through the external opening during external flaming. The results of the sensitivity analysis show that using 2 cm or 1 cm grid cell size shows a small difference in the results. However using 2 cm grid cell size shows accurate simulation results, the author simulates all CFD models with both grid cell sizes to investigate the empirical correlation of the simulated actual HRR and the mass inflow rate.

Actual HRR

The result of the averaged actual HRR inside the model during external flaming is approximately 25.0% below the measured average actual HRR inside the cubic scale model. This means that the simulated actual HRR does not comply with the empirical correlation of $1500\,A\sqrt{H}$. The constant value of 1500 kW/m$^{5/2}$ does not predict the actual HRR inside the model during external flaming. The constant value which is simulated complies with 1130.7 kW/m$^{5/2}$. This deviation is mainly related to the air inflow rate and the completeness of the use of oxygen for combustion inside the model.

Mass in- and outflow

The prediction of the average mass flow rate through the opening in under-ventilated conditions is of great importance, because it determines the extent of burning inside and outside the simulated model. The result of the averaged mass inflow rate during the combustion process is approximately 18.0% below the measured average mass inflow rate inside the cubic scale model. This means that the simulated mass inflow rate does not comply with the empirical correlation of $0.5\ A\sqrt{H}$. The constant value of 0.5 kg/s$^{5/2}$ does not predict the mass inflow rate through the opening. The constant value which is simulated complies with 0.41 kg/s$^{5/2}$. Figure 9 and Figure 10 show the inflow rate through an opening geometry of 0.2 m x 0.3 m and 0.3 m x 0.3 m. The average mass inflow rate calculated with the empirical correlation should equal 0.016 kg/s and 0.025 kg/s.

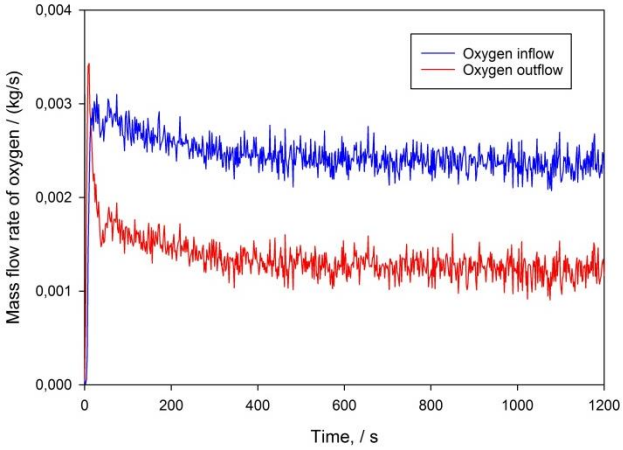

Figure 9: The simulated mass inflow rate of oxygen through the opening geometry 0.2 m x 0.3 m and a fire source of 80 kW inside the model, case 24 (Zhao, Beji, & Merci, 2015).

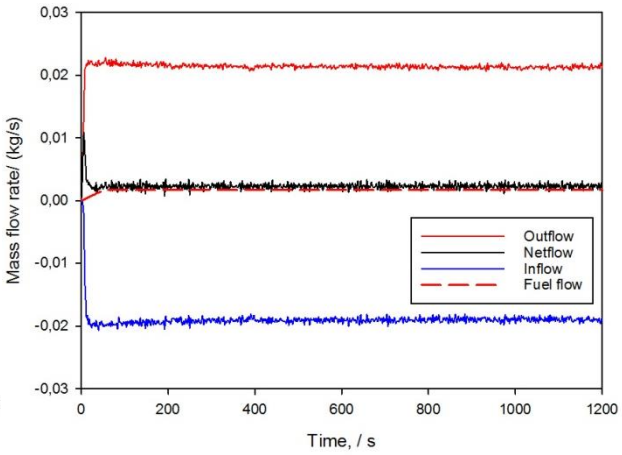

Figure 10: The simulated mass inflow rate of oxygen through the opening geometry 0.3 m x 0.3 m and a fire source of 80 kW inside the model, case 27 (Zhao, Beji, & Merci, 2015).

Gas temperature

The simulated gas temperature at different heights for two opposite corners (front and back) of different opening geometries is given in Figure 11. The temperature progression of the front and back corner are similar. Higher temperatures are observed for bigger openings and thus a higher actual HRR inside the model during external flaming.

The time-averaged gas temperatures at the front corner are compared with experimental data for case 8, 11, 31 and 32 (Figure 12). All these cases correspond to an opening size of 0.2 m x 0.2 m but with different theoretical HRR. Figure 12 shows that simulated gas temperatures of 10 cm height from floor level or above are approximately uniform. The selected graphs show the difference between measured and simulated gas temperatures. The simulated gas temperatures are under-predicted with an average deviation of 13.0% with the measured gas temperatures. This deviation can be related to the under-predicted actual HRR inside the cubic scale model. If the actual HRR inside is decreased the gas temperature inside the model will decrease as well.

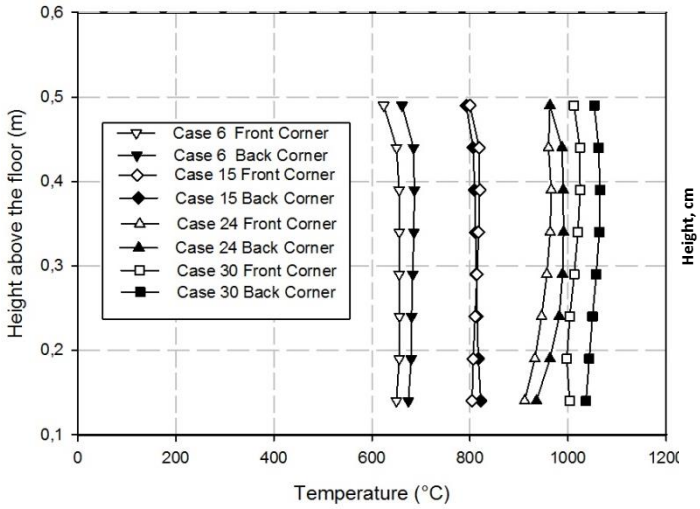

Figure 11: The temperature distribution inside the model obtained from the front and back corner thermocouple trees for four different opening geometries, see Table 6.1.1 for case numbers (Zhao, Beji, & Merci, 2015).

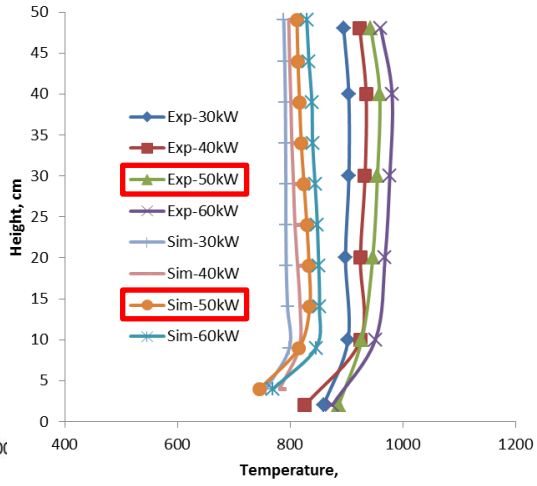

Figure 12: Comparison of average temperatures obtained with FDS 6.0.1 to experimental results for case 8, 11, 31 and 32, see Table 6.1.1 for case numbers (Zhao, Beji, & Merci, 2015).

Air velocity (opening)

At a certain height at the opening the horizontal velocity is zero. This height is called the 'neutral plane height'. The neutral plane height value is determined as the position where the average horizontal velocity profile crosses the dashed zero velocity line in Figure 13 and Figure 14. Figure 13 shows the average horizontal air velocity through the opening geometry 0.2 m x 0.3 m with a fire source of 80 kW simulated with 4 cm, 2 cm and 1 cm. Figure 14 shows the average horizontal air velocity through the opening geometry 0.3 m x 0.3 m with a fire source of 80 kW simulated with 4 cm, 2 cm and 1 cm. The average horizontal air velocity is calculated during external flaming (between 8 minutes and 20 minutes after the ignition).

The height of the neutral plane should be validated with the experimental results of the empirical correlation 0.4H. The external opening height of both models is 0.3 m high. This means that the simulated neutral plane of both models should equal 0.12 m. Figure 13 and Figure 14 shows that the calculated neutral plane is 0.12 m from floor level. Using 2 cm or 1 cm grid cell size show similar results concerning the neutral plane height.

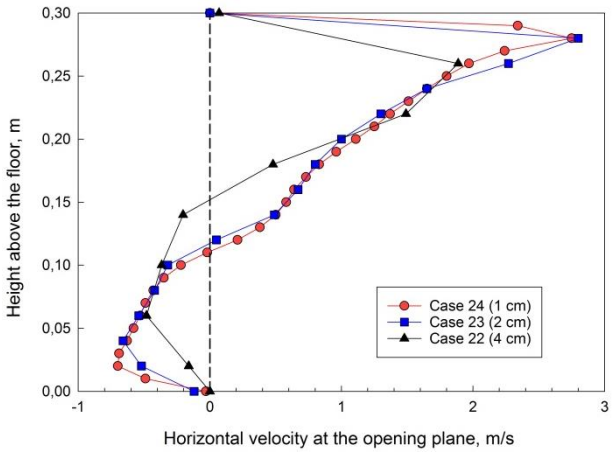

Figure 13: Cell size effect on the horizontal velocity along the centerline of the opening for an opening geometry of 0.2 m x 0.3 m and a fire source of 80 kW (Zhao, Beji, & Merci, 2015).

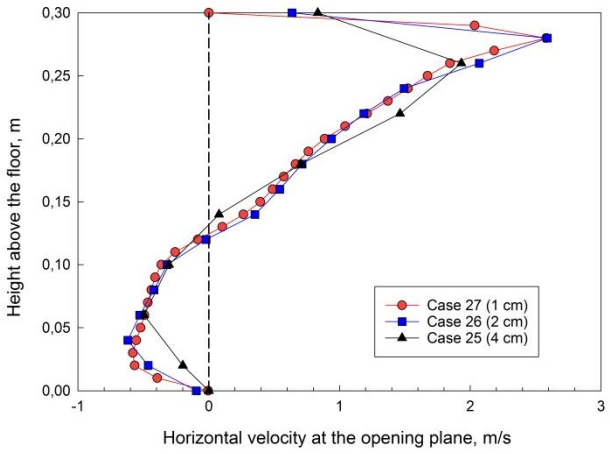

Figure 14: Cell size effect on the horizontal velocity along the centerline of the opening for an opening geometry of 0.3 m x 0.3 m and a fire source of 80 kW (Zhao, Beji, & Merci, 2015).

Gas temperature (opening)

The average gas temperature through the opening at different height is simulated as well. The average gas temperature through the opening is simulated during external flaming occurs. The gas temperature at the calculated neutral plane height can be determined. Figure 15 shows the gas temperature through the opening geometry 0.2 m x 0.3 m and Figure 16 shows the gas temperature through the opening geometry 0.3 m x 0.3 m. Both graphs show that using 2 cm grid cell size or finer is sufficient to ensure the grid insensitivity of the simulation results.

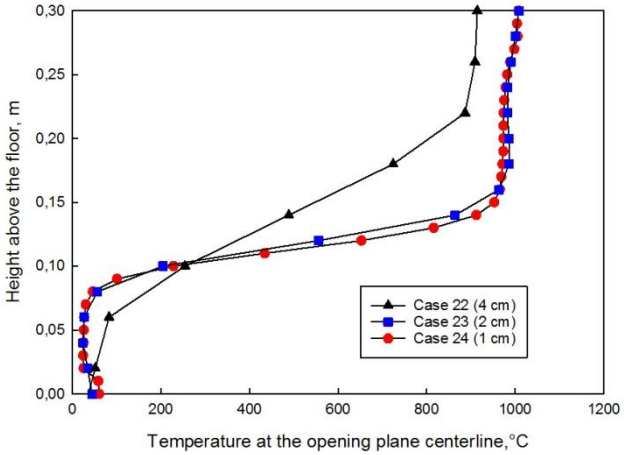

Figure 15: Cell size effect on the gas temperature along the centerline of the opening for an opening geometry of 0.2 x 0.3 m and a fire source of 80 kW (Zhao, Beji, & Merci, 2015).

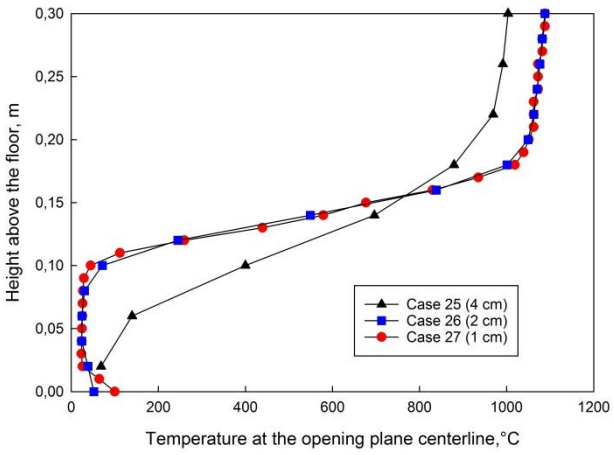

Figure 16: Cell size effect on the gas temperature along the centerline of the opening for an opening geometry of 0.3 x 0.3 m and a fire source of 80 kW (Zhao, Beji, & Merci, 2015).

External flame height

As mentioned before two different methods have been used in the post-processing of the simulation results to determine the flame height. The first one is used on a temperature reference value of 520 °C to define the flame tip. The second method is based on the heat release rate per unit volume (HRRPUV) of the flame. Two reference values of the HRRPUV are considered 0.5 MW/m³ and 1.2 MW/m³. If all these reference values are exceeded a flame is supposed to be present. All calculated flame heights are determined from the neutral plane height (0.4H), see Table 6.4. 1.

For the same ventilation factor the amount of fuel consumed inside the enclosure should remain approximately the same. For a higher total HRR more excess fuel will burn outside and a higher flame height value is expected. This is confirmed in the results regardless of the method used the flame height value increases with the fire HRR. And the obtained results using 0.5 MW/m^3 are higher than using 1.2 MW/m^3. When using temperature based method FDS over-predicts the external flame height with a maximum relative deviation of approximately 18.0% (case 8). When using HRRPUV based method (e.g., taking 1.2 MW/m^3 as reference value) FDS over-predicts the external flame height with a maximum relative deviation of approximately 21.0% (case 8). From these results it can be concluded that it is important to use a correct method for the flame height determination.

Table 6.4. 1: Comparison of the flame height calculated from the neutral plane by using different methods between simulation results and experimental results for the opening geometries 0.2 m x 0.2 m (Zhao, Beji, & Merci, 2015).

Case No.	HRR_{Total} (kW)	$Z_{f\text{-}exp}$ (m)	$Z_{f\text{-}hrrpuv\ (1.2MW/m^3)}$ (m)	$Z_{f\text{-}hrrpuv\ (0.5\ MW/m^3)}$ (m)	$Z_{f\text{-}tem\ (520\ °C)}$ (m)	$(Z_{f\text{-}hrrpuv\ (1.2)}-Z_{f\text{-}exp})/Z_{f\text{-}exp}$ (%)	$(Z_{f\text{-}hrrpuv\ (0.5)}-Z_{f\text{-}exp})/Z_{f\text{-}exp}$ (%)	$(Z_{f\text{-}tem}-Z_{f\text{-}exp})/Z_{f\text{-}exp}$ (%)
11	60	0.70	0.87	1.09	0.81	24.51	56.00	15.71
8	50	0.56	0.67	0.77	0.66	20.52	38.51	17.85
31	40	0.40	0.45	0.58	0.46	12.74	45.30	15.00
32	30	0.34	0.37	0.49	0.37	9.38	44.85	8.82

Discussion

This research is performed at the University of Ghent to investigate the accuracy of using CFD models with external flames of ventilation-controlled fires. Therefore a CFD model of 0.5 m x 0.5 m x 0.5 m is simulated by FDS 6.0.1 and is validated with experimental results.

Not all results of the validated CFD model are presented in the scientific article. Through lack of information it is difficult to judge if these results are suitable for predicting the external flames in ventilation-controlled fires. Below the research gaps are given:

- The simulated actual HRR inside the model is not presented for all 32 simulation models with the measured actual HRR inside the cubic scale model.
- The simulated in- and outflow through the opening of the validated model is only presented for the geometry openings of 0.2 m x 0.3 m and 0.3 m x 0.3 m. Only the deviation and the new empirical correlation are given for the simulated actual HRR (inside) and the simulated mass inflow rate through the opening geometry 0.2 m x 0.2 m. It can be helpful if the deviation between simulated and measured data results were shown in one graph.
- In the experimental set-up 7 heat flux sensors are placed above the opening at different heights. In this research 10 heat flux devices are placed above the opening at different heights. The results of the simulated heat flux are calculated by FDS but not presented and thus not compared with the experimental results.
- The oxygen concentration inside the model is not presented. The oxygen concentration shows when the fire becomes ventilation-controlled. Using a critical flame temperature of 1700 K shows that the oxygen concentration inside the model is zero when external flames occur.
- The results of the average gas temperature and the average horizontal air velocity through the opening are given for the opening geometries 0.2 m x 0.3 m and 0.3 m x 0.3 m. The calculated neutral plane height of both models is 0.12 m high because of the empirical correlation of 0.4H. These results belong not to the validated model with experimental results. Based on this simulation results it can be concluded that using a 2 cm grid cell size shows accurate simulation results.
- The flame height is determined from the temperature cross-section (y=0). The time-averaged temperatures are calculated per cell. The time-averaged temperature distribution is used to validate the simulated external flame height with the measured flame height of external flaming. The used calculation method will not result in the measured flame height which appears 50% of the time. The measured flame height is 0.59 m from the neutral plane height. The simulated flame height is compared with 0.56 m from neutral plane height, see Table 6.4. 1.

From the results of this research it can be concluded that the simulated results deviate with the experimental results. Despite all these uncertainties above, this CFD simulation model will be used for a new validation study with FDS 6.5.2. Some of the assumptions and basic principles from this research may be partially implemented for the following validation study with the newest version of FDS (FDS

6.5.2). To perform a good validation study all measured variables should be simulated by FDS. In this research it is assumed that the CFD simulation results shows similar results by using FDS 6.0.1 or FDS 6.5.1. This means that all simulated variables should be compared to the experimental results. For a better comparison with the experimental results some of the applied assumptions have to be adjusted. Below all adjustments to the model are presented which will be done for the next validation study with the same experimental results:

- Both simulated thermocouple trees are located 5 cm from the front and back corner. In the experiments the used thermocouple trees are located 10 cm from the front and back corner. This means that the simulated results are not comparable with the measured thermocouple tree results. In the next validation study the thermocouple tree will be simulated 10 cm from the front corner. This means that only the simulated thermocouple tree of the front corner will be used. The results of the measured thermocouple tree at the back corner are not available and therefore not simulated.
- The simulated thermocouple tree is located at 10 different heights (Z= 0.04 m, 0.09 m, 0.14 m, 0.19 m, 0.24 m, 0.29 m, 0.34 m, 0.39 m, 0.44 m and 0.49 m) while the measured temperature heights are located at 6 different heights. The measured temperatures are located at Z= 0.00 m, 0.05 m, 0.10 m, 0.20 m, 0.30 m, 0.40 m and 0.50 m. In the next validation model the temperature at 6 different heights will be simulated (Z= 0.01 m, 0.05 m, 0.10 m, 0.20 m, 0.30 m, 0.40 m and 0.49 m). The simulated temperature should be 1 cm from the floor and ceiling, otherwise the wall temperature will be simulated.
- The measured façade heat flux is located at 7 different heights from floor level (Z= 0.32 m, 0.47 m, 0.62 m, 0.77 m, 0.92 m, 1.07 m and 1.27 m). These different heights will be used to simulate the heat flux on the façade by FDS. The results of the simulated heat flux will be compared with the experimental results.
- The oxygen concentration will be simulated at different heights to check if external flames occur because of a limited oxygen concentration inside the model.
- The burner in the experiments is modelled as a rectangular sandbox below the cubic scale model. In the simulated model the burner inside the model is positioned at 2 cm from floor level. In the next validation study the burner will be simulated at floor level like in the experimental research.
- In this validation study for the radiative fraction 0.3 is used for the propane fires while in FDS a radiative fraction of 0.35 is preferred for propane fires. In the next validation study a radiative fraction 0.35 for propane fires will be used in FDS.
- A new calculation method will be investigated to calculate the flame height which occurs 50% of the time. The flame height will only be determined from the temperature distribution because an increased temperature results in an increased HRRPUV. Thus using different criteria for the flame height will in fact always show different flame heights.

Based on the grid sensitivity analysis 2 cm grid cell size will be used for all measured variables. By using 2 cm grid cell size all simulated variables will be compared with the experiments. An additional 1 cm grid cell size will be used to verify the difference between the results simulated with 2 cm grid cell size or 1 cm grid cell size (grid sensitivity analysis). Thus in the next validation study two grid cell sizes will be compared with the experimental results.

Conclusion

Numerical simulations of under-ventilated enclosure fires with external flames have been discussed. FDS version 6.0.1 has been applied with the default settings. Four different opening geometries are considered: 0.1 m x 0.2 m, 0.2 m x 0.2 m, 0.2 m x 0.3 m and 0.3 m x 0.3 m. There are 32 simulations with different theoretical HRR inside the models. The accuracy of the obtained results have been discussed and compared with the experimental data and empirical correlations (Lee Y. , et al., 2007), (Lee, Delichatsios, & Silcock, 2007), (Lee, Delichatsios, & Silcock, 2008).

Due to the importance of the flow through the opening the required fineness of the grid has been discussed by analysing the length scale for cell grid size calculations (McGrattan). The results of the simulated horizontal air velocity and the simulated gas temperature show that using 2 cm grid cell size provides accurate simulation results.
The actual heat release rate inside the model obtained from FDS shows a linear relationship with the ventilation factor. The linear regression coefficient is 1130.7 kW/m$^{2.5}$, which is lower than the 'classical' value 1500 kW/m$^{2.5}$. The result of the averaged actual HRR inside the model during external flaming is approximately 25.0% below the measured average actual HRR inside the cubic scale model. This has been explained by the lower mass flow rate of incoming air and incomplete consumption of oxygen flowing into the compartment. The air inflow rate through the opening is found correlating linearly to the ventilation factor $C.A\sqrt{H}$. The obtained C value is 0.41 which means a deviation of 18.0% with the experimental results.

The simulated gas temperatures at different heights of two opposite corners do not show identical temperatures. The average deviation between the simulated and measured gas temperature of different height is approximately 13.0%. Two methods, namely a temperature based method and a volumetric heat release rate based method were employed to define the flame height. The external flame height is over-predicted by these methods which is in line with the presumed under-prediction of the heat release rate inside the model and the mass flow rate through the opening. If the heat release rate and mass inflow are under-predicted there is relatively more excess fuel which leads to combustion outside the model. The flame height calculated with the time-averaged temperature distribution shows the lowest deviation with the experimental results (18.0%). Although there are still deviations between simulated and measured variables the neutral plane height for various configurations shows accurate results with the empirical correlations.

Appendix III: external flame height

Appendix III-a: calculation method 1

The advantage and disadvantages of calculation method 1 is given below. This calculation method is established to determine the external flame height which is caused by a ventilation-controlled fire.

Method 1

The first method determines the flame height from all temperature cross sections of external flaming ($\Delta t = 720\ s$). Each cross section shows the temperature distribution per second. Figure 17 shows an example of the temperature cross section along the opening centerline. The simulated temperature cross section is calculated during external flaming with 1 cm grid cell size. The flame height outside the model is determined by a virtual temperature distribution.

The virtual temperature distribution is obtained from the temperature per grid cell during 12 minutes of external flaming. Per grid cell the minimum, maximum, median, first quartile and third quartile is calculated as a virtual flame visualization. This means that the simulated temperature of each grid cell is ranked by the boxplot during external flaming.

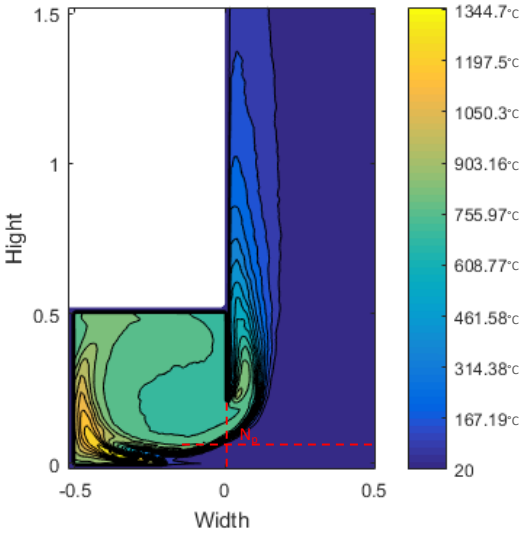

Figure 17: An example of the simulated temperature distribution cross section during external flaming with use of Matlab. The red dotted line shows the neutral plane height where the velocity is zero.

The flame height which occurs 50% of the time is determined from the calculated virtual temperature distribution. The flame height is calculated when outside a flame tip of 520 °C ($\Delta t = 500$ °C and $t_{ambient}$= 20 °C) is reached. Below the advantages and disadvantages of using calculation method 1 are given.

Advantages

- Shows the flame height which appears 50% of the simulation time;
- The flame height is calculated based on the temperature per grid cell;
- This calculation method eliminates the high and low temperatures because of data ranking.

Disadvantages

This calculation method shows a virtual temperature distribution of all simulated records during external flaming. The flame height is calculated from this virtual visualization.

Appendix III-b: calculation method 2

The advantage and disadvantages of calculation method 2 is given below. This calculation method is established to determine the external flame height which is caused by a ventilation-controlled fire.

Method 2

The second method is to determine the visibility of the external flame from the simulated flame temperature distribution per second. This means the flame height is calculated per second (720 s). The flame height at the first seconds of external flaming will be low. By increasing the simulation time the flame height will increase at the end of the simulation time. Because of the increased actual HRR outside the model the temperature and thus the flame height will increase as result. All flame heights are sorted by the boxplot from the begin of the simulation (low) to the end of the simulation (high). This information can be used to view the fluctuations in flame height during external flaming (Figure 18). In this calculation method the minimum, maximum, median, first quartile and third quartile are calculated from one specific record. Below the advantages and disadvantages of using calculation method 2 are given.

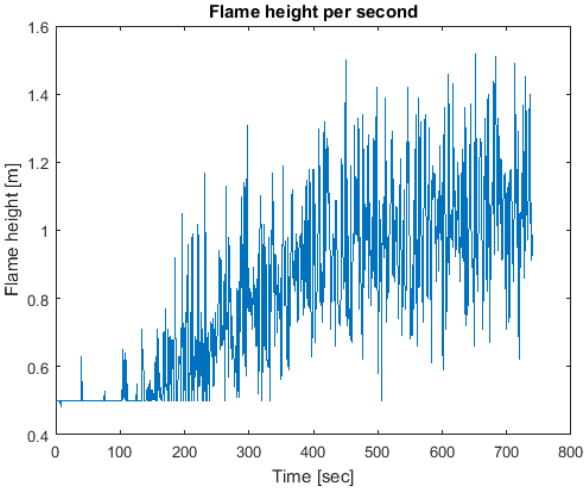

Figure 18: The flame height calculated per simulated temperature distribution during external flaming (method 2) given by Matlab.

Advantages

- The flame height is calculated from each simulated temperature distribution;
- The flame height per second is viewed during external flaming;

Disadvantages

- Shows only one second record;
- Viewing the flame height per second does not show the influence of the simulated temperature distribution between each second;
- Calculating the flame height which occurs 50% of the time is averaged based on the flame height between Q1 and Q3;
- Determining the flame height with this method shows more results for the same median, maximum and minimum flame height.

Appendix IV: FDS/Matlab script

Appendix IV-a: fds2ascii script

This script is needed to generate from fdsascii the temperature distribution per second during the period of external flaming. The period of external flaming can be determined from the actual HRR inside the model. The temperature distribution per second should be exported for both domains.

```
'------------Script config------------------
Const TEMP = 13 'number of exported variable, depends on the export data
Const mesh = "H" 'can be changed in "H" (mesh 2) or "L"(mesh 1)
Const StepSize = 1 'every second the data will be saved
Const strStartTime = 360 'start time external flaming [s]
Const strStopTime = 1200 'end time external flaming [s], mostly the end of
the simulation time
'-------------------------------------

'Const ForReading = 1
'Const ForWriting = 2
Const DontShowWindow = 0
Const WaitUntilFinished = true

'Dim rfso
Dim wfso
Dim oShell

'Set rfso = CreateObject("Scripting.FileSystemObject")
Set wfso = CreateObject("Scripting.FileSystemObject")
Set oShell = WScript.CreateObject ("WScript.Shell")

'Set timeObjFile = rfso.OpenTextFile("fds2ascii-time.txt", 1)
'Set timeObjFile = rfso.OpenTextFile("fds2ascii-time.txt", ForReading)

'strStartTime = timeObjFile.Readline
'strStopTime = timeObjFile.Readline

'timeObjFile.Close

For i=strStartTime to strStopTime-1 Step StepSize 'i is the counter
variable and it is incremented by 2
      Set configObjFile = wfso.OpenTextFile("fds2ascii-configs.txt", 2)
      'Set configObjFile = wfso.OpenTextFile("fds2ascii-configs.txt",
ForWriting)
      strContents = "validated model" & vbNewLine & "2" & vbNewLine & "1" &
vbNewLine & "n" & vbNewLine & i & " " & i+StepSize & vbNewLine & "1" &
vbNewLine & TEMP & vbNewLine & "TEMP" & TEMP & "_" & mesh & i+StepSize &
".csv" & vbNewLine
      configObjFile.Write(strContents)
      configObjFile.Close
      command = "cmd /c fds2ascii.exe < fds2ascii-configs.txt"
      oShell.Run command, DontShowWindow, WaitUntilFinished
Next

'Set configObjFile = objFSO.OpenTextFile("fds2ascii-time.txt", ForReading)
'strText = objFile.ReadAll
'objFile.Close
'strNewText = Replace(strText, "Jim ", "James ")
'Set objFile = objFSO.OpenTextFile("C:\Scripts\Text.txt", ForWriting)
'objFile.WriteLine strNewText
'objFile.Close
```

Appendix IV-b: Matlab script

This Matlab script reads all fdsascii output for the temperature distribution per second per domain. From these temperature distributions two calculation methods are investigated. Flame height of both calculation methods are calculated with this Matlap script.

```
clear all
close all
% ------------------------- Self defines ------------------------------
startOfSampleTime   = 460;    % start time external flaming [s]
stopOfSampleTime    = 1200;   % end time external flaming [s]
sampleStep          = 1;      % step size
mesh1           = 'L';        % mesh 1 (low)
mesh2           = 'H';        % mesh 2 (high)
aveTemp         = 13;         % number of exported variable for mesh 1
medQ2Temp       = 37;         % number of exported variable for mesh 2
meshStep        = 0.01;       % grid step [m]

mesh1Xstart     = -0.52;      % read from starting grid point of mesh 1 [m]
mesh1Xstop      = 0.50;       % read till end grid point of mesh 1 [m]

mesh1Zstart     = -0.02;      % read from starting grid point of mesh 1 [m]
mesh1Zstop      = 0.52;       % read till end grid point of mesh 1 [m]

mesh2Xstart     = 0.00;       % read from starting grid point of mesh 2 [m]
mesh2Xstop      = 0.50;       % read till end grid point of mesh 2 [m]

mesh2Zstart     = 0.52;       % read from starting grid point of mesh 2 [m]
mesh2Zstop      = 1.52;       % read till end grid point of mesh 2 [m]

flameThreshold  = 520;        % Flame tip threshold temperature [˚C]
% ---------------------------------------------------------------------
% ------------------ Auto build (amount of grid cells)-----------------
simulationTime     = stopOfSampleTime-startOfSampleTime; % Total cell grids
numberOfX1samples  = length(mesh1Xstart:meshStep:mesh1Xstop); % Number of X
Samples for mesh 1
numberOfZ1samples  = length(mesh1Zstart:meshStep:mesh1Zstop); % Number of Z
Samples for mesh 1

numberOfX2samples  = length(mesh2Xstart:meshStep:mesh2Xstop); % Number of X
Samples for mesh 2
numberOfZ2samples  = length(mesh2Zstart:meshStep:mesh2Zstop); % Number of Z
Samples for mesh 2

flameHeightPerTime  = nan(1,simulationTime); % flame height per second
flameHeightPerTimeOut = nan(1,simulationTime); % external flame height per
second
finalFlameHeight   = nan(1,10); % all flame heights (saved in one file)

% Calculating the total grid size of all points
minX    = min([mesh1Xstart mesh2Xstart]);
maxX    = max([mesh1Xstop mesh2Xstop]);
minZ    = min([mesh1Zstart mesh2Zstop]);
maxZ    = max([mesh1Zstart mesh2Zstop]);

numberOfXsamplesInMat = length(minX:meshStep:maxX); % Number of X Samples
for the total mesh
numberOfZsamplesInMat = length(minZ:meshStep:maxZ); % Number of Y Samples
for the total mesh
```

```
% this section is for plot, image processing and data read:
% inputMat contains the total inputs (for all readings)
inputMat  = nan(numberOfZsamplesInMat,numberOfXsamplesInMat,
simulationTime);
% resultMat contains the total inputs with some results (it can not be
presented due to its size)
resultMat = nan(numberOfZsamplesInMat,numberOfXsamplesInMat, 10); % for 10
results, it can be used such as average, median, std etc.

minimumTempOfmodel = 1000;
maximumTempOfmodel = 0;
minimumTempOfOutside = 1000;
maximumTempOfOutside = 0;
counter = 1;

% loading all data from csv's (depends on the mesh position)
for i=startOfSampleTime+1:sampleStep:stopOfSampleTime
    filename1 = sprintf('temp%d_%s%d.csv',aveTemp,mesh1,i);
    filename2 = sprintf('temp%d_%s%d.csv',medQ2Temp,mesh2,i);

    for j=1:sampleStep:numberOfZ1samples
        inputMat(j,:,counter) = csvread(filename1,2+(numberOfX1samples*(j-
1)),2, [ 2+(numberOfX1samples*(j-1)) 2 (j*numberOfX1samples)+1 2]); % is
not good because its fixed !
    end

    for h=1:sampleStep:numberOfZ2samples
        inputMat(j+h-1,numberOfXsamplesInMat-
numberOfX2samples+1:numberOfXsamplesInMat,counter) =
csvread(filename2,2+(numberOfX2samples*(h-1)),2, [ 2+(numberOfX2samples*(h-
1)) 2 (h*numberOfX2samples)+1 2]); % is not good yet because its fixed !
    end
    counter = counter + 1;
end

% Calculating temperature per grid cell (ave,med,std)
%  min,max are among all points
for i = 1:numberOfZsamplesInMat
    for j = 1:numberOfXsamplesInMat
% Creating a temporary vector to hold the all measurements at pixel (i,j)
        tmpVec = zeros(1,simulationTime);
        for h = 1:simulationTime
            tmpVec(h) = inputMat(i,j,h);
        end

% Calculating min and max temperature of all grid points of the model among
all reads
        minT = min(tmpVec);
        maxT = max(tmpVec);
        if (minT<minimumTempOfmodel)
            minimumTempOfmodel = minT;
        end
        if (maxT>maximumTempOfmodel)
            maximumTempOfmodel = maxT;
        end

        Q2 = median(tmpVec);  %median Q2 temperature
        Q1 = median(tmpVec(tmpVec<=Q2)); %median Q1 temperature
        Q3 = median(tmpVec(tmpVec>=Q2)); %median Q3 temperature
```

```
        aveBtwnQ1andQ3 = mean(tmpVec(tmpVec>=Q1 & tmpVec<=Q3)); %average
temperature of all samples between median Q1 and median Q3
        aveBtwnQ2andQ3 = mean(tmpVec(tmpVec>=Q2 & tmpVec<=Q3)); %average
temperature of all samples between median Q2 and median Q3
        aveBtwnQ1andQ2 = mean(tmpVec(tmpVec>=Q1 & tmpVec<=Q2)); %average
temperature of all samples between median Q1 and median Q2

        resultMat(i,j,1) = std(tmpVec); % standard deviation for point
(i,j) among all sample reads
        resultMat(i,j,2) = Q2; % median (Q2) for point (i,j) among all
sample reads
        resultMat(i,j,3) = mean(tmpVec);  % average for point (i,j) among
all sample reads
        resultMat(i,j,4) = max(tmpVec); % maximum for point (i,j) among all
samples reads
        resultMat(i,j,5) = min(tmpVec); % minimum for point (i,j) among all
samples reads
        resultMat(i,j,6) = Q1; % Q1 (median from minimum to median Q2) for
point (i,j) among all sample reads
        resultMat(i,j,7) = Q3; % Q3 (median from median Q2 to maximum) for
point (i,j) among all sample reads
        resultMat(i,j,8) = aveBtwnQ1andQ3; % average from Q1 to Q3 for
point (i,j) among all sample reads
        resultMat(i,j,9) = aveBtwnQ2andQ3; % average from Q2 to Q3 for
point (i,j) among all sample reads
        resultMat(i,j,10)= aveBtwnQ1andQ2; % average from Q1 to Q2 for
point (i,j) among all sample reads

% Calculating the minimum and maximum temperature of the outside points of
the model among all samples
        if(i>numberOfXsamplesInMat-numberOfX2samples)
            if (minT<minimumTempOfOutside)
                minimumTempOfOutside = minT;
            end
            if (maxT>maximumTempOfOutside)
                maximumTempOfOutside = maxT;
            end
        end
    end
end

[allx,allz] = meshgrid(minX:meshStep:maxX,minZ:meshStep:maxZ);
stdTemp     = resultMat(:,:,1);
medQ2Temp   = resultMat(:,:,2);
aveTemp     = resultMat(:,:,3);
maxTemp     = resultMat(:,:,4);
minTemp     = resultMat(:,:,5);
medQ1Temp   = resultMat(:,:,6);
medQ3Temp   = resultMat(:,:,7);
aveQ1Q3Temp = resultMat(:,:,8);
aveQ2Q3Temp = resultMat(:,:,9);
aveQ1Q2Temp = resultMat(:,:,10);

% Cutting the total mesh, reading only outside temperature distribution:
% starting off with creating mesh grid size outside without the walls
[outx,outz] = meshgrid(mesh2Xstart:meshStep:mesh2Xstop,minZ:meshStep:maxZ);
%cell location
% copy only outside sample grid cells
stdTempOut     = resultMat(:,numberOfXsamplesInMat-
numberOfX2samples+1:numberOfXsamplesInMat,1);
```

```
medQ2TempOut   = resultMat(:,numberOfXsamplesInMat-
numberOfX2samples+1:numberOfXsamplesInMat,2);
aveTempOut     = resultMat(:,numberOfXsamplesInMat-
numberOfX2samples+1:numberOfXsamplesInMat,3);
maxTempOut     = resultMat(:,numberOfXsamplesInMat-
numberOfX2samples+1:numberOfXsamplesInMat,4);
minTempOut     = resultMat(:,numberOfXsamplesInMat-
numberOfX2samples+1:numberOfXsamplesInMat,5);
medQ1TempOut   = resultMat(:,numberOfXsamplesInMat-
numberOfX2samples+1:numberOfXsamplesInMat,6);
medQ3TempOut   = resultMat(:,numberOfXsamplesInMat-
numberOfX2samples+1:numberOfXsamplesInMat,7);
aveQ1Q3TempOut = resultMat(:,numberOfXsamplesInMat-
numberOfX2samples+1:numberOfXsamplesInMat,8);
aveQ2Q3TempOut = resultMat(:,numberOfXsamplesInMat-
numberOfX2samples+1:numberOfXsamplesInMat,9);
aveQ1Q2TempOut = resultMat(:,numberOfXsamplesInMat-
numberOfX2samples+1:numberOfXsamplesInMat,10);

% Building facade index at the matrix finalResult:
buildingFacade = 3;
% Calculating flame height per sample inside and outside the model for all
data
% Scanning from top to down for the highest flame temperature tip (520 ˚C)
for all data per sample
for t = 1:simulationTime
    for j = numberOfZsamplesInMat:-sampleStep:1
        if (max(inputMat(j,:,t))>=flameThreshold)
            flameHeightPerTime(t) = allz(j,1);
            break
        end
    end
end

% Calculating external flame height per sample for all data
% Scanning from top to down for the highest flame tip in the model per
sample
for t = 1:simulationTime
    for j = numberOfZsamplesInMat:-sampleStep:1
        if (max(inputMat(j,numberOfXsamplesInMat-
numberOfX2samples+1+buildingFacade:numberOfXsamplesInMat,t))>=flameThreshol
d)
            flameHeightPerTimeOut(t) = outz(j,1);
            break
        end
    end
end

% Calculating external flame height:
% Scanning from top to down for the highest flame in the medQ2TempOut
matrix
for i = numberOfZsamplesInMat:-sampleStep:1
    if (max(max(medQ2TempOut(i,buildingFacade:end)))>=flameThreshold)
        finalFlameHeight(2) = outz(i,1);
        break
    end
end

% Scanning from top to down for the highest flame tip in the aveTempOut
matrix
for i = numberOfZsamplesInMat:-sampleStep:1
```

```
    if (max(max(aveTempOut(i,buildingFacade:end)))>=flameThreshold)
        finalFlameHeight(3) = outz(i,1);
        break
    end
end

% Scanning from top to down for the highest flame tip in the maxTempOut
matrix
for i = numberOfZsamplesInMat:-sampleStep:1
    if (max(max(maxTempOut(i,buildingFacade:end)))>=flameThreshold)
        finalFlameHeight(4) = outz(i,1);
        break
    end
end

% Scanning from top to down for the highest flame tip in the minTempOut
matrix
for i = numberOfZsamplesInMat:-sampleStep:1
    if (max(max(minTempOut(i,buildingFacade:end)))>=flameThreshold)
        finalFlameHeight(5) = outz(i,1);
        break
    end
end

% Scanning from top to down for the highest flame tip in the medQ1TempOut
matrix
for i = numberOfZsamplesInMat:-sampleStep:1
    if (max(max(medQ1TempOut(i,buildingFacade:end)))>=flameThreshold)
        finalFlameHeight(6) = outz(i,1);
        break
    end
end

% Scanning from top to down for the highest flame tip in the medQ3TempOut
matrix
for i = numberOfZsamplesInMat:-sampleStep:1
    if (max(max(medQ3TempOut(i,buildingFacade:end)))>=flameThreshold)
        finalFlameHeight(7) = outz(i,1);
        break
    end
end

% Scanning from top to down for the highest flame tip in the aveQ1Q3TempOut
matrix
for i = numberOfZsamplesInMat:-sampleStep:1
    if (max(max(aveQ1Q3TempOut(i,buildingFacade:end)))>=flameThreshold)
        finalFlameHeight(8) = outz(i,1);
        break
    end
end

% Scanning from top to down for the highest flame tip in the aveQ2Q3TempOut
matrix
for i = numberOfZsamplesInMat:-sampleStep:1
    if (max(max(aveQ2Q3TempOut(i,buildingFacade:end)))>=flameThreshold)
        finalFlameHeight(9) = outz(i,1);
        break
    end
end
```

```
% Scanning from top to down for the highest flame tip in the aveQ1Q2TempOut
matrix
for i = numberOfZsamplesInMat:-sampleStep:1
    if (max(max(aveQ1Q2TempOut(i,buildingFacade:end)))>=flameThreshold)
        finalFlameHeight(10) = outz(i,1);
        break
    end
end

figure; %plot the external flame height per sample
plot(flameHeightPerTimeOut);
title('Flame height per second')
xlabel('Time [sec]')
ylabel('Flame height [m]')

figure;
subplot(231);
resolution = 20; % is needed for the legend (colors)
contourf(allx, allz, aveTemp, resolution);
tic = linspace(min(min(aveTemp)),max(max(aveTemp)),resolution);
tickz = tic(1:resolution/10:end);
colorbar('TickLabels',tickz,'Ticks',tickz);
title('Mean flame')
xlabel('Width')
ylabel('Hight')
axis image

subplot(232);
contourf(allx, allz, medQ2Temp, resolution);
tic = linspace(min(min(medQ2Temp)),max(max(medQ2Temp)),resolution);
tickz = tic(1:resolution/10:end);
colorbar('TickLabels',tickz,'Ticks',tickz);
title('Median flame')
xlabel('Width')
ylabel('Hight')
axis image

subplot(233);
contourf(allx, allz, stdTemp, 20);
tic = linspace(min(min(stdTemp)),max(max(stdTemp)),resolution);
tickz = tic(1:resolution/10:end);
colorbar('TickLabels',tickz,'Ticks',tickz);
title('Std flame')
xlabel('Width')
ylabel('Hight')
axis image

subplot(234);
resolution = 10;
contourf(outx, outz, aveTempOut, resolution);
tic = linspace(min(min(aveTempOut)),max(max(aveTempOut)),resolution);
tickz = tic(1:resolution/10:end);
colorbar('TickLabels',tickz,'Ticks',tickz);
title('Mean flame outside')
xlabel('Width')
ylabel('Hight')
axis image

subplot(235);
contourf(outx, outz, medQ2TempOut, resolution);
```

```
tic = linspace(min(min(medQ2TempOut)),max(max(medQ2TempOut)),resolution);
tickz = tic(1:resolution/10:end);
colorbar('TickLabels',tickz,'Ticks',tickz);
title('Median flame outside')
xlabel('Width')
ylabel('Hight')
axis image

subplot(236);
contourf(outx, outz, stdTempOut, resolution);
tic = linspace(min(min(stdTempOut)),max(max(stdTempOut)),resolution);
tickz = tic(1:resolution/10:end);
colorbar('TickLabels',tickz,'Ticks',tickz);
title('Std flame outside')
xlabel('Width')
ylabel('Hight')
axis image

% --------------- Plotting all results separately ---------------------
% Setting plot resolution. It must be multiple of 8!!
resolution = 8;

% Plotting aveTempOut (average temperature outside)
figure
contourf(outx, outz, aveTempOut, resolution+1);
tic = linspace(min(min(aveTempOut)),820,resolution+1);
tickz = tic(1:end);
caxis([20, 820]);
colorbar('TickLabels',tickz,'Ticks',tickz,'Limits', [20,820], 'LimitsMode',
'manual');
title('Average flame result')
xlabel('Width')
ylabel('Hight')
axis image

% Plotting medQ2TempOut (median Q2 temperature outside)
figure
contourf(outx, outz, medQ2TempOut, resolution+1);
tic = linspace(min(min(medQ2TempOut)),820,resolution+1);
tickz = tic(1:end);
caxis([20, 820]);
colorbar('TickLabels',tickz,'Ticks',tickz,'Limits', [20,820], 'LimitsMode',
'manual');
title('Median flame result')
xlabel('Width')
ylabel('Hight')
axis image

% Plotting maxTempOut (maximum temperature outside)
figure
contourf(outx, outz, maxTempOut, resolution+1);
tic = linspace(min(min(maxTempOut)),820,resolution+1);
tickz = tic(1:end);
caxis([20, 820]);
colorbar('TickLabels',tickz,'Ticks',tickz,'Limits', [20,820], 'LimitsMode',
'manual');
title('Maximum flame result')
xlabel('Width')
ylabel('Hight')
axis image
```

```
% Plotting minTempOut (minimum temperature outside)
figure
contourf(outx, outz, minTempOut, resolution+1);
tic = linspace(min(min(minTempOut)),820,resolution+1);
tickz = tic(1:end);
caxis([20, 820]);
colorbar('TickLabels',tickz,'Ticks',tickz,'Limits', [20,820], 'LimitsMode',
'manual');
title('Minimum flame result')
xlabel('Width')
ylabel('Hight')
axis image

% Plotting medQ1TempOut (median Q1 temperature outside)
figure
contourf(outx, outz, medQ1TempOut, resolution+1);
tic = linspace(min(min(medQ1TempOut)),820,resolution+1);
tickz = tic(1:end);
caxis([20, 820]);
colorbar('TickLabels',tickz,'Ticks',tickz,'Limits', [20,820], 'LimitsMode',
'manual');
title('Median Q1 flame result')
xlabel('Width')
ylabel('Hight')
axis image

% Plotting medQ3TempOut (median Q3 temperature outside)
figure
contourf(outx, outz, medQ3TempOut, resolution+1);
tic = linspace(min(min(medQ3TempOut)),820,resolution+1);
tickz = tic(1:end);
caxis([20, 820]);
colorbar('TickLabels',tickz,'Ticks',tickz,'Limits', [20,820], 'LimitsMode',
'manual');
title('Median Q3 flame result')
xlabel('Width')
ylabel('Hight')
axis image

% Plotting aveQ1Q3TempOut (average temperature between Q1 and Q3 outside)
figure
contourf(outx, outz, aveQ1Q3TempOut, resolution+1);
tic = linspace(min(min(aveQ1Q3TempOut)),820,resolution+1);
tickz = tic(1:end);
caxis([20, 820]);
colorbar('TickLabels',tickz,'Ticks',tickz,'Limits', [20,820], 'LimitsMode',
'manual');
title('Average between Q1 and Q3 flame result')
xlabel('Width')
ylabel('Hight')
axis image

% Plotting aveQ2Q3TempOut (average temperature between Q2 and Q3 outside)
figure
contourf(outx, outz, aveQ2Q3TempOut, resolution+1);
tic = linspace(min(min(aveQ2Q3TempOut)),820,resolution+1);
tickz = tic(1:end);
caxis([20, 820]);
```

```
colorbar('TickLabels',tickz,'Ticks',tickz,'Limits', [20,820], 'LimitsMode',
'manual');
title('Average between Q2 and Q3 flame result')
xlabel('Width')
ylabel('Hight')
axis image

% Plotting aveQ1Q2TempOut (average temperature between Q1 and Q2 outside)
figure
contourf(outx, outz, aveQ1Q2TempOut, resolution+1);
tic = linspace(min(min(aveQ1Q2TempOut)),820,resolution+1);
tickz = tic(1:end);
caxis([20, 820]);
colorbar('TickLabels',tickz,'Ticks',tickz,'Limits', [20,820], 'LimitsMode',
'manual');
title('Average between Q1 and Q2 flame result')
xlabel('Width')
ylabel('Hight')
axis image

%  1 = stdTempOut = NaN
%  2 = medQ2TempOut
%  3 = aveTempOut
%  4 = maxTempOut
%  5 = minTempOut
%  6 = medQ1TempOut
%  7 = medQ3TempOut
%  8 = aveQ1Q3TempOut
%  9 = aveQ2Q3TempOut
% 10 = aveQ1Q2TempOut

Q2Method2 = median(flameHeightPerTimeOut)
Q1Method2 = median(flameHeightPerTimeOut(flameHeightPerTimeOut<=Q2Method2))
Q3Method2 = median(flameHeightPerTimeOut(flameHeightPerTimeOut>=Q2Method2))
aveBtwnQ1andQ3Method2 =
mean(flameHeightPerTimeOut(flameHeightPerTimeOut>=Q1Method2 &
flameHeightPerTimeOut<=Q3Method2))
aveBtwnQ2andQ3Method2 =
mean(flameHeightPerTimeOut(flameHeightPerTimeOut>=Q2Method2 &
flameHeightPerTimeOut<=Q3Method2))
aveBtwnQ1andQ2Method2 =
mean(flameHeightPerTimeOut(flameHeightPerTimeOut>=Q1Method2 &
flameHeightPerTimeOut<=Q2Method2))

finalFlameHeight

clear i h j maxT maxX maxZ minT minX minZ t counter
```

Appendix V: FDS script

Appendix V: FDS script (full-scale model)

This FDS script is the full scale simulation model with external flames (chapter 9).

```
&HEAD CHID='model1'/
&TIME T_END=120.0/ simulation time of 2 minutes
&DUMP DT_RESTART=10.0, NFRAMES=120/ the results will be per second saved
&MISC EXTINCTION_MODEL='EXTINCTION 1'/ using extinction model 1 (default=
EXTINCTION_MODEL 2), see paragraph 4.4

&MESH ID='Mesh1', IJK=208,108,108, XB=-0.2,10.2,-0.2,5.2,-0.2,5.2 / cell
size 5 cm (inside/outside)
&MESH ID='Mesh2', IJK=104,108,204, XB=5.0,10.2,-0.2,5.2,5.2,15.2 / cell
size 5 cm (outside)

**********cellulose fire***********
&SPEC ID='Cellulose'/ Cellulose fire

&REAC ID='CELLulose',
      FUEL='REAC_FUEL',
      FORMULA='C4H6O3',
      CRITICAL_FLAME_TEMPERATURE=1427.0,
      RADIATIVE_FRACTION=0.35,
      SOOT_YIELD=0.01/

**********Adiabatic walls***********
&SURF ID='adiabatic',
      RGB=146,202,166,
      ADIABATIC=.TRUE./

**********fire surface***********
&SURF ID='Surface01',
      COLOR='RED',
      HRRPUA=5000.0,
      RAMP_Q='Surface01_RAMP_Q'/ a maximum HRR of 10 000 kW during 2
minutes

&RAMP ID='Surface01_RAMP_Q', T=0.0, F=1.0/
&RAMP ID='Surface01_RAMP_Q', T=60, F=1.0/
&RAMP ID='Surface01_RAMP_Q', T=120, F=1.0/

**********construction full-scale model (25 m²)***********
&OBST XB=-0.2,5.2,-0.2,0.0,0.0,5.0, SURF_ID='adiabatic'/ wall
&OBST XB=-0.2,5.2,5.0,5.2,0.0,5.0, SURF_ID='adiabatic'/ wall
&OBST XB=-0.2,5.2,-0.2,5.2,5.0,5.2, SURF_ID='adiabatic'/ roof
&OBST XB=-0.2,5.2,-0.2,5.2,-0.2,0.0, SURF_ID='adiabatic'/ floor
&OBST XB=5.0,5.2,0.0,5.0,0.0,5.0, SURF_ID='adiabatic'/ wall with opening
&OBST XB=-0.2,0.0,0.0,5.0,0.0,5.0, SURF_ID='adiabatic'/ rear wall
&OBST XB=5.0,5.2,-0.2,5.2,5.2,15.2, SURF_ID='adiabatic'/ upper wall

&HOLE XB=5.0,5.2,1.5,3.5,0.0,2.0/ external opening of 2.0 m by 2.0 m
&VENT SURF_ID='Surface01', XB=2.0,3.0,1.5,3.5,0.0,0.0/ burning area with a
specific fuel and HRR

**********open boundary***********
&VENT MB='XMAX', SURF_ID='OPEN'/
&VENT MB='XMIN', SURF_ID='OPEN'/
&VENT MB='YMAX', SURF_ID='OPEN'/
&VENT MB='YMIN', SURF_ID='OPEN'/
&VENT MB='ZMAX', SURF_ID='OPEN'/
&VENT MB='ZMIN', SURF_ID='OPEN'/
```

```
**********outputs************
&SLCF QUANTITY='HRRPUV', VECTOR=.TRUE., PBY=2.5/ slice file of the HRR Per
Unit Volume per grid cell per second
&SLCF QUANTITY='U-VELOCITY', VECTOR=.TRUE., PBY=2.5/ slice file of the
horizontal velocity (neutral plane)per grid cell per second
&SLCF QUANTITY='TEMPERATURE', VECTOR=.TRUE., PBY=2.5/ slice file of the
temperature distribution (external flame height)per grid cell per second

**********devices************
&DEVC ID='FLOW out', QUANTITY='MASS FLOW +', XB=5.2,5.2,1.5,3.5,0.0,2.0/
the mass outflow rate through the external opening per second
&DEVC ID='FLOW in', QUANTITY='MASS FLOW -', XB=5.2,5.2,1.5,3.5,0.0,2.0/ the
mass inflow rate through the external opening per second
&DEVC ID='HRR 3', QUANTITY='HRR', XB=-0.2,5.2,-0.2,5.2,-0.2,5.2/ the actual
HRR inside the model [kW]
&DEVC ID='HRR 2', QUANTITY='HRR', XB=5.2,10.2,-0.2,5.2,-0.2,5.2/ the actual
HRR outside upper part [kW]
&DEVC ID='HRR 1', QUANTITY='HRR', XB=5.2,10.2,-0.2,5.2,5.2,15.2/ the actual
HRR outside lower part [kW]

&TAIL / end script
```

Appendix VI: simulation results

Appendix VI-a: HRR Per Unit Volume

The cubic scale model cross section with the HRRPUV is given below. The HRRPUV inside and outside the cubic scale model are given after each 2 minutes of ignition. The result of the HRRPUV is averaged per 30 seconds.

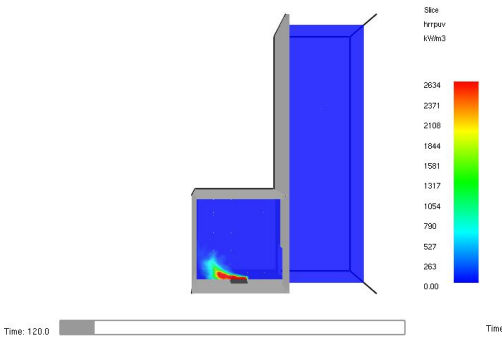

after 2 minute of ignition

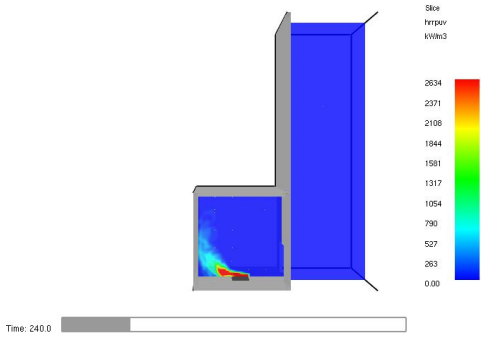

after 4 minute of ignition

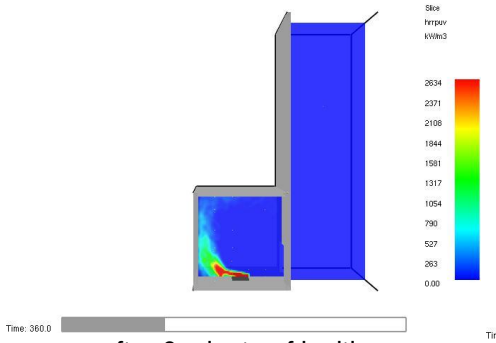

after 6 minute of ignition

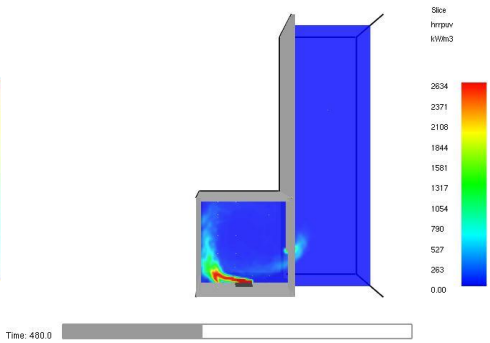

after 8 minute of ignition

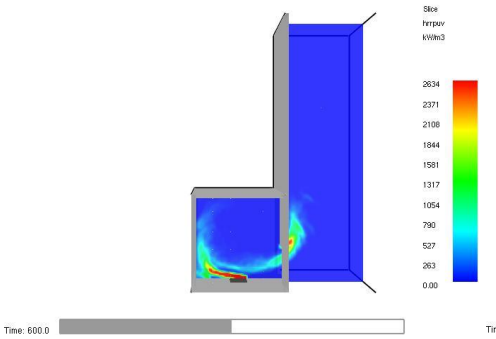

after 10 minute of ignition

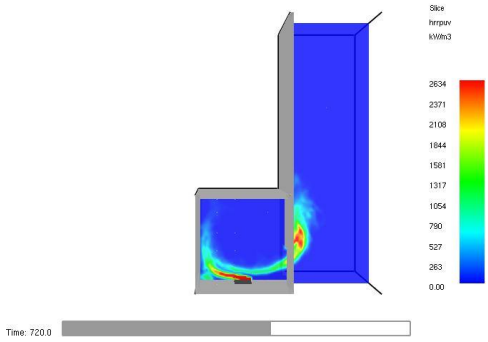

after 12 minute of ignition

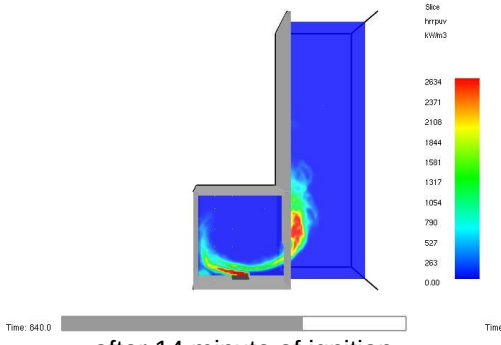

after 14 minute of ignition

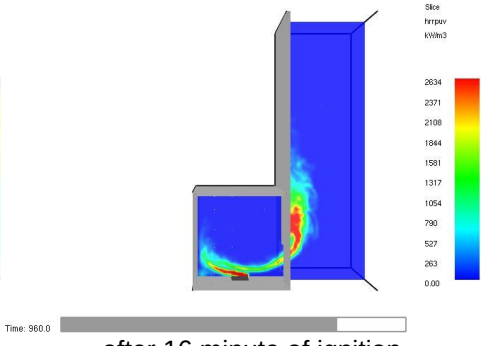

after 16 minute of ignition

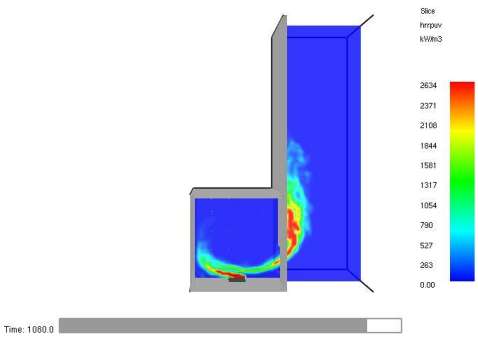

after 18 minute of ignition

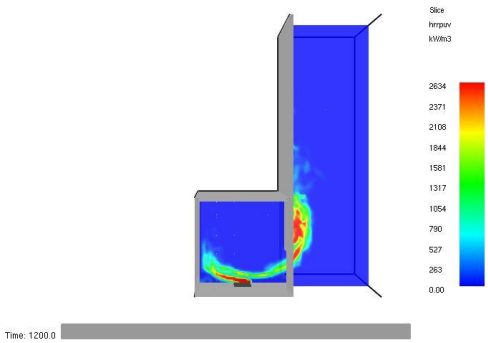

after 20 minute of ignition

Appendix VI-b: gas temperature

The cubic scale model cross section with the gas temperature is given below. The gas temperature inside and outside the cubic scale model are given after each 2 minutes of ignition. The result of the gas temperature is averaged per 30 seconds.

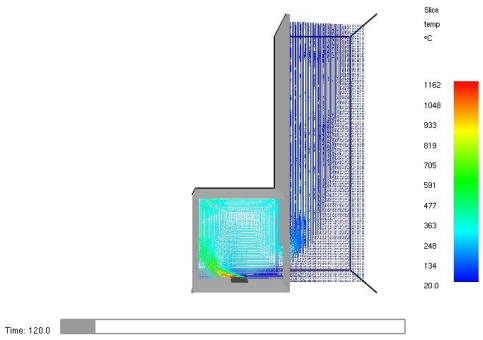

after 2 minute of ignition

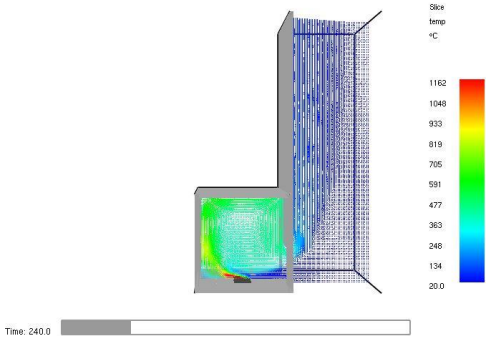

after 4 minute of ignition

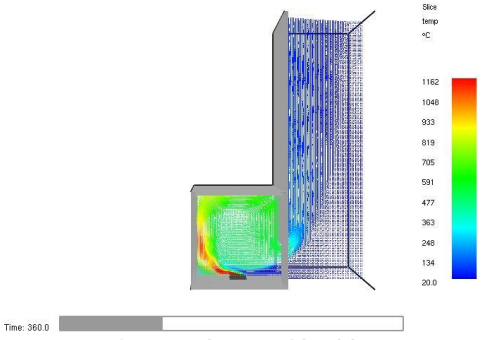

after 6 minute of ignition

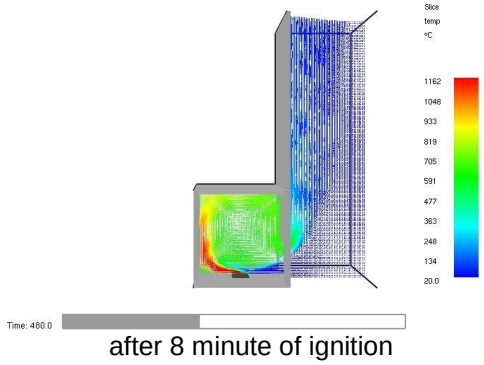

after 8 minute of ignition

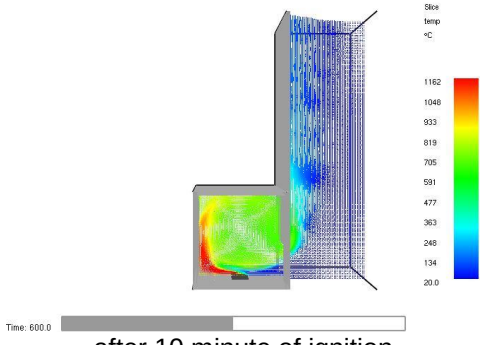

after 10 minute of ignition

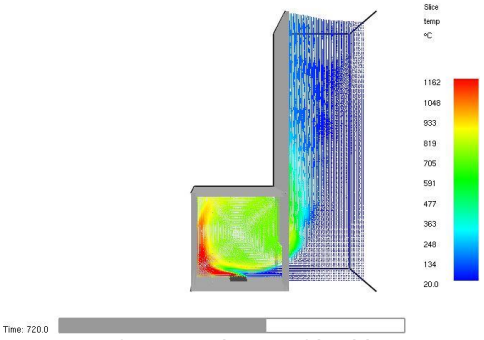

after 12 minute of ignition

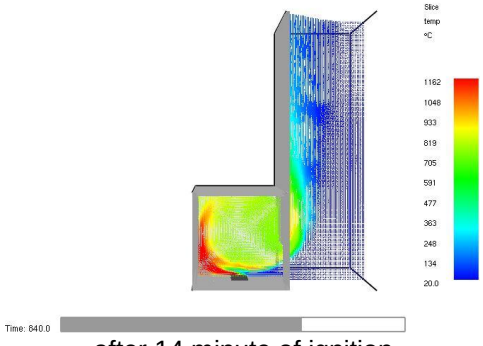

after 14 minute of ignition

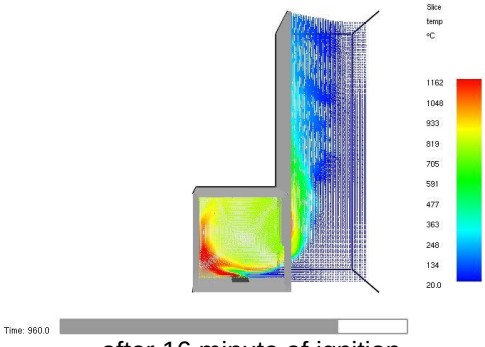

after 16 minute of ignition

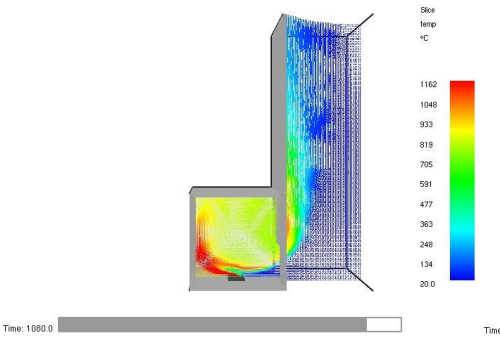

after 18 minute of ignition

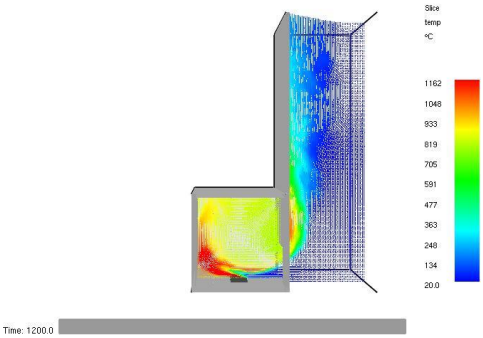

after 20 minute of ignition

Appendix VI-c: horizontal air velocity

The cubic scale model cross section with the horizontal air velocity is given below. The air velocity inside and outside the cubic scale model are given after each 2 minutes of ignition. The inflow show a negative air velocity and the outflow show a positive air velocity in the figures below. Both flows are averaged per 30 seconds.

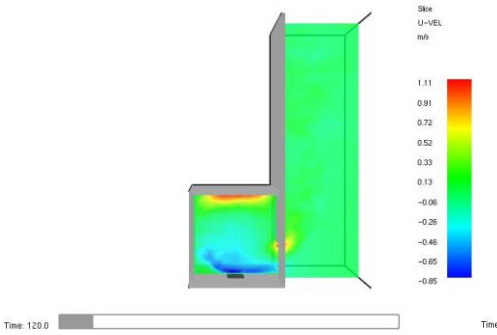

after 2 minute of ignition

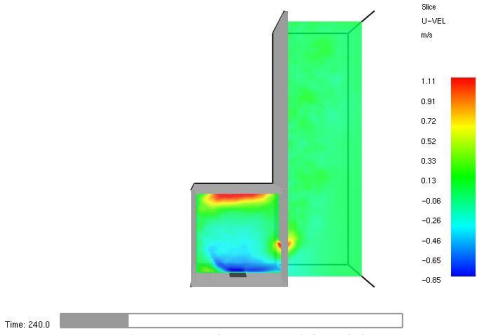

after 4 minute of ignition

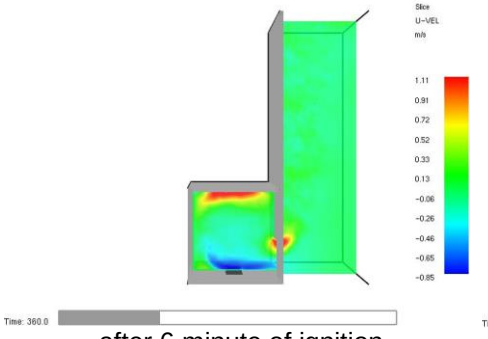

after 6 minute of ignition

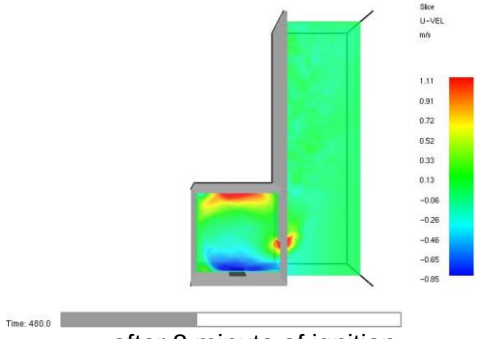

after 8 minute of ignition

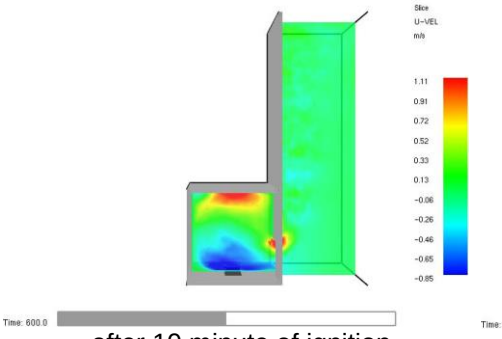

after 10 minute of ignition

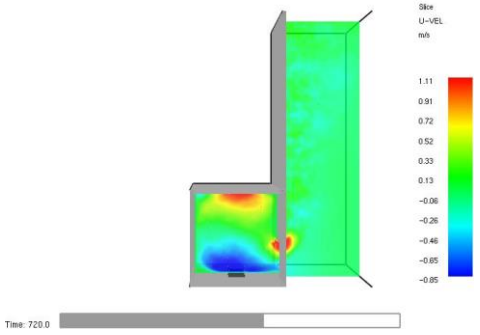

after 12 minute of ignition

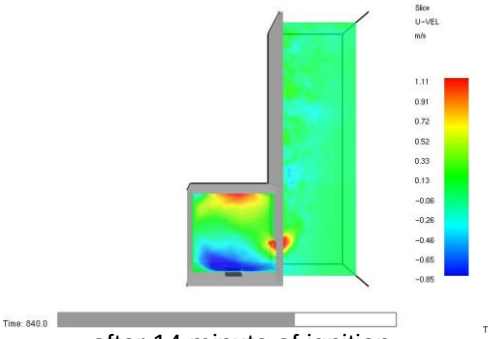

after 14 minute of ignition

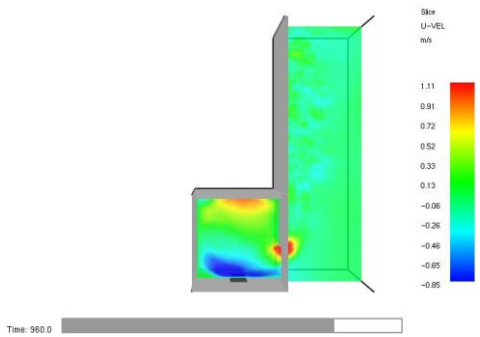

after 16 minute of ignition

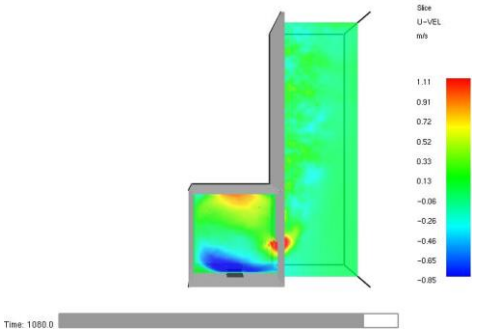

after 18 minute of ignition

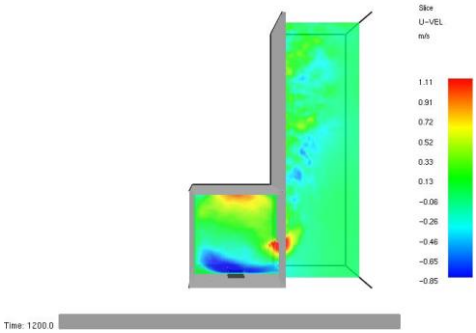

after 20 minute of ignition

Appendix VI-d: external flame

The flame cross section inside and outside the cubic scale model is given below. The soot mass fraction and the HRRPUV are given after each 2 minutes of ignition. The results of the soot mass fraction and the HRRPUV are averaged per 30 seconds.

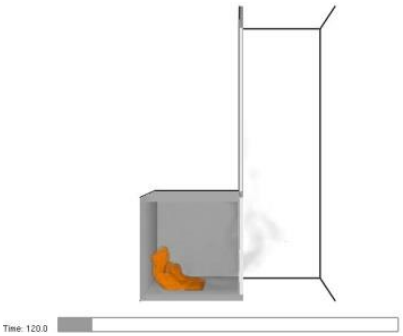

after 2 minute of ignition

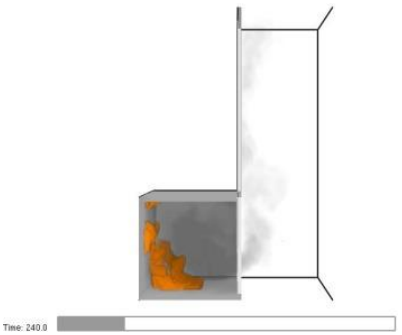

after 4 minute of ignition

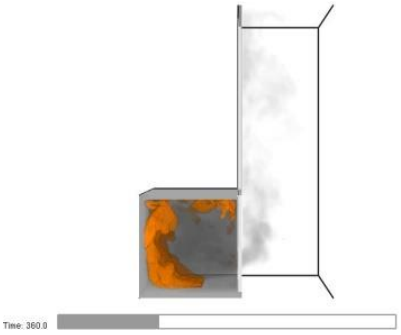

after 6 minute of ignition

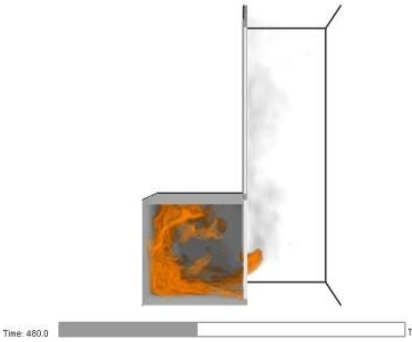

after 8 minute of ignition

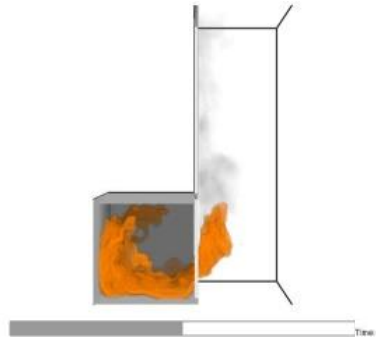

after 10 minute of ignition

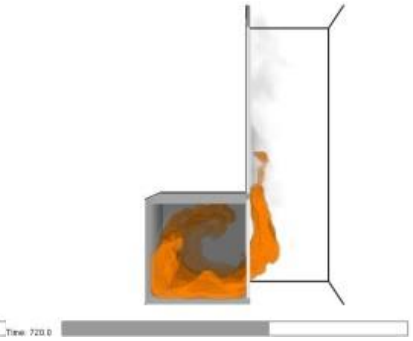

after 12 minute of ignition

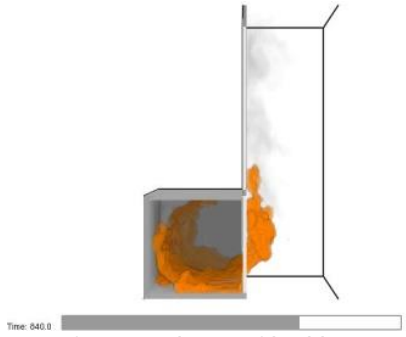

after 14 minute of ignition

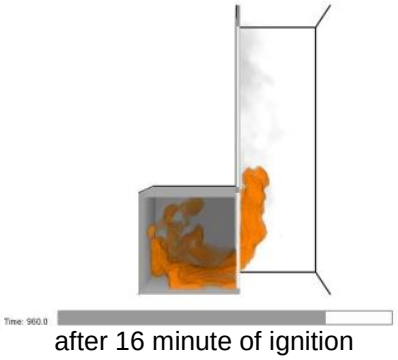

after 16 minute of ignition

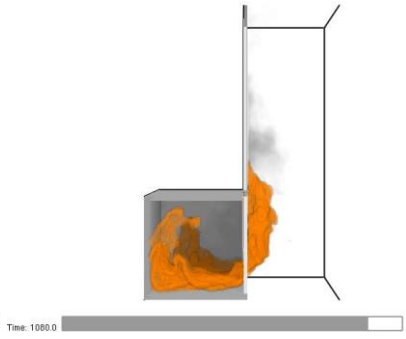

after 18 minute of ignition

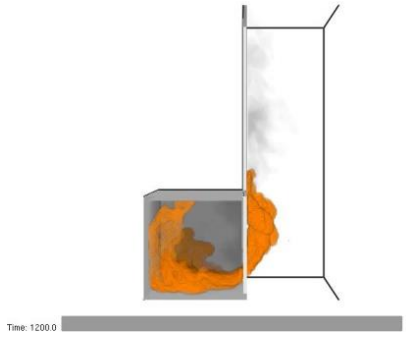

after 20 minute of ignition

Appendix VII: simulation results

Appendix VII-a: simulation results sensitivity of building and fire parameters

Simulation model 1: window-like opening

Actual HRR

Figure 19 shows the actual HRR inside the model simulated with 2 cm grid cell size by shifting the door-like opening to the middle of the front façade (window-like opening). The actual HRR inside the model (green solid line) equals before external flaming the theoretical HRR of the fire source (black solid line). The actual HRR inside the model and the theoretical HRR show in the validated model similar results (green and black dashed lines). After external flaming occurs the actual HRR inside the model should be stabilized like the actual HRR of the validated model (Figure 19: green dashed line) with 1 cm grid cell size. Because shifting the opening geometry from a door-like opening to a window-like opening should show similar actual HRR as in the reference model. Thus the actual HRR inside the model calculated (green solid line) with 2 cm grid cell size should equal the actual HRR of the reference model (green dashed line). The actual HRR inside the model with a window-like opening simulated with 2 cm grid cell size equals the empirical correlation of $1500\ \mathrm{A}\sqrt{\mathrm{H}}$ while the actual HRR inside the model with a door-like opening simulated with 2 cm grid cell size equals the empirical correlation of $1150\ \mathrm{A}\sqrt{\mathrm{H}}$ during external flaming.

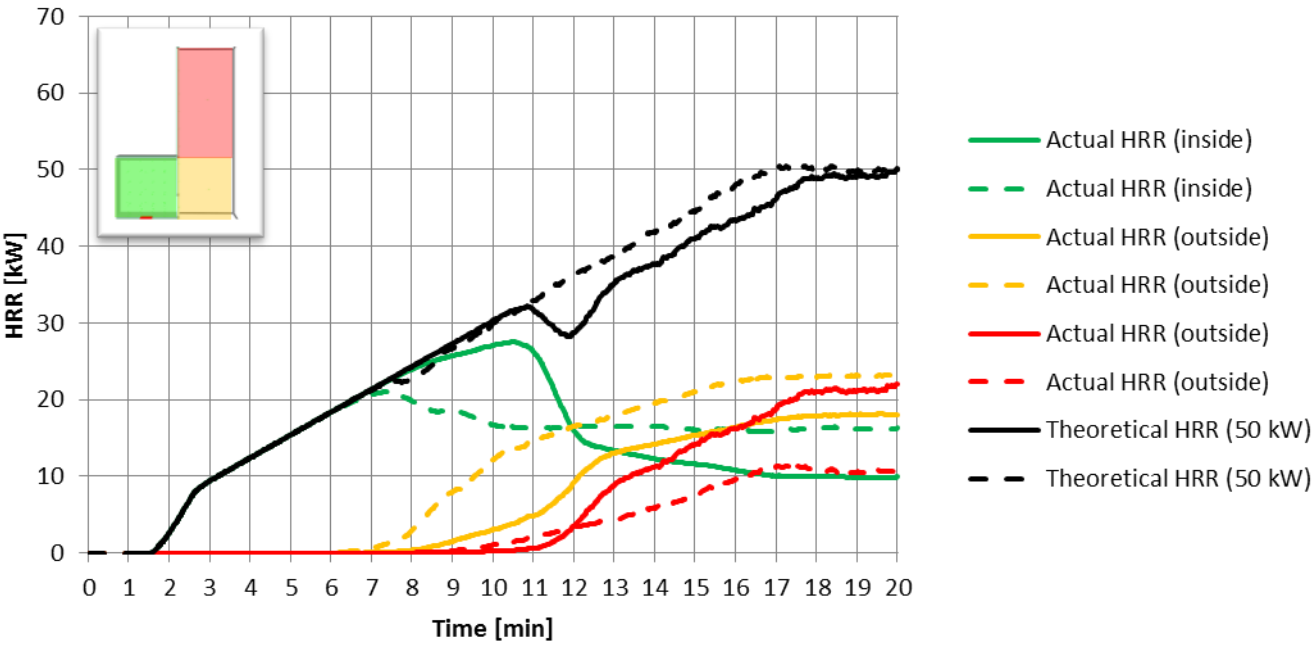

Figure 19: The effect of a window-like opening on the actual HRR inside the model simulated with 2 cm grid cell size. The dashed lines show the HRR of the reference model simulated with 2 cm grid cell size.

The actual HRR inside the model of a window-like opening shows a good agreement with the experimental results while the actual HRR inside the model of a door-like opening shows a deviation of 23.3% with the experimental results. When the reference model is used as the reference model then the deviation with the shifted opening is 23.3% as well. After approximately 11 minutes of ignition the actual HRR inside the model with a window-like opening decreases to a constant value of $550\ \mathrm{A}\sqrt{\mathrm{H}}$. At the end of the simulation time the deviation with the reference model by using 2 cm grid cell size is approximately 38.8%. While the reference model deviates 40.0% with the experimental results.

This means by shifting the opening from a door-like to a window-like opening the actual HRR inside the model will increase. When the actual HRR inside the model during external flaming increases the actual

HRR at the outside part will decrease (yellow and red lines). The actual HRR at the outside lower part (yellow line) is decreased compared to the reference model with a door-like opening. This is due to two reasons. The first reason is the increased actual HRR inside the model with a window-like opening. The second reason is the influence of the shifted opening in relation to the external flame. At the lower part of the front façade do not occur external flaming. So there is no actual HRR at the outside lower part. The actual HRR of the outside upper part becomes higher because of the shifted opening position a large part of the produced HRR will appear at the outside upper part (red line). The total of the actual HRR of all areas should equal the theoretical HRR of the fire source (black line). If the total HRR of all areas does not equal the theoretical HRR this means that the simulation results are not accurate. Because the produced energy should equal the energy which is available in the different areas.

Figure 20 shows the actual HRR inside the model simulated with 1 cm grid cell size by shifting the door-like opening to the middle of the front façade (so it is a window-like opening). The actual HRR inside the model (green solid line) equals before external flaming the theoretical HRR of the fire source (black solid line). The actual HRR inside the model and the theoretical HRR shows in the reference model similar results (green and black dashed lines).

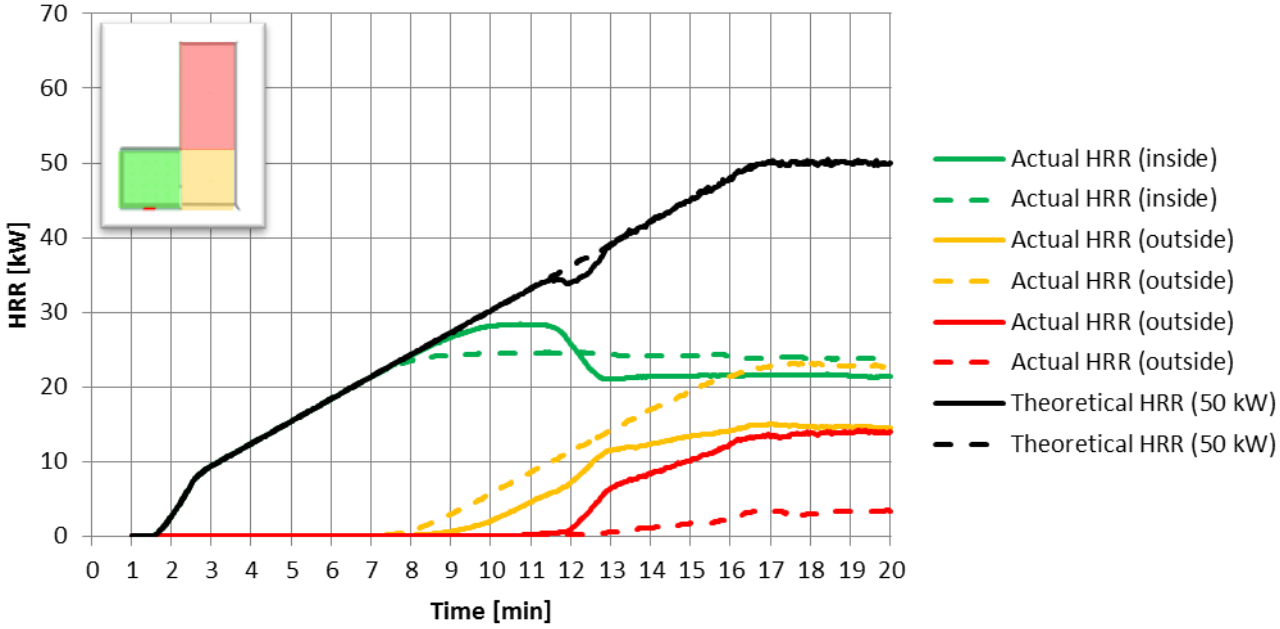

Figure 20: The effect of a window-like opening on the actual HRR inside the model simulated with 1 cm grid cell size. The dashed lines show the HRR of the reference model simulated with 1 cm grid cell size.

After external flaming occurs the actual HRR inside the model should be stabilized like the actual HRR of the reference model (green dashed line). The actual HRR inside the model with a window-like opening simulated with 1 cm grid cell size equals the empirical correlation of $1600\ \mathrm{A}\sqrt{\mathrm{H}}$ while the actual HRR inside the model with a door-like opening simulated with 1 cm grid cell size equals the empirical correlation of $1350\ \mathrm{A}\sqrt{\mathrm{H}}$ during external flaming. The actual HRR inside the model of a window-like opening shows a deviation of 6.3% with the experimental results while the actual HRR inside the model of a door-like opening shows a deviation of 10% with the experimental results. When the reference model results are used as the reference model then the deviation with the shifted opening is approximately 15.6%. After approximately 12 minutes of ignition the actual HRR inside the model with a window-like opening decreases to a constant value of $1200\ \mathrm{A}\sqrt{\mathrm{H}}$.

This means by shifting the opening from a door-like to a window-like opening will increase the actual HRR inside the model. When the actual HRR inside the model during external flaming increases the actual HRR at the outside part will decrease (yellow and red lines). The actual HRR at the outside lower

part (yellow line) is decreased compared to the results of the CFD reference model with a door-like opening (like as simulated with 2 cm grid cell size). The actual HRR of the outside upper part becomes higher because of the increased opening position a large part of the produced fire release will appear at the upper part (red line). The total actual HRR of all areas should equal the theoretical HRR of the fire source (black line). The total HRR of different areas simulated by 1 cm grid cell size shows a good agreement with the theoretical HRR.

Both graphs show that the theoretical HRR and the actual HRR inside the model are similar before external flames occur. After external flames occur the actual HRR inside the room will decrease. In fact this shows that using 1 cm grid cell size is not accurate for predicting the actual HRR inside the model. Because the actual HRR inside the model should be stabilized during external flaming. Using 1 cm grid cell size shows bigger deviation with the experimental results than using 2 cm grid cell size. Using the reference model as reference it shows a smaller deviation with the results of the reference model of 1 cm grid cell size. In Table 2 the results of the actual HRR of the window-like opening simulated by 2 cm and 1 cm are compared to the experimental results and the CFD reference model. Because the actual HRR inside the model with a window-like opening is not stabilized during external flaming the results do not show accurate predictions. For more accurate simulation results the model of the window-like opening should be simulated with a finer grid cell size (grid cell size < 1 cm).

Table 2: The simulated actual HRR inside the model of a window-like opening model by two different grid cell sizes.

reference model vs experiments			
door-like model	empirical correlation HRR (experiments)	empirical correlation HRR (reference model)	deviation
2 cm grid cell size	$1500.\,A\sqrt{H}$	$1150.\,A\sqrt{H}$ / $900.\,A\sqrt{H}$	23.3% - 40.0%
1 cm grid cell size	$1500.\,A\sqrt{H}$	$1350.\,A\sqrt{H}$	10%
model with window-like opening vs experiments			
window-like model	empirical correlation HRR (experiments)	empirical correlation HRR (variant)	deviation
2 cm grid cell size	$1500.\,A\sqrt{H}$	$1500.\,A\sqrt{H}$ / $550.\,A\sqrt{H}$	0.0% - 63.3%
1 cm grid cell size	$1500.\,A\sqrt{H}$	$1600.\,A\sqrt{H}$ / $1200.\,A\sqrt{H}$	6.3% - 20%
model with window-like opening vs reference model			
	empirical correlation HRR (reference model)	empirical correlation HRR (variant)	deviation
2 cm grid cell size	$1150.\,A\sqrt{H}$ / $900.\,A\sqrt{H}$	$1500.\,A\sqrt{H}$ / $550.\,A\sqrt{H}$	23.3% - 38.8%
1 cm grid cell size	$1350.\,A\sqrt{H}$	$1600.\,A\sqrt{H}$ / $1200.\,A\sqrt{H}$	15.6% - 11.1%

Mass inflow rate

Because of the increased actual HRR inside the model with a window-like opening the mass inflow rate through the opening will increase for both grid cell sizes as well. In Table 3 the simulated mass inflow rate through the opening is given by using 2 cm and 1 cm grid cell size. The simulated mass inflow rate shows similar decreasement in the line progression like the mass inflow rate of the validated model. The simulation model with a window-like opening show for 2 cm grid cell size a lower deviation with the experimental results. In fact using a finer grid cell size should result in a lower deviation with the experiments. The mass inflow rate of the simulated model with window-like opening model is compared to the CFD reference model. Using a 1 cm grid cell size shows a lower deviation (Table 3). From the actual HRR inside the model and the mass inflow rate through the opening of a window-like opening model it can be concluded that the actual HRR and the mass inflow rate do not comply with the empirical correlation from the experiments. By changing the opening position at the front façade will not equal the empirical correlation which is used to predict the actual HRR and the mass inflow rate of a door-like opening model.

Table 3: The simulated mass inflow rate of a window-like opening model by two different grid cell sizes.

reference model vs experiments			
door-like model	empirical correlation inflow rate (experiments)	empirical correlation inflow rate (reference model)	deviation
2 cm grid cell size	$0.5.\mathrm{A}\sqrt{\mathrm{H}}$	$0.41.\mathrm{A}\sqrt{\mathrm{H}}$ / $0.36.\mathrm{A}\sqrt{\mathrm{H}}$	18.0% - 28.1%
1 cm grid cell size	$0.5.\mathrm{A}\sqrt{\mathrm{H}}$	$0.47.\mathrm{A}\sqrt{\mathrm{H}}$	5.6%
model with window-like opening vs experiments			
window-like model	empirical correlation inflow rate (experiments)	empirical correlation inflow rate (variant)	deviation
2 cm grid cell size	$0.5.\mathrm{A}\sqrt{\mathrm{H}}$	$0.50.\mathrm{A}\sqrt{\mathrm{H}}$ / $0.34.\mathrm{A}\sqrt{\mathrm{H}}$	0.0% - 32.0%
1 cm grid cell size	$0.5.\mathrm{A}\sqrt{\mathrm{H}}$	$0.53.\mathrm{A}\sqrt{\mathrm{H}}$ / $0.45.\mathrm{A}\sqrt{\mathrm{H}}$	6.0% - 10%
model with window-like opening vs reference model			
	empirical correlation inflow rate (reference model)	empirical correlation inflow rate (variant)	deviation
2 cm grid cell size	$0.41.\mathrm{A}\sqrt{\mathrm{H}}$ / $0.36.\mathrm{A}\sqrt{\mathrm{H}}$	$0.50.\mathrm{A}\sqrt{\mathrm{H}}$ / $0.34.\mathrm{A}\sqrt{\mathrm{H}}$	18.0% - 5.6%
1 cm grid cell size	$0.47.\mathrm{A}\sqrt{\mathrm{H}}$	$0.53.\mathrm{A}\sqrt{\mathrm{H}}$ / $0.45.\mathrm{A}\sqrt{\mathrm{H}}$	11.3% - 4.3%

Neutral plane

The neutral plane height of the window-like opening model is calculated with 2 cm and 1 cm grid cell size, see Table 4. The neutral plane height of the window-like opening model calculated with 1 cm grid cell size shows a lower deviation with the experimental results. By using the validated CFD model as a reference model the deviation of the neutral plane height of using 1 cm grid cell size is lower as well.

Table 4: The simulated neutral plane height of a window-like opening model by two different grid cell sizes.

reference model vs experiments			
door-like model	neutral plane height (experiments)	neutral plane height (reference model)	deviation
2 cm grid cell size	0.080 m	0.060 m	25.0%
1 cm grid cell size	0.080 m	0.083 m	3.8%
model with window-like opening vs experiments			
window-like model	neutral plane height (experiments)	neutral plane height (variant)	deviation
2 cm grid cell size	0.230 m	0.243 m	5.7%
1 cm grid cell size	0.230 m	0.231 m	0.4%
model with window-like opening vs reference model			
	neutral plane height from opening bottom (reference model)	neutral flame height from opening bottom (variant)	deviation
2 cm grid cell size	0.060 m	0.093 m	35.5%
1 cm grid cell size	0.083 m	0.081 m	2.4%

External flame height

In Table 5 the simulated external flame height which is determined by calculation method 1 is given for the two grid cell sizes of a window-like opening model. The result of the window-like opening model is compared to the validated external flame height simulated with 1 cm grid cell size. From the grid sensitivity analysis it can be concluded that using 1 cm grid cell size shows a good agreement with all measured variables. Therefore the reference model is compared with 2 cm and 1 cm grid cell size of a window-like opening.

Because of a shifted opening the flame height will be not be surprisingly higher than the door-like opening model. This means that using a window-like opening model the risk for fire spread will increase. The flame height simulated by using 2 cm grid cell size deviates 23.9% from the flame height simulated by 1 cm grid cell size of the door-like opening. Using 1 cm grid cell size shows a deviation of 29.3% with the door-like opening. Using 1 cm grid cell size shows that the external flame height of the window-like

opening increases 29.3% relatively compared to the external flame height of the reference model with a door-like opening.

Table 5: The simulated external flame height of a window-like opening model with two different grid cell sizes.

	external flame height (simulations)
validated model (door-like)	0.58 m
2 cm grid cell size (window-like)	0.76 m
1 cm grid cell size (window-like)	0.82 m

Simulation model 2: narrowed opening

Actual HRR

Figure 21 shows the actual HRR inside the model simulated with 2 cm grid cell size by narrowing the opening to an opening geometry of 0.1 m x 0.2 m. The actual HRR inside the model (green solid line) equals before external flaming the theoretical HRR of the fire source (black solid line). The actual HRR inside the model and the theoretical HRR shows in the validated model similar results (green and black dashed lines). After external flaming occurs the actual HRR inside the model should be stabilized like the actual HRR of the reference model simulated by 1 cm grid cell size (green dashed line). Because of the decreased opening area the mass inflow rate through the opening will be lower. So the actual HRR will decrease. Results of the actual HRR shows that narrowing the opening gives a huge influence on the actual HRR of the outside upper part.

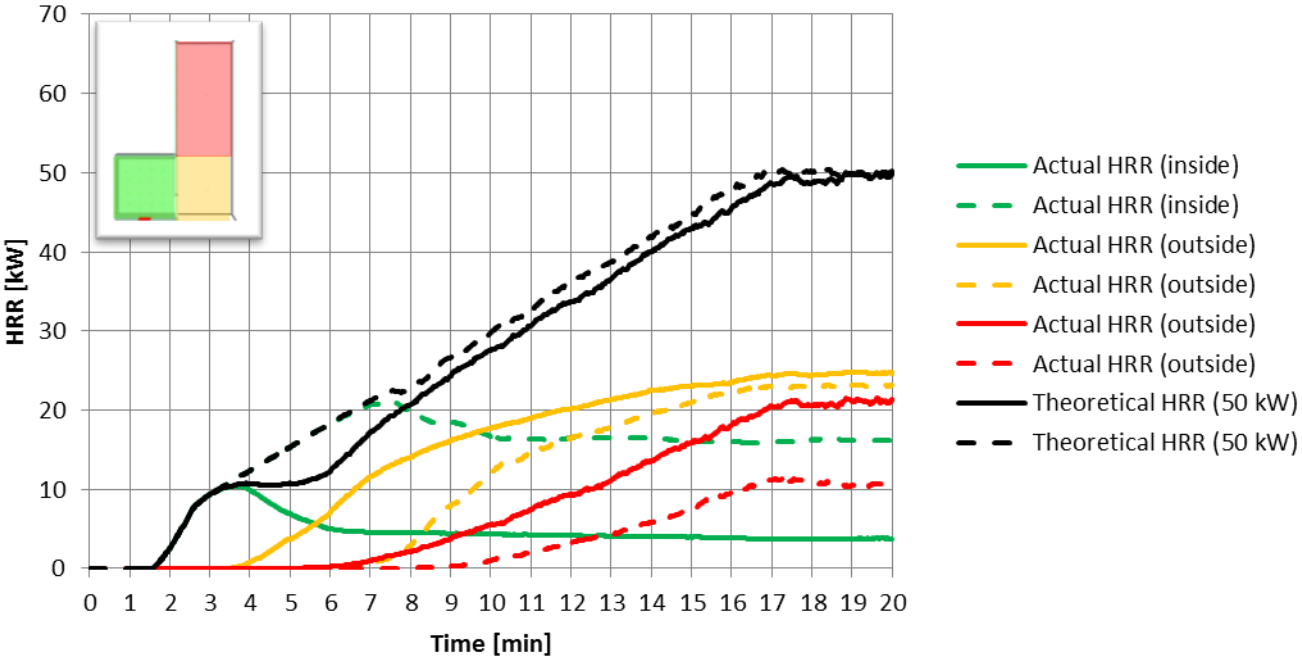

Figure 21: The effect of narrowing the opening on the actual HRR inside the model simulated with 2 cm grid cell size. The dashed lines show the HRR of the reference model simulated with 2 cm grid cell size.

The actual HRR inside the model with an opening geometry of 0.1 m x 0.2 m simulated with 2 cm grid cell size equals the empirical correlation of $1200\,A\sqrt{H}$ while the actual HRR inside the model with opening size 0.2 m x 0.2 m simulated with 2 cm grid cell size equals the empirical correlation of $1150\,A\sqrt{H}$ during external flaming. The actual HRR inside the model of a narrowed window opening shows a lower deviation with the experimental results then the simulation model with 0.2 m x 0.2 m opening. The deviation of the actual HRR of the narrowed opening model shows a deviation of 20% with

the empirical correlation from the experiments. After approximately 4 minutes of ignition the actual HRR inside the model with a narrowed opening size decreases to a constant value of $500\ A\sqrt{H}$. At the end of the simulation time the deviation with the experimental results is approximately 66.7%.
However the decreased opening surface the actual HRR inside the model when external flaming occurs should be lower than the actual HRR inside the model with a bigger opening surface (e.g. reference model). When the actual HRR inside the model during external flaming decrease the actual HRR at the outside part will increase (yellow and red lines). The actual HRR at the outside lower part (yellow line) is increased compared to the reference model with a narrowed opening. This is due to a lower actual HRR inside the model. The total actual HRR of all areas should equal the theoretical HRR of the fire source (black line). If the total HRR of all areas do not equal the theoretical HRR this means the simulated results shows discontinuity and thus are not accurate (numerical error).

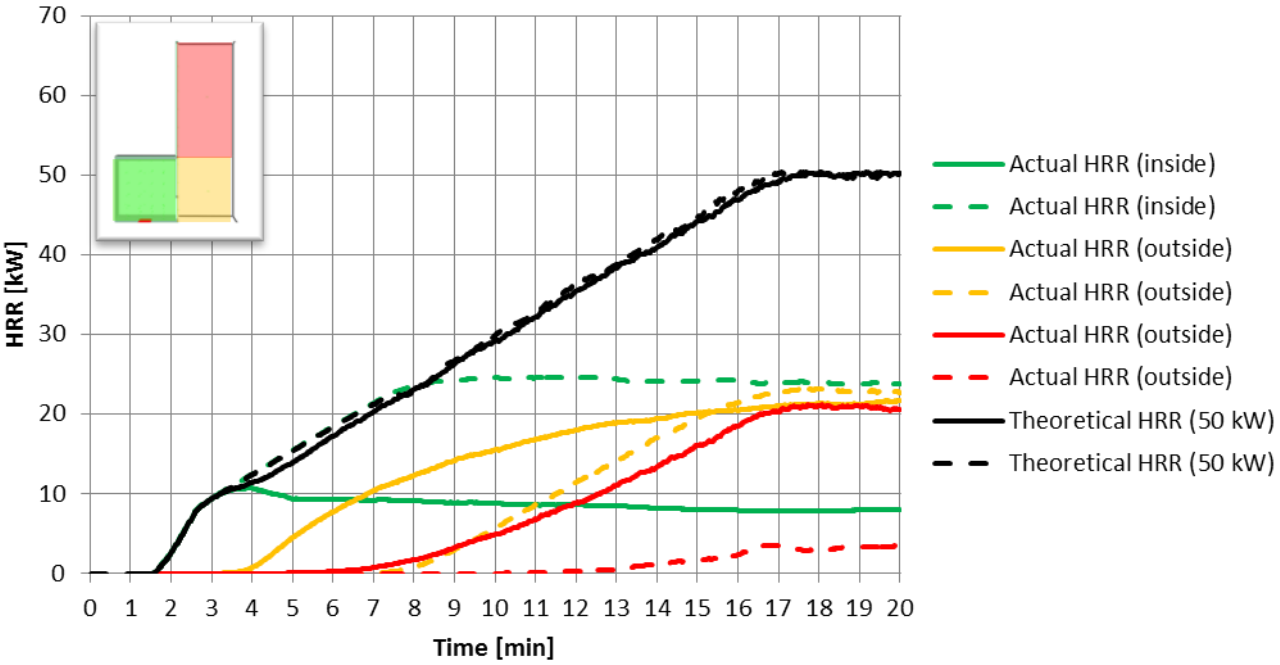

Figure 22: The effect of narrowing the opening on the actual HRR inside the model simulated with 1 cm grid cell size. The dashed lines show the HRR of the reference model simulated with 1 cm grid cell size.

Figure 22 shows the actual HRR inside the model simulated with 1 cm grid cell size by narrowing the opening to an opening geometry of 0.1 m x 0.2 m. The actual HRR inside the model (green solid line) equals before external flaming the theoretical HRR of the fire source (black solid line). The actual HRR inside the model and the theoretical HRR shows similar results with the reference model (green and black dashed lines). The actual HRR inside the model should stabilize during external flaming (green line) like the actual HRR of the reference model (green dashed line). Because the actual HRR inside the model will be influenced by the mass inflow rate through the opening a lower horizontal plateau will be reached than the horizontal plateau of the reference model. The actual HRR inside the model should equal an actual HRR of 13.4 kW conform the empirical correlation for the actual HRR. The simulated actual HRR inside the model is approximately 11.2 kW instead of an actual HRR of 13.4 kW. The actual HRR inside the model with a narrowed opening simulated with 1 cm grid cell size equals the empirical correlation of $1250\ A\sqrt{H}$ while the actual HRR inside the model of an opening geometry of 0.2 m x 0.2 m simulated with 1 cm grid cell size equals the empirical correlation of $1350\ A\sqrt{H}$ during external flaming. A few minutes after external flaming occurs the actual HRR inside the model is semi stabilized conform the empirical correlation of $850\ A\sqrt{H}$. The actual HRR inside the model with a narrowed opening shows a deviation of 16.7% with the experimental results while the actual HRR inside the model with an opening geometry of 0.2 m x 0.2 m shows a deviation of 10% with the experimental results. When the reference

model is used as reference model then the deviation of the narrowed opening is approximately 7.4%. The actual HRR at the outside lower part (yellow line) begins at approximately 4 minutes after the ignition and will be lower than the actual HRR at the outside lower part of the reference model at the end of the simulation time. The actual HRR of the upper part (red line) of the narrowed opening model shows a huge increasement compared to the results of the reference model.

Both graphs show that the theoretical HRR and the actual HRR inside the model are similar before external flames occurs. After external flames occurs the actual HRR inside the room will be differently because of the adjusted opening surface which will influence the mass inflow rate and the actual HRR inside the model. Using 2 cm or 1 cm grid cell size does not show a stabilized actual HRR during external flaming. The total HRR of all areas (black line) should equal the theoretical HRR of the propane burner. If the total HRR of all areas does not equals the theoretical HRR this means that there is loss of energy in the simulation. In Table 6 the results of the actual HRR by narrowing the opening are compared to the experimental results and the CFD reference model. Decreasing the opening surface means a decreased mass inflow rate through the opening and thus a decreased actual HRR inside the model. The empirical correlation based on the experimental results shows a lower actual HRR inside the model by decreasing the opening surface.

Table 6: The simulated actual HRR of a narrowed opening model (0.1 m x 0.2 m) by two different grid cell sizes.

reference model vs experiments			
opening size: 0.2 m x 0.2 m	empirical correlation HRR (experiments)	empirical correlation HRR (reference model)	deviation
2 cm grid cell size	$1500.\,A\sqrt{H}$	$1150.\,A\sqrt{H}$ / $900.\,A\sqrt{H}$	23.3% - 40.0%
1 cm grid cell size	$1500.\,A\sqrt{H}$	$1350.\,A\sqrt{H}$	10%
model with a narrowed opening vs experiments			
opening size: 0.1 m x 0.2 m	empirical correlation HRR (experiments)	empirical correlation HRR (variant)	deviation
2 cm grid cell size	$1500.\,A\sqrt{H}$	$1250.\,A\sqrt{H}$ / $500.\,A\sqrt{H}$	16.7% - 66.7%
1 cm grid cell size	$1500.\,A\sqrt{H}$	$1250.\,A\sqrt{H}$ / $850.\,A\sqrt{H}$	16.7% - 43.3%
model with a narrowed opening vs reference model			
	empirical correlation HRR (reference model)	empirical correlation HRR (variant)	deviation
2 cm grid cell size	$1150.\,A\sqrt{H}$ / $900.\,A\sqrt{H}$	$1250.\,A\sqrt{H}$ / $500.\,A\sqrt{H}$	8.0% - 44.4%
1 cm grid cell size	$1350.\,A\sqrt{H}$	$1250.\,A\sqrt{H}$ / $850.\,A\sqrt{H}$	7.4% - 37.0%

Mass inflow rate

In Table 7 the simulated mass inflow rate through the opening with opening geometry 0.1 m x 0.2 m and the results of the reference model are given for 2 cm and 1 cm grid cell sizes. The simulated mass inflow rate with 2 cm grid cell size shows a bigger deviation with the experimental results. Using 1 cm grid cell size to determine the mass inflow rate shows a large deviation with the experimental results as well. The reference model shows a lower deviation with experimental results for the mass inflow rate. Using the reference model as a reference model will result in a lower deviation for both grid cell sizes. Using 2 cm grid cell size shows a lower deviation with the reference model instead of using 1 cm grid cell size.

Table 7: The simulated mass inflow rate of a narrowed opening model (0.1 m x 0.2 m) by two different grid cell sizes.

reference model vs experiments			
opening size: 0.2 m x 0.2 m	empirical correlation inflow rate (experiments)	empirical correlation inflow rate (reference model)	deviation
2 cm grid cell size	$0.5.\mathrm{A}\sqrt{\mathrm{H}}$	$0.41.\mathrm{A}\sqrt{\mathrm{H}}$ / $0.36.\mathrm{A}\sqrt{\mathrm{H}}$	18.0% - 28.1%
1 cm grid cell size	$0.5.\mathrm{A}\sqrt{\mathrm{H}}$	$0.47.\mathrm{A}\sqrt{\mathrm{H}}$	5.6%
model with a narrowed opening vs experiments			
opening size: 0.1 m x 0.2 m	empirical correlation inflow rate (experiments)	empirical correlation inflow rate (variant)	deviation
2 cm grid cell size	$0.5.\mathrm{A}\sqrt{\mathrm{H}}$	$0.41.\mathrm{A}\sqrt{\mathrm{H}}$ / $0.29.\mathrm{A}\sqrt{\mathrm{H}}$	18.0% - 42.0%
1 cm grid cell size	$0.5.\mathrm{A}\sqrt{\mathrm{H}}$	$0.40.\mathrm{A}\sqrt{\mathrm{H}}$ / $0.31.\mathrm{A}\sqrt{\mathrm{H}}$	20.0% - 38.0%
model with a narrowed opening vs reference model			
	empirical correlation inflow rate (reference model)	empirical correlation inflow rate (variant)	deviation
2 cm grid cell size	$0.41.\mathrm{A}\sqrt{\mathrm{H}}$ / $0.36.\mathrm{A}\sqrt{\mathrm{H}}$	$0.41.\mathrm{A}\sqrt{\mathrm{H}}$ / $0.29.\mathrm{A}\sqrt{\mathrm{H}}$	0.0% - 19.4%
1 cm grid cell size	$0.47.\mathrm{A}\sqrt{\mathrm{H}}$	$0.40.\mathrm{A}\sqrt{\mathrm{H}}$ / $0.35.\mathrm{A}\sqrt{\mathrm{H}}$	14.9% - 25.5

Neutral plane

The neutral plane height of a narrowed opening is calculated by 2 cm and 1 cm grid cell size, see Table 8. The neutral plane height of the narrowed opening model simulated with 1 cm grid cell size shows zero deviation with the experimental results. By using the validated CFD model as a reference model the deviation of the neutral plane height is lower by using 1 cm grid cell size as well.

Table 8: The simulated neutral plane height of a narrowed opening model (0.1 m x 0.2 m) by two different grid cell sizes.

reference model vs experiments			
opening size: 0.2 m x 0.2 m	neutral plane height (experiments)	neutral plane height (reference model)	deviation
2 cm grid cell size	0.080 m	0.060 m	25.0%
1 cm grid cell size	0.080 m	0.083 m	3.8%
model with a narrowed opening vs experiments			
opening size: 0.1 m x 0.2 m	neutral plane height (experiments)	neutral plane height (variant)	deviation
2 cm grid cell size	0.080 m	0.112 m	40.0%
1 cm grid cell size	0.080 m	0.080 m	0.0%
model with a narrowed opening vs reference model			
	neutral plane height from opening bottom (reference model)	neutral flame height from opening bottom (variant)	deviation
2 cm grid cell size	0.060 m	0.112 m	46.4%
1 cm grid cell size	0.083 m	0.080 m	3.6%

External flame height

In Table 9 the simulated external flame height which is determined by calculation method 1 is given for two grid cell sizes. The result of the model with a narrowed opening is compared to the validated external flame height simulated with 1 cm grid cell size. From the grid sensitivity analysis it can be concluded that using 1 cm grid cell size shows a good agreement with all measured variables. Therefore the reference model is compared with simulation results of 2 cm and 1 cm grid cell size. The external flame height simulated by using 2 cm grid cell size deviates 0.0% from the validated flame height simulated with 1 cm grid cell size. Using 1 cm grid cell size shows a deviation of 34.5% from the validated external flame height. Using 1 cm grid cell size shows that the external flame height of a narrowed opening shows an increasement of 34.5% relatively compared to the external flame height of the reference model.

Table 9: The simulated external flame height of a narrowed opening model (0.1 m x 0.2 m).

	external flame height (simulations)
validated model	0.58 m
2 cm grid cell size	0.58 m
1 cm grid cell size	0.78 m

Simulation model 3: adiabatic construction

Actual HRR

Below simulation model 3 is given by using 2 cm and 1 cm grid cell size. In simulation model 3 adiabatic construction are used instead of fiberboard. Figure 23 shows the influence of using adiabatic construction instead of using fiberboard construction on the actual HRR inside and outside the model simulated with 2 cm grid cell size. The actual HRR inside the model (green solid line) equals before external flaming the theoretical HRR of the fire source (black solid line). The actual HRR inside the model and the theoretical HRR show similar results like in the reference model (green and black dashed lines). In both simulation models external flames occurs after 7 minutes after the ignition. After external flaming occurs the actual HRR inside the model is stabilized (green line) like the actual HRR of the validated model (green dashed line) during external flaming simulated with 1 cm grid cell size. Both the actual HRR inside the model with adiabatic construction and fiberboard construction simulated with 2 cm grid cell size equal the empirical correlation of $1150\ A\sqrt{H}$. Both simulation models show a deviation of 23.3% from the experimental results. Using adiabatic construction instead of fiberboard show a constant HRR value of 20.8 kW during external flaming. After approximately 11 minutes of ignition the actual HRR inside the model with fiberboard construction decreases to a constant value of $900\ A\sqrt{H}$. Decreasing the actual HRR inside the model after external flames occurs means that there is more energy loss to the outside area. Therefore the use of adiabatic construction shows a constant HRR inside the model. This constant HRR does not influence the external flaming at the outside lower part (yellow line). Because of this constant HRR the external flaming at the outside upper part (red line) is decreased.

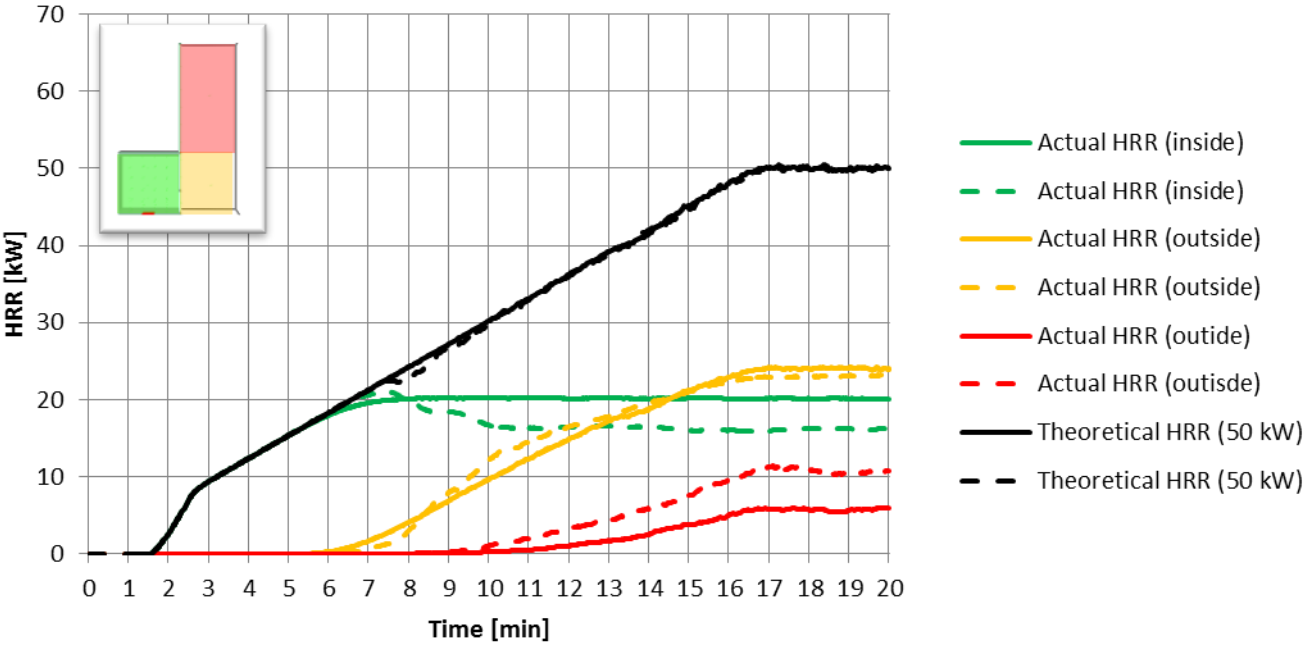

Figure 23: The effect of using adiabatic construction instead of fiberboard construction on the actual HRR inside the model simulated with 2 cm grid cell size. The dashed lines show the HRR of the reference model simulated with 2 cm grid cell size.

Figure 24 shows the actual HRR inside the model simulated with 1 cm grid cell size by using adiabatic construction instead of fiberboard construction. The actual HRR inside the model (green solid line) equals before external flaming the theoretical HRR of the fire source (black solid line). The actual HRR inside the model and the theoretical HRR shows in the reference model similar results (green and black dashed lines). After external flaming occur the actual HRR inside the model is stabilized like the actual HRR of the reference model (green dashed line). The actual HRR inside the model with adiabatic construction simulated with 1 cm grid cell size equals the empirical correlation of $1250\ \mathrm{A}\sqrt{\mathrm{H}}$ while the actual HRR inside the model with fiberboard construction simulated with 1 cm grid cell size equals the empirical correlation of $1350\ \mathrm{A}\sqrt{\mathrm{H}}$ during external flaming. The difference between these two models is approximately 1.8 kW during external flaming.

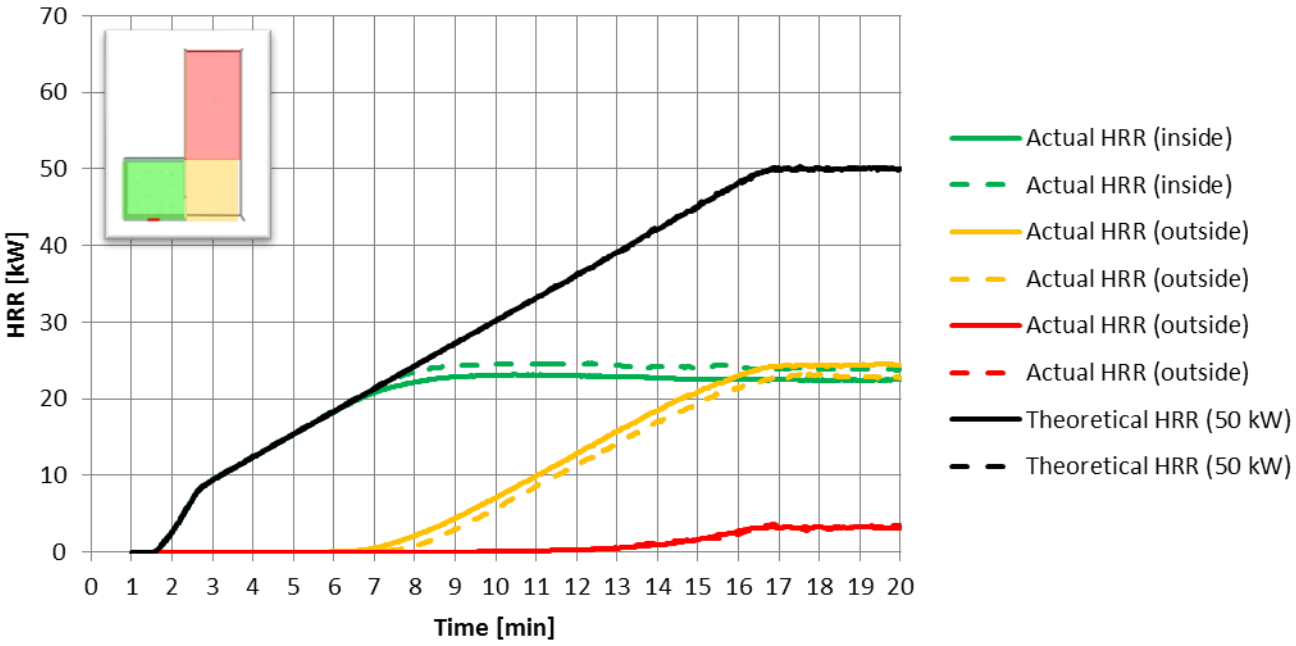

Figure 24: The effect of using adiabatic construction instead of fiberboard on the actual HRR inside the model simulated with 1 cm grid cell size. The dashed lines show the HRR of the reference model simulated with 1 cm grid cell size.

The actual HRR inside the model with adiabatic construction shows a deviation of 16.7% with the experimental results while the actual HRR inside the model with fiberboard construction shows a deviation of 10% with the experimental results. When the reference model is used as the reference model then the deviation of using adiabatic construction instead of fiberboard construction is approximately 7.4%. The actual HRR at the outside lower part (yellow line) is increased compared to the reference model with fiberboard construction by 1.8 kW during the simulation time. The actual HRR of the outside upper part of the CFD model with adiabatic construction (red line) equals the actual HRR of the outside upper part of the CFD model with fiberboard construction (red dashed line).

Both graphs show that the theoretical HRR and the actual HRR inside the model are similar before external flames occur. The actual HRR inside the model simulated with 2 cm and 1 cm grid cell size shows a constant value during external flaming. Using 1 cm grid cell size instead of 2 cm grid cell size increases the actual HRR inside the model. This means that the actual HRR outside is decreased as a result of the increased actual HRR. In Table 10 the results of the actual HRR by using adiabatic construction and fiberboard construction are compared to the experimental results and the CFD reference model.

Table 10: The simulated actual HRR of a model with adiabatic construction by two different grid cell sizes.

reference model walls vs experiments			
fiberboard construction	empirical correlation HRR (experiments)	empirical correlation HRR (reference model)	deviation
2 cm grid cell size	$1500.\,A\sqrt{H}$	$1150.\,A\sqrt{H}$ / $900.\,A\sqrt{H}$	23.3% - 40.0%
1 cm grid cell size	$1500.\,A\sqrt{H}$	$1350.\,A\sqrt{H}$	10%
model with adiabatic construction vs experiments			
adiabatic construction	empirical correlation HRR (experiments)	empirical correlation HRR (variant)	deviation
2 cm grid cell size	$1500.\,A\sqrt{H}$	$1150.\,A\sqrt{H}$	23.3%
1 cm grid cell size	$1500.\,A\sqrt{H}$	$1250.\,A\sqrt{H}$	16.7%
model with adiabatic construction vs reference model			
	empirical correlation HRR (reference model)	empirical correlation HRR (variant)	deviation
2 cm grid cell size	$1150.\,A\sqrt{H}$ / $900.\,A\sqrt{H}$	$1150.\,A\sqrt{H}$	0.0% - 21.7%
1 cm grid cell size	$1350.\,A\sqrt{H}$	$1250.\,A\sqrt{H}$	7.4%

Mass inflow rate

Although the actual HRR inside the model with adiabatic construction is not similar to the actual HRR of the reference model, the mass inflow rate through the opening will be different for both grid cell sizes. This is because of the decreased actual HRR inside the room. In Table 11 the simulated mass inflow rate through the opening of an adiabatic construction model and fiberboard construction model is given by using 2 cm and 1 cm grid cell size. The simulated mass inflow rate shows a bigger deviation with the experimental results by using adiabatic construction then using fiberboard construction. The simulated model with adiabatic construction is compared to the reference model. Using 1 cm grid cell size shows a deviation of approximately 14.0%. From the actual HRR inside the model and the mass inflow rate of an adiabatic construction model it can be concluded that the actual HRR and the mass inflow rate do not comply with the empirical correlation from the experiments. By changing the material properties to adiabatic construction the actual HRR and the mass inflow rate show a bigger deviation with the experiments.

Table 11: The simulated mass inflow rate of a model with adiabatic construction by two different grid cell sizes.

reference model vs experiments			
fiberboard construction	empirical correlation inflow rate (experiments)	empirical correlation inflow rate (reference model)	deviation
2 cm grid cell size	$0.5.\,A\sqrt{H}$	$0.41.\,A\sqrt{H}$ / $0.36.\,A\sqrt{H}$	18.0% - 28.1%
1 cm grid cell size	$0.5.\,A\sqrt{H}$	$0.47.\,A\sqrt{H}$	5.6%
model with adiabatic construction vs experiments			
adiabatic construction	empirical correlation inflow rate (experiments)	empirical correlation inflow rate (variant)	deviation
2 cm grid cell size	$0.5.\,A\sqrt{H}$	$0.40.\,A\sqrt{H}$	20.0%
1 cm grid cell size	$0.5.\,A\sqrt{H}$	$0.43.\,A\sqrt{H}$	14.0%
model with adiabatic construction vs reference model			
	empirical correlation inflow rate (reference model)	empirical correlation inflow rate (variant)	deviation
2 cm grid cell size	$0.41.\,A\sqrt{H}$ / $0.36.\,A\sqrt{H}$	$0.40.\,A\sqrt{H}$	2.4% - 10.0%
1 cm grid cell size	$0.47.\,A\sqrt{H}$	$0.43.\,A\sqrt{H}$	8.5%

Neutral plane

The neutral plane height of the adiabatic construction model is calculated with 2 cm and 1 cm grid cell size. The neutral plane height of the adiabatic construction model calculated with 1 cm grid cell size shows zero deviation with the experimental results, see Table 12. By using the validated CFD model as reference model the deviation of the neutral plane height by using 1 cm grid cell size is lower with the experimental results as well.

Table 12: The simulated neutral plane height of a model with adiabatic construction by two different grid cell sizes.

reference model walls vs experiments			
fiberboard construction	neutral plane height (experiments)	neutral plane height (reference model)	deviation
2 cm grid cell size	0.080 m	0.060 m	25.0%
1 cm grid cell size	0.080 m	0.083 m	3.8%
model with adiabatic construction vs experiments			
Adiabatic construction	neutral plane height (experiments)	neutral plane height (variant)	deviation
2 cm grid cell size	0.080 m	0.063 m	21.3%
1 cm grid cell size	0.080 m	0.080 m	0.0%
model with adiabatic construction vs reference model			
	neutral plane height from opening bottom (reference model)	neutral flame height from opening bottom (variant)	deviation
2 cm grid cell size	0.060 m	0.063 m	4.8%
1 cm grid cell size	0.083 m	0.080 m	3.6%

External flame height

In Table 13 the simulated external flame height which is determined by calculation method 1 is given for two grid cell sizes. From the grid sensitivity analysis it can be concluded that using 1 cm grid cell size shows a good agreement with all measured variables. Therefore the external flame height of the model with adiabatic construction will be compared to the external flame height of the reference model simulated by 1 cm grid cell size.

The external flame height simulated by using 2 cm grid cell size deviates 6.5% from the validated flame height simulated with 1 cm grid cell size. Using 1 cm grid cell size shows a deviation of 10.8% compared to the validated external flame height. Using 1 cm grid cell size shows that the external flame height of using adiabatic construction gives an increasement of 10.8% relatively compared to the external flame height of the reference model.

Table 13: The simulated external flame height of a model with adiabatic construction by two different cell sizes.

	external flame height (simulations)
validated model (fiberboard construction)	0.58 m
2 cm grid cell size (adiabatic construction)	0.62 m
1 cm grid cell size (adiabatic construction)	0.65 m

Simulation model 4: increased theoretical HRR

Actual HRR

The results of the actual and the theoretical HRR simulated with 2 cm grid cell size and 1 cm grid cell size are given in Figure 25 and Figure 26. In Figure 25 the actual and theoretical HRR with a maximum of 50 kW and 60 kW fire release rate simulated with 2 cm grid cell size is given. The actual HRR inside the model (green solid line) equals the theoretical HRR of the fire source (black solid line) before external flaming occurs. The actual HRR inside the model and the theoretical HRR show in the reference model similar results (green and black dashed lines). The results of the reference model shows that external flames occur after approximately 7 minutes while increasing the theoretical HRR shows that external flames occur after approximately 6 minutes. This is because of the increased fire release of the propane burner, the fire inside becomes earlier ventilation-controlled because of the limited oxygen concentration. The actual HRR inside the model during external flaming of both models simulated with 2 cm grid cell size varies between 20.6 kW and 16.1 kW. The correlation which belongs to this graph is between $1150\,\mathrm{A}\sqrt{\mathrm{H}}$ and $900\,\mathrm{A}\sqrt{\mathrm{H}}$. Both simulation models show a deviation of 23.3% from the experimental results. Although the actual HRR inside the model remain as without increasing the theoretical HRR the rest of the produced heat should be pushed out to the outside area. This means that the actual HRR outside the model is at the lower and upper outside part increased (yellow and red

lines). These results confirm that increased theoretical HRR inside the model does not influence the actual HRR inside the model during external flaming ($1150\ A\sqrt{H}$), but will influence the external flames outside.

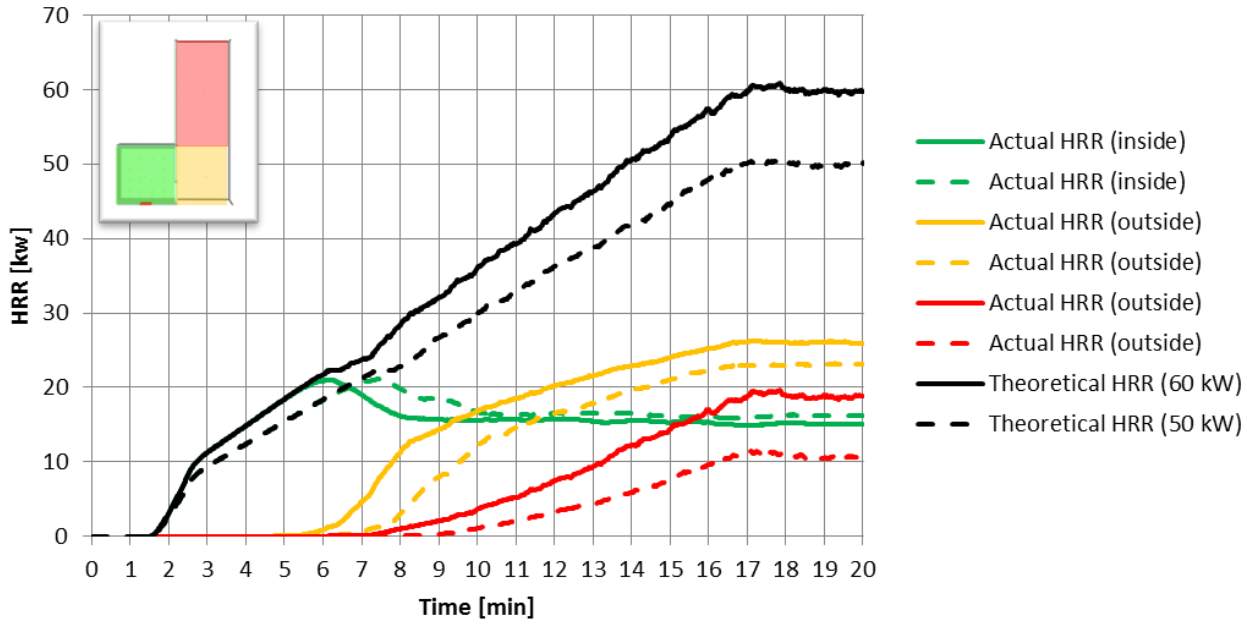

Figure 25: The effect of increasing the theoretical HRR inside the model simulated with 2 cm grid cell size. The dashed lines show the HRR of the reference model with 2 cm grid cell size.

In Figure 26 the actual and theoretical HRR with a maximum HRR of 50 kW and 60 kW are shown for a 1 cm grid cell size. The actual HRR inside the model (green solid line) equals the theoretical HRR of the fire source (black solid line) before external flaming. The actual HRR inside the model and the theoretical HRR show in the validated model similar results (green and black dashed lines). During external flaming the actual HRR inside the model is stabilized like the actual HRR of the reference model (green dashed line). Because increasing the theoretical HRR does not influence the actual HRR inside the model, the actual HRR inside the model with increased theoretical HRR should equal the actual HRR inside the model of the reference model.

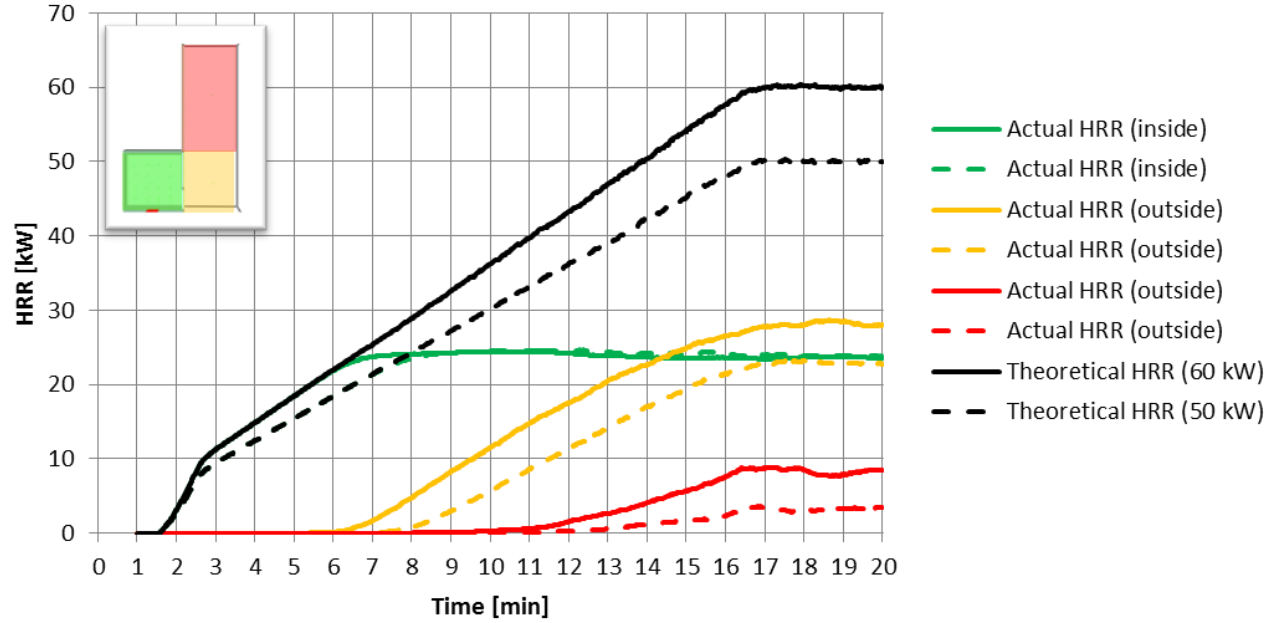

Figure 26: The effect of increasing the theoretical HRR inside the model simulated with 1 cm grid cell size. The dashed lines show the HRR of the reference model with 1 cm grid cell size.

This means that the actual HRR inside the model of both CFD models simulated with 1 cm grid cell size equals the empirical correlation of $1350\,A\sqrt{H}$. The actual HRR inside the model by increasing the theoretical HRR shows a deviation of 10.0% with the experimental results. When the reference model is used as reference model then the deviation will be zero. The actual HRR at the outside lower part (yellow line) is increased compared to the validated model with a theoretical HRR of maximum HRR of 50 kW. The actual HRR of the upper part is increased as well (red line). The result of the reference model simulated with 1 cm grid cell size shows that external flames occur after approximately 8 minutes while increasing the theoretical HRR shows that external flames occur after approximately 6.5 minutes. The actual HRR inside the model during external flaming of both models simulated with 1 cm grid cell size is 24.1 kW. If the actual HRR inside the model is similar to the actual HRR of the reference model, the mass inflow rate through the opening should be similar to the mass inflow rate of the reference model.

Both graphs show similar progression inside the model (actual HRR) before external flames occur. The actual and theoretical HRR are similar until the fire becomes ventilation-controlled. The actual HRR inside the model simulated with 50 kW or 60 kW shows similar results during external flaming. By an increased theoretical HRR the external flames will develop earlier outside the model. External flames will reach the upper floors earlier as well. This is because of the increased theoretical HRR inside the model. Therefore the rest of the actual HRR will be visible at the outside area. Both simulation models (2 cm or 1 cm grid cell size) comply with the results of the experiments which is that an increased theoretical HRR does not influence the actual HRR inside the model. In Table 14 the results of the actual HRR by increasing the theoretical HRR compared to the experimental results and the reference model are given. By increasing the theoretical HRR inside the model show similar actual HRR like the actual HRR of the reference model simulated with 1 cm grid cell size.

Table 14: The simulated actual HRR of a model with an increased theoretical HRR by two different grid cell sizes.

reference model vs experiments			
theoretical HRR (50 kW)	empirical correlation HRR (experiment)	empirical correlation HRR (reference model)	deviation
2 cm grid cell size	$1500.\,\mathrm{A}\sqrt{\mathrm{H}}$	$1150.\,\mathrm{A}\sqrt{\mathrm{H}}$ / $900.\,\mathrm{A}\sqrt{\mathrm{H}}$	23.3% - 40.0%
1 cm grid cell size	$1500.\,\mathrm{A}\sqrt{\mathrm{H}}$	$1350.\,\mathrm{A}\sqrt{\mathrm{H}}$	10%
model with an increased theoretical HRR vs experiments			
theoretical HRR (60 kW)	empirical correlation HRR (experiments)	empirical correlation HRR (variant)	deviation
2 cm grid cell size	$1500.\,\mathrm{A}\sqrt{\mathrm{H}}$	$1150.\,\mathrm{A}\sqrt{\mathrm{H}}$ / $900.\,\mathrm{A}\sqrt{\mathrm{H}}$	23.3% - 40.0%
1 cm grid cell size	$1500.\,\mathrm{A}\sqrt{\mathrm{H}}$	$1350.\,\mathrm{A}\sqrt{\mathrm{H}}$	10%
Model with an theoretical HRR vs reference model			
	empirical correlation HRR (reference model)	empirical correlation HRR (variant)	deviation
2 cm grid cell size	$1150.\,\mathrm{A}\sqrt{\mathrm{H}}$ / $900.\,\mathrm{A}\sqrt{\mathrm{H}}$	$1150.\,\mathrm{A}\sqrt{\mathrm{H}}$ / $900.\,\mathrm{A}\sqrt{\mathrm{H}}$	0.0% - 0.0%
1 cm grid cell size	$1350.\,\mathrm{A}\sqrt{\mathrm{H}}$	$1350.\,\mathrm{A}\sqrt{\mathrm{H}}$	0.0%

Mass inflow rate

Because the actual HRR inside the model with an increased theoretical HRR shows similar results, the mass inflow rate through the opening should show similar mass inflow rate through the opening as well. In Table 15 the simulated mass inflow rate through the opening with an increased theoretical HRR and the results of the reference model are given by using 2 cm and 1 cm grid cell sizes.

Table 15: The simulated mass inflow rate of a model with an increased theoretical HRR by two different grid cell sizes.

reference model vs experiments			
theoretical HRR 50 kW	empirical correlation inflow rate (experiments)	empirical correlation inflow rate (reference model)	deviation
2 cm grid cell size	$0.5 \cdot A\sqrt{H}$	$0.41 \cdot A\sqrt{H}$ / $0.36 \cdot A\sqrt{H}$	18.0% - 28.1%
1 cm grid cell size	$0.5 \cdot A\sqrt{H}$	$0.47 \cdot A\sqrt{H}$	5.6%
model with an increased theoretical HRR vs experiments			
theoretical HRR 60 kW	empirical correlation inflow rate (experiments)	empirical correlation inflow rate (variant)	deviation
2 cm grid cell size	$0.5 \cdot A\sqrt{H}$	$0.41 \cdot A\sqrt{H}$ / $0.36 \cdot A\sqrt{H}$	18.0% - 28.1%
1 cm grid cell size	$0.5 \cdot A\sqrt{H}$	$0.47 \cdot A\sqrt{H}$	5.6%
model with an increased theoretical HRR vs reference model			
	empirical correlation inflow rate (reference model)	empirical correlation inflow rate (variant)	deviation
2 cm grid cell size	$0.41 \cdot A\sqrt{H}$ / $0.36 \cdot A\sqrt{H}$	$0.41 \cdot A\sqrt{H}$ / $0.36 \cdot A\sqrt{H}$	0.0% - 0.0%
1 cm grid cell size	$0.47 \cdot A\sqrt{H}$	$0.47 \cdot A\sqrt{H}$	0.0%

Neutral plane

In Table 16 the neutral plane height above floor level is compared by two different fire release rates. The difference between using 2 cm and 1 cm grid cell size with a fire release rate of 50 kW does not equal the difference between using 2 cm and 1 cm grid cell size with a fire release rate of 60 kW. This means the neutral plane height will be increased by increasing the theoretical HRR. The neutral plane height shows a lower deviation with the neutral plane height of the reference model.

Table 16: The simulated neutral plane height of a model with an increased theoretical HRR by two different grid cell sizes.

reference model vs experiments			
theoretical HRR 50 kW	neutral plane height (experiments)	neutral plane height (reference model)	deviation
2 cm grid cell size	0.080 m	0.060 m	25.0%
1 cm grid cell size	0.080 m	0.083 m	3.8%
model with an increased theoretical HRR vs experiments			
theoretical HRR 60 kW	neutral plane height (experiments)	neutral plane height (variant)	deviation
2 cm grid cell size	0.080 m	0.090 m	12.5%
1 cm grid cell size	0.080 m	0.085 m	6.3%
model with an increased theoretical HRR vs reference model			
	neutral plane height from opening bottom (reference model)	neutral flame height from opening bottom (variant)	deviation
2 cm grid cell size	0.060 m	0.090 m	33.3%
1 cm grid cell size	0.083 m	0.085 m	2.4%

External flame height

In Table 17 the simulated external flame height is given which is determined by calculation method 1 for two grid cell sizes. Because of the increased theoretical HRR the flame height will be increased for this reason. The external flame height simulated by using 2 cm grid cell size deviates 17.1% from the validated flame height simulated with 1 cm grid cell size. Using 1 cm grid cell size shows a deviation of 18.3% from the validated external flame height. Using 1 cm grid cell size shows that for the external flame height of the model with an increased theoretical HRR an increasement of 18.3% relatively compared to the external flame height of the reference model.

Table 17: The simulated external flame height of a model with an increased theoretical HRR by two different grid cell sizes.

	external flame height (simulations)
validated model (50 kW)	0.58 m
2 cm grid cell size (60 kW)	0.70 m
1 cm grid cell size (60 kW)	0.71 m

Appendix VII-b: simulation results – linear correlation

Below is the linear correlation between the opening geometry factor and the predicted actual HRR and mass inflow rate of the reference model. The dashed line shows a deviation of 10.0% above and below the linear correlation line.

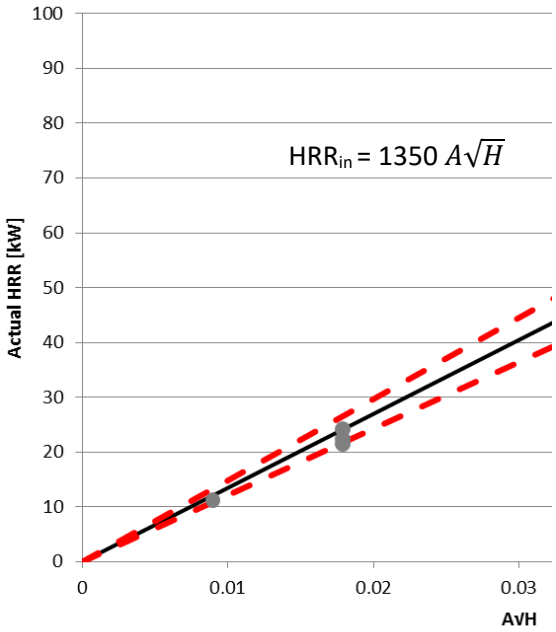

Figure 27: The linear correlation between the opening geometry factor and the predicted actual HRR inside the model of the reference model. The red dashed boundary shows a deviation of 10.0% above and below the linear correlation line. The grey dots show the simulated actual HRR of all simulation models.

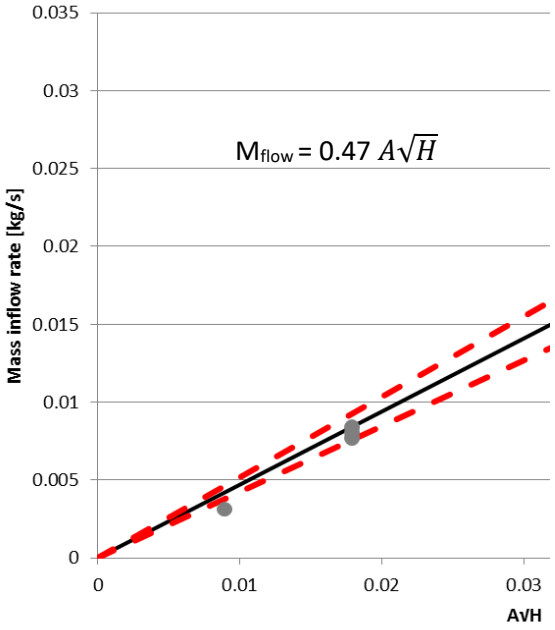

Figure 29: The linear correlation between the opening geometry factor and the predicted mass inflow rate of the reference model. The red dashed boundary shows a deviation of 10.0% above and below the linear correlation line. The grey dots show the simulated mass inflow rate of all simulation models.

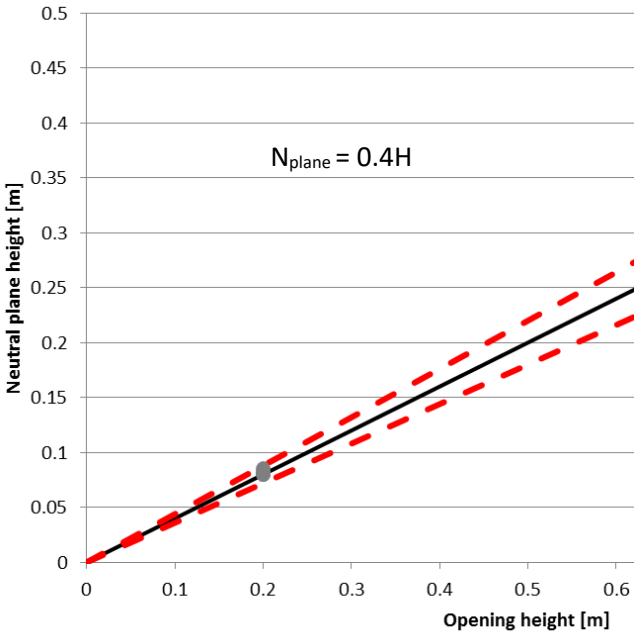

Figure 28: The linear correlation between the opening geometry factor and the predicted neutral plane height of the reference model. The red dashed boundary shows a deviation of 10.0% above and below the linear correlation line. The gray dots show the simulated neutral plane height of all simulation models.

Appendix VIII: simulation results

Appendix VIII-a: full-size model with propane fire (10 cm grid cell size)

The simulation results of the actual HRR, mass inflow rate and neutral plane height during external flaming are given below.

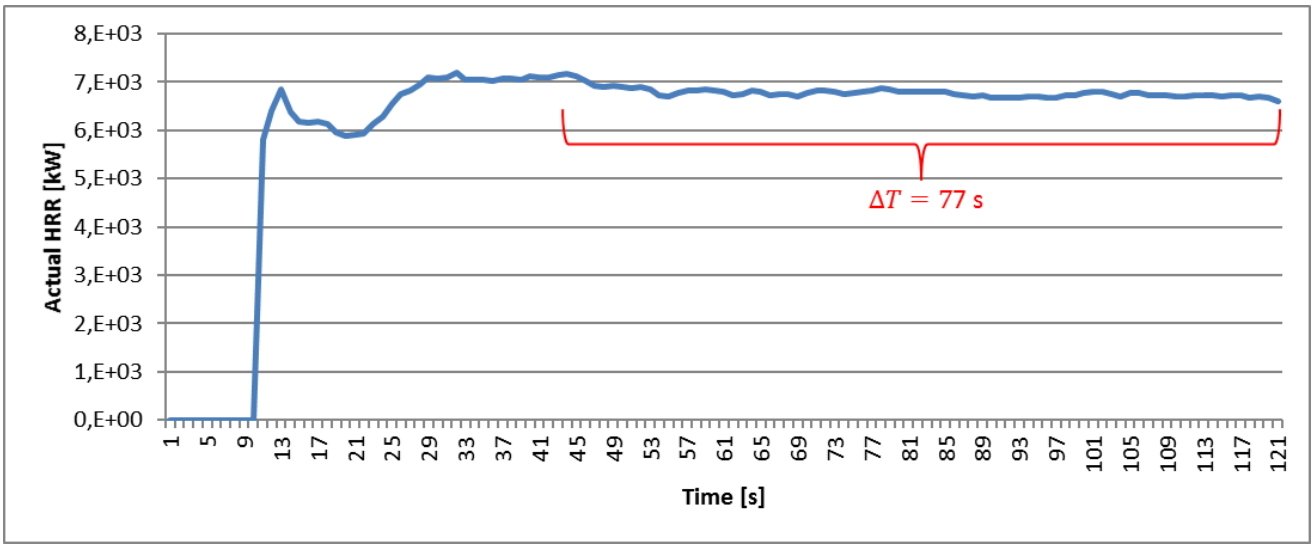

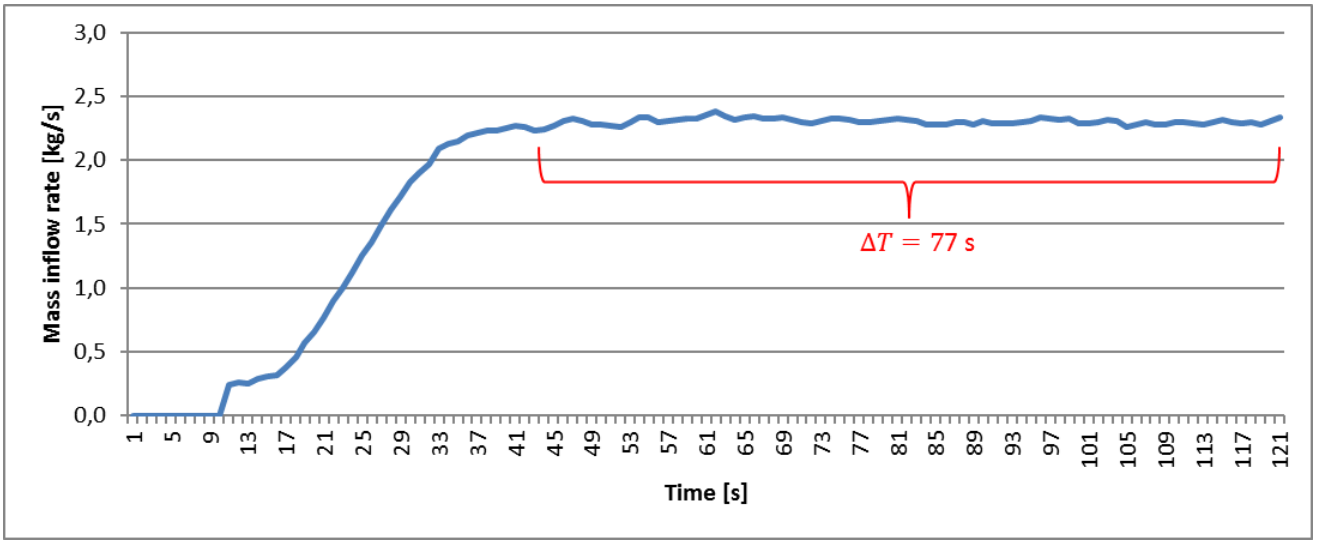

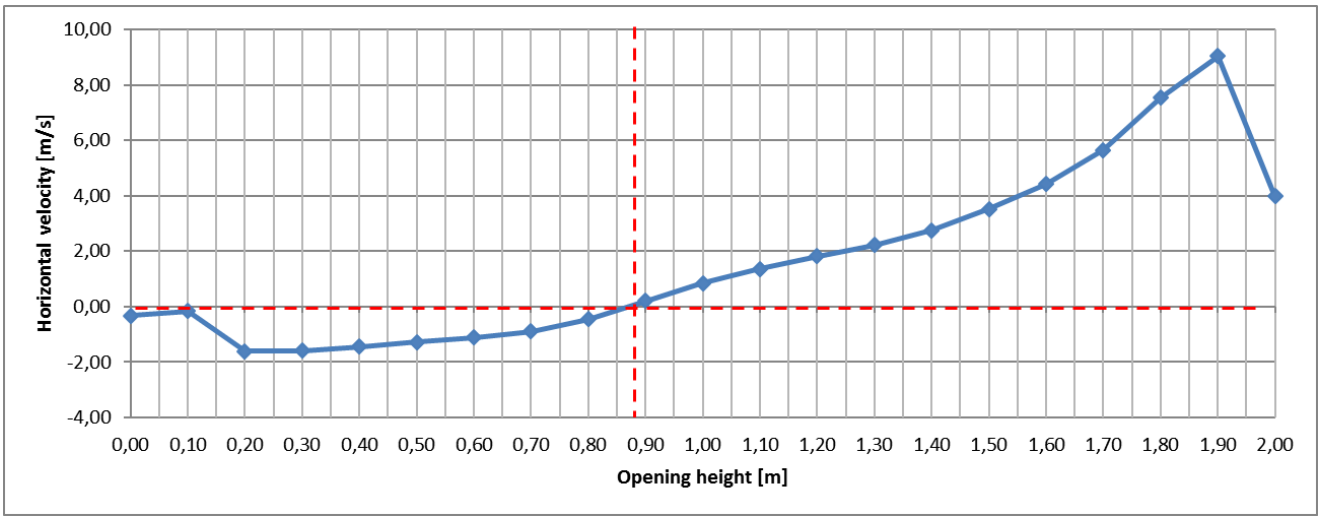

Appendix VIII-b: full-size model with cellulose fire (10 cm grid cell size)

The simulation results of the actual HRR, mass inflow rate and neutral plane height during external flaming are given below.

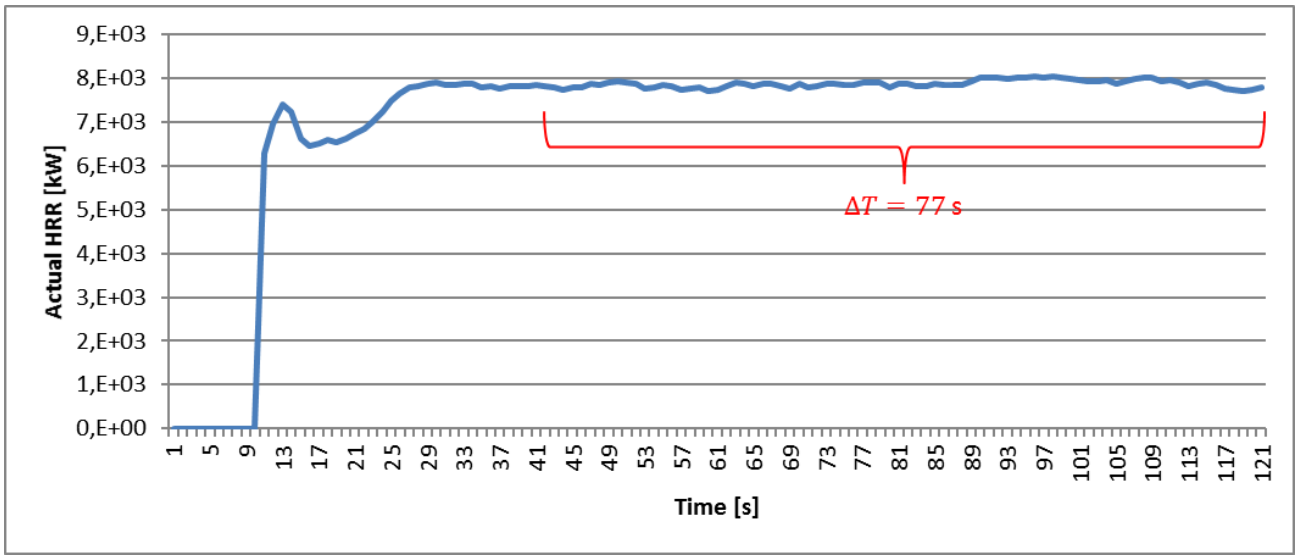

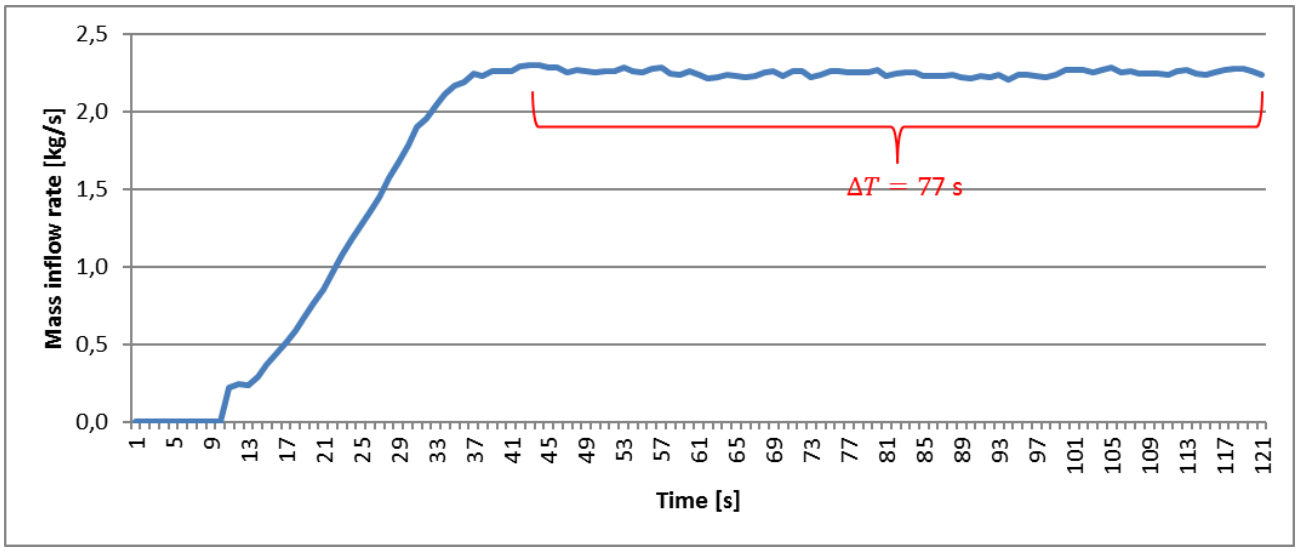

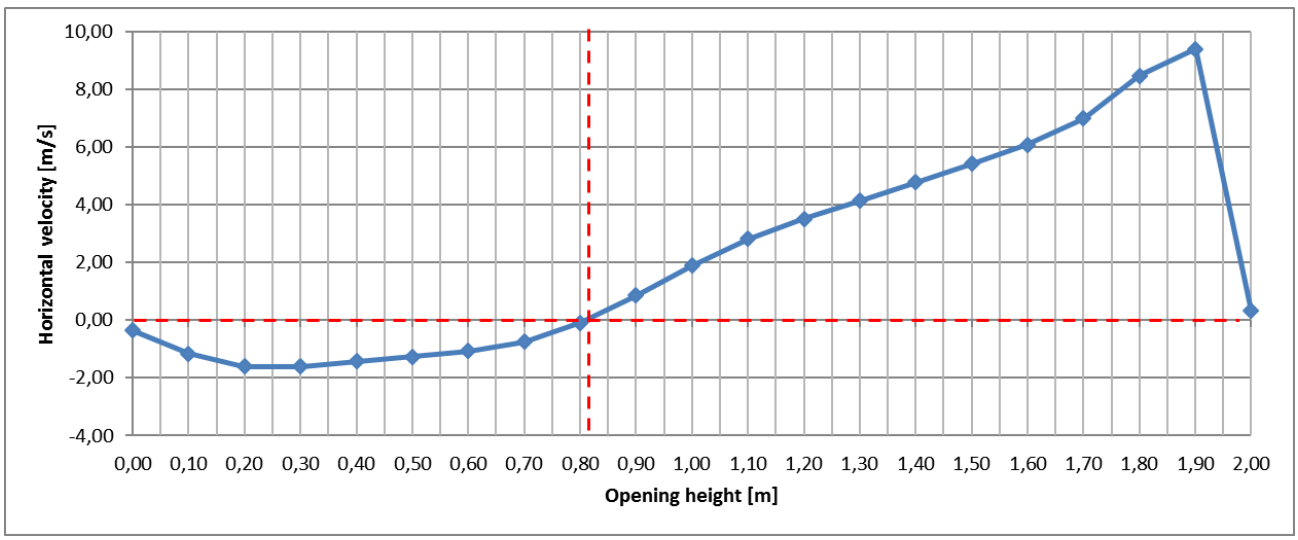

Appendix VIII-c: full-size model with cellulose fire (5 cm grid cell size)

The simulation results of the actual HRR, mass inflow rate and neutral plane height during external flaming are given below.